

Zero waste Heat vessel towards relevant Energy savings also thanks to IT technologies



D 5.5 | Technology benchmark and competitor analysis of ZHENIT WH2X systems

WP5 – Technologies evaluation and impact assessment towards replication

HORIZON-CL5-2021-D5-01-10

Clean and competitive solutions for all transport modes -
Innovative on-board energy saving solutions

Version 1.0 | May 2026



Danelec

tecnal.a
UNIVERSITY OF SASSARI RESEARCH & TECHNOLOGY CENTER



bound4blue



This project has received funding from the European Union's Horizon Europe research and innovation programme under grant agreement No 101056801.



Funded by the
European Union

Disclaimer

Funded by the European Union. The content of this deliverable reflects the authors' views. Views and opinions expressed are however those of the author(s) only and do not necessarily reflect those of the European Union or the European Climate, Infrastructure and Environment Executive Agency (CINEA). Neither the European Union nor the granting authority can be held responsible for them.

Copyright Message

This report, if not confidential, is licensed under a Creative Commons Attribution 4.0 International License (CC BY 4.0). A copy is available here:

<https://creativecommons.org/licenses/by/4.0/>.

You are free to share (copy and redistribute the material in any medium or format) and adapt (remix, transform, and build upon the material for any purpose, even commercially) under the following terms: (i) attribution (you must give appropriate credit, provide a link to the license, and indicate if changes were made; you may do so in any reasonable manner, but not in any way that suggests the licensor endorses you or your use); (ii) no additional restrictions (you may not apply legal terms or technological measures that legally restrict others from doing anything the license permits).

Document History

Project Acronym	ZHENIT
Project Title	ZHENIT - Zero waste Heat vessel towards relevant Energy savings also thanks to IT technologies
Project coordination	RINA-C
Project duration	47 months – from 1/06/2022 to 30/04/2026
Title	Technology benchmark and competitor analysis of ZHENIT WH2X systems
Dissemination Level	PU - Public
Status	Final
Version	1.0
Work Package	WP5
Lead Beneficiary	UoB
Other Beneficiaries	UoB, RINA-C, Tecnalia, and CNR
Author(s)	Lorenzo Ciappi (UoB), Konstantinos Braimakis (NTUA), Carol Pascual Ortiz (Tecnalia), Andrea Frazzica (CNR), Walter Mittelbach (Sorption Technologies GmbH), Andrea Welti (RINA-C), Yulong Ding (UoB), and Adriano Sciacovelli (UoB)

Date	Ver.	Contributors	Comment
05/03/2025	0.1	Lorenzo Ciappi (UoB) and Adriano Sciacovelli (UoB)	Initial structure
21/05/2025	0.2	Lorenzo Ciappi (UoB)	Section 2 and Subsections from 3.1 to 3.7
18/06/2025	0.3	Lorenzo Ciappi (UoB) and Andrea Welti (RINA-C)	Subsection 3.8
29/06/2025	0.4	Adriano Sciacovelli (UoB)	Review of Section 2 and Section 3
16/07/2025	0.5	Lorenzo Ciappi (UoB) and Konstantinos Braimakis (NTUA)	Section 4
22/09/2025	0.6	Lorenzo Ciappi (UoB) and Carol Pascual Ortiz (Tecnalia)	Section 5
30/10/2025	0.7	Yulong Ding (UoB)	Review of Sections from 2 to 5

D 5.5 | Technology benchmark and competitor analysis of ZHENIT
WH2X systems

21/11/2025	0.8	Lorenzo Ciappi (<i>UoB</i>), Andrea Frazzica (<i>CNR</i>), and Walter Mittelbach (<i>Sorption Technologies GmbH</i>)	Section 6
02/12/2025	0.9	Lorenzo Ciappi (<i>UoB</i>)	Section 1
25/01/2026	0.10	Lorenzo Ciappi (<i>UoB</i>)	Section 7
28/04/2026	0.11	Sander Roosjen (<i>ECT</i>) and Bjarte Lund (<i>Danelec</i>)	Review
15/05/2026	0.12	Lorenzo Ciappi (<i>UoB</i>)	Final version
19/05/2026	1.0	Fiorella Valenti (RINA-C)	Document ready for submission

D 5.5 | Technology benchmark and competitor analysis of ZHENIT
WH2X systems

List of Organisations

	Participant	Abbreviation	Country	Logo
1	<i>RINA Consulting S.p.A.</i>	<i>RINA-C</i>	Italy	
1.1	<i>RINA Services S.p.A.</i>	<i>RINA-S</i>	Italy	
2	<i>Ethnicon Metsovion Polytechnion / National Technical University of Athens</i>	<i>NTUA</i>	Greece	
3	<i>Danelec Marine A/S</i>	<i>Danelec</i>	Norway	
4	<i>Fundación Tecnalia Research & Innovation</i>	<i>Tecnalia</i>	Spain	
4.1	<i>Universidad del País Vasco / Euskal Herriko Unibertsitatea</i>	<i>UPV/EHU</i>	Spain	
5	<i>Attica Group</i>	<i>Attica</i>	Greece	
6	<i>Consiglio Nazionale delle Ricerche</i>	<i>CNR</i>	Italy	
6.1	<i>Consorzio di ricerca per l'innovazione tecnologica, Sicilia Trasporti Navali, Commerciali e da Diporto S.c.a.r.l.</i>	<i>Navtec</i>	Italy	
7	<i>Sorption Technologies GmbH</i>	<i>SorTech</i>	Germany	
7.1	<i>Sorption Technologies S.r.l.</i>	<i>SorTIT</i>	Italy	
8	<i>Bound4blue S.L.</i>	<i>B4B</i>	Spain	
9	<i>Encontech B.V.</i>	<i>ECT</i>	Netherlands	
10	<i>Gruppo SIGLA S.r.l.</i>	<i>SIGLA</i>	Italy	
11	<i>The University of Birmingham</i>	<i>UoB</i>	United Kingdom	

Table of Content

Abbreviations and acronyms.....	12
1 Executive summary	13
2 Introduction	16
3 Latent heat thermal energy storage prototype	19
3.1 Configuration of the LHTES prototype.....	19
3.2 Geometry of the LHTES prototype.....	21
3.3 Working principle of the LHTES prototype	22
3.4 Principal components of the LHTES prototype.....	23
3.4.1 Tank and lid	25
3.4.2 Pillow plates.....	27
3.4.3 Phase change material	28
3.4.4 Thermal sensors	29
3.5 Design choices, novel features, and technology readiness level of the LHTES prototype	30
3.5.1 Main design choices for the LHTES prototype	31
3.5.2 Novel features of the LHTES prototype.....	32
3.5.3 Technology readiness level of the LHTES prototype	33
3.6 Operating conditions and performance of the LHTES prototype.....	33
3.7 Cost overview for the LHTES prototype.....	37
3.8 Thermal energy storage technologies for maritime applications.....	39
4 Organic Rankine cycle prototype.....	51
4.1 Working principle of the ORC prototype	53
4.1.1 Organic Rankine cycle – Electricity production modes	53
4.1.2 Ejector cooling cycle – Cooling mode.....	54
4.1.3 Ejector-vapour compression cycle configuration – Cooling mode.....	55
4.1.4 Parallel ORC–EVCC configuration	55
4.2 Principal components of the ORC–ejector integrated heat pump prototype.....	56
4.2.1 Heat exchangers.....	56
4.2.2 Pump and motor.....	57
4.2.3 Expanders and motors.....	57
4.2.4 Compressors.....	58
4.2.5 Ejector.....	59
4.2.6 Expansion valve	60

D 5.5 | Technology benchmark and competitor analysis of ZHENIT
WH2X systems

4.2.7	Sensors	60
4.2.8	Control hardware and cabinet	61
4.3	Design choices, novel features, and technology readiness level of the ORC prototype	62
4.3.1	Main design choices for the ORC prototype	62
4.3.2	Novel features of the ORC prototype	63
4.3.3	Technology readiness level of the ORC prototype	64
4.4	Operating conditions and performance of the ORC prototype	64
4.5	Organic Rankine cycle technologies for maritime applications	69
5	Isobaric expansion engine prototype	73
5.1	Working principle of the IEE prototype	74
5.2	Principal components of the IEE prototype	75
5.2.1	Core components of the IEE prototype	76
5.2.2	Auxiliary components of the IEE prototype	77
5.3	Design choices, novel features, and technology readiness level of the IEE prototype	80
5.3.1	Main design choices for the IEE prototype	80
5.3.2	Novel features of the IEE prototype	80
5.3.3	Technology readiness level of the IEE prototype	81
5.4	Operating conditions and performance of the IEE prototype	81
5.5	Cost overview for the IEE prototype	84
5.6	Isobaric expansion engine technologies for maritime applications	84
6	Sorption desalination and cooling prototype	87
6.1	Working principle of the SDC prototype	88
6.2	Principal components of the SDC prototype	89
6.3	Design choices, novel features, and technology readiness level of the SDC prototype	93
6.3.1	Main design choices for the SDC prototype	93
6.3.2	Novel features of the SDC prototype	94
6.3.3	Technology readiness level of the SDC prototype	95
6.4	Operating conditions and performance of the SDC prototype	95
6.5	Sorption desalination and cooling technologies for maritime applications	97
7	Conclusions	103
	Bibliography	108

List of Figures

Figure 1 – Photograph of the latent heat thermal energy storage prototype developed by The University of Birmingham.	20
Figure 2 – Rendering of the LHTES prototype revealing its external structure and the internal arrangement of its principal components.....	22
Figure 3 – Photograph of the thermally insulated tank and lid, the drain valve with washer, the bundle of pillow plates with the spacers, the PCM, and the thermocouples with the dedicated wire and compression fittings.	25
Figure 4 – Photographs of the thermally insulated tank: (left) isometric view and (right) side view. .	25
Figure 5 – Photographs of the thermal insulation, aluminium cladding, and heat-resistant silicone of the tank: (left) isometric view and (right) close-up of the side walls.	26
Figure 6 – Photographs of the tank: (left) top view of the lid mounted on the tank and (right) closed configuration of the two finger plates.	27
Figure 7 – Side view photograph of the pillow plate bundle, showing the plates, pipes, manifolds, brackets, and stands, with the test rig in the background.....	27
Figure 8 – Photographs of the pillow plate bundle depicting the plates, pipes, manifolds, brackets, and stands: (left) close-up of the pipes and manifold and (right) front view of the region close to the pipes.	28
Figure 9 – Photographs of the sacks containing the phase change material RT80HC: (left) side view and (right) top view.....	29
Figure 10 – Photographs of the tank containing the phase change material RT80HC and the pillow plate bundle: (left) side view and (right) close-up of the pipes, manifold, and storage medium.	29
Figure 11 – Top view photograph of the eight thermocouples with sockets, the insulated thermocouple cable, and the miniature thermocouple plugs utilised for the commissioning tests....	30
Figure 12 – Time series of (a) the liquid mass fraction and (b) the average static temperature of RT80HC determined with the analytical model for different water mass flow rates.....	34
Figure 13 – Time series of (a) the outlet temperature of the water and (b) its average static temperature determined with the analytical model for different water mass flow rates.....	35
Figure 14 – Time series of (a) the liquid mass fraction and (b) the average static temperature of RT80HC determined with the CFD model for different water mass flow rates.....	35

D 5.5 | Technology benchmark and competitor analysis of ZHENIT
WH2X systems

Figure 15 – Time series of (a) the outlet temperature of the water and (b) its average static temperature determined with the CFD model for different water mass flow rates. 36

Figure 16 – Time series of the average static temperature of RT80HC measured during the experiments performed with water volume flow rates of (a) 2 m³/h and (b) 3 m³/h imposed at the inlet. 37

Figure 17 – Piping and instrumentation diagram of the ORC–ejector integrated heat pump prototype developed by the National Technical University of Athens. 53

Figure 18 – Photograph of the ORC–ejector integrated heat pump prototype installed at the National Technical University of Athens. 56

Figure 19 – Photograph of the working fluid pump and motor installed on the ORC–ejector integrated heat pump prototype. 57

Figure 20 – Photograph of the expanders and motors installed on the ORC–ejector integrated heat pump prototype. 58

Figure 21 – Photograph of the compressors installed on the ORC–ejector integrated heat pump prototype. 58

Figure 22 – Rendering of the standard view of the ejector designed for its application in the ORC–ejector integrated heat pump prototype. 59

Figure 23 – Rendering of the sectional view of the ejector designed for its application in the ORC–ejector integrated heat pump prototype. 59

Figure 24 – Photograph of the thermally insulated ejector installed on the ORC–ejector integrated heat pump prototype. 60

Figure 25 – Photograph of the Coriolis flow meters installed on the ORC–ejector integrated heat pump prototype. 61

Figure 26 – Simplified piping and instrumentation diagram of the isobaric expansion engine prototype. 75

Figure 27 – Isometric view of the assembly of the expander of the IEE prototype. 76

Figure 28 – Photograph of a low-pressure check valve VYC 179 installed in the IEE prototype. 77

Figure 29 – Photograph of the high-pressure accumulator H4000R utilised in the IEE prototype. 78

Figure 30 – Photograph of the hydro-pneumatic converter CCT63-100 included in the IEE prototype. 78

D 5.5 | Technology benchmark and competitor analysis of ZHENIT
WH2X systems

Figure 31 – Photograph of the gearwheel volume sensor Profimess VM-01.2.1 used in the IEE prototype. 79

Figure 32 – Schematic of the structure of the IEE prototype with indication of the frame dimensions. 79

Figure 33 – Hydraulic power output and thermal efficiency as functions of the oil pressure difference at various temperatures of the cold side, for a fixed temperature of 90°C on the hot side. 83

Figure 34 – Hydraulic power output and thermal efficiency as functions of the oil pressure difference at various temperatures of the cold side, for a fixed temperature of 80°C on the hot side. 83

Figure 35 – Photograph of the fishing vessel Teseo I of Tringali S.r.l. selected for the installation and testing of the sorption desalination and cooling prototype. 91

Figure 36 – Side view of the rendering of one SDC prototype illustrating the external dimensions and the internal arrangement of the principal components. 92

Figure 37 – Top view of the rendering of one SDC prototype illustrating the external dimensions and the internal arrangement of the principal components. 92

List of Tables

Table 1 – Bill of materials of the LHTES prototype designed and assembled by The University of Birmingham. 23

Table 2 – Main materials constituting the LHTES prototype with their Chemical Abstracts Service numbers, and the hazard number of the selected phase change material. 32

Table 3 – Inlet water conditions considered for the design of the LHTES prototype with the analytical and CFD models and applied in the experiments performed at the laboratory of Tecnalìa. 34

Table 4 – Key performance indicators of the LHTES prototype determined with the analytical and CFD models. 37

Table 5 – List of component and subassembly costs, packaging, shipping, and customs expenses, and total costs inclusive of value-added tax for the LHTES prototype. 38

Table 6 – Properties of materials commonly used in sensible heat thermal energy storage systems [32]. 40

Table 7 – Properties of phase change materials typically utilised for waste heat recovery in internal combustion engines [38]. 41

Table 8 – Properties of materials commonly used in thermochemical storage systems [40]. 41

D 5.5 | Technology benchmark and competitor analysis of ZHENIT
WH2X systems

Table 9 – Thermal energy storage typologies and media suited for on-board applications.	43
Table 10 – Design assumptions applied for the electricity production and CHP modes of the ORC prototype.	65
Table 11 – Results obtained for the electricity-only mode and the combined heat and power mode of the ORC prototype.	65
Table 12 – Design assumptions applied for the parallel ORC–EVCC configuration of the ORC prototype.	66
Table 13 – Results of the ORC–EVCC combined cooling and power production modes of the ORC prototype.	68
Table 14 – Configuration, temperature levels, and performance of organic Rankine cycle systems for marine applications [7].	70
Table 15 – Technical specifications of the heat exchangers installed in the IEE prototype.	76
Table 16 – Operating conditions of the isobaric expansion engine applied at the laboratory of Tecnalia during experimental testing.....	82
Table 17 – List of the most relevant components and the related costs for the IEE prototype.....	84
Table 18 – Operating conditions and performance of isobaric expansion engines compared to a thermal power pump [7].....	85
Table 19 – Bill of materials of the two developed sorption desalination and cooling prototypes.....	90
Table 20 – Prototype characteristics, test conditions, and operating environments for the SDC prototypes installed at the laboratory of Tecnalia and on board the ship Teseo I of Tringali S.r.l. for testing.....	91
Table 21 – Principal dimensions, footprint, and total mass of one sorption desalination and cooling prototype.	92
Table 22 – Operating conditions of the sorption desalination and cooling prototype imposed during the experiments.	96
Table 23 – Key performance indicators, target values, and verification methods for the SDC prototype.	96
Table 24 – Working pairs, temperature levels, and performance of absorption refrigeration systems considered for integration on board ships [7].	98
Table 25 – Model, cooling power, specific cost, and advancement level of three reference adsorption chillers [7].....	100

Table 26 – Temperature levels, cooling power, coefficient of performance, and specific cost of reference hybrid refrigeration systems for maritime applications [7]. 101

Abbreviations and acronyms

Acronym	Description
CAD	Computer-aided design
CAS	Chemical Abstracts Service
CFD	Computational fluid dynamics
CHP	Combined heat and power
CNR	<i>Consiglio Nazionale delle Ricerche</i>
COP	Coefficient of performance
ECC	Ejector cooling cycle
EVCC	Ejector–vapour compression cooling
EXVCC	Ejector-expansion vapour compression cycle
HTF	Heat transfer fluid
IEE	Isobaric expansion engine
IMO	<i>International Maritime Organization</i>
ITAE	<i>Institute of Advanced Technologies for Energy</i>
LHTES	Latent heat thermal energy storage
NTUA	<i>National Technical University of Athens</i>
ORC	Organic Rankine cycle
PCM	Phase change material
SDC	Sorption desalination and cooling
SHTES	Sensible heat thermal energy storage
SorTech	<i>Sorption Technologies GmbH</i>
TCS	Thermochemical storage
TES	Thermal energy storage
TRL	Technology readiness level
UoB	<i>The University of Birmingham</i>
VCC	Vapour compression cooling
WHR	Waste heat recovery

1 Executive summary

The ZHENIT project aims to identify, develop, and assess potential solutions for waste heat recovery on board maritime vessels. Specifically, Work Package 5 regards the implementation of the innovative technologies conceived within the project and their evaluation and impact assessment towards replication and on-board integration. As outlined in the work plan for Task 5.3, this report characterises the four realised prototypes and provides the technology benchmark and competitor analysis for each of them, establishing their principal achievements and positioning within the current state of the art.

The deliverable consists of seven sections: the *Executive summary*, the *Introduction*, the *Latent heat thermal energy storage prototype*, the *Organic Rankine cycle prototype*, the *Isobaric expansion engine prototype*, the *Sorption desalination and cooling prototype*, and the *Conclusions*.

The *Introduction* outlines the background to energy availability and management on board various types of vessels and defines the main waste heat sources associated with maritime energy systems. The most important traditional and novel systems for the effective use of waste heat are discussed, and the advantages of their integration within ship energy systems are presented. The rationale and objectives of the research are defined, together with the hypotheses applied and their influence on results.

The following four sections present the innovative technologies realised within the project according to a consistent assessment framework. For each prototype, the report describes the operating principle, components, design choices, novel features, technology readiness level, operating conditions, and performance. The relevant modelling results, experimental data, cost information, and benchmark comparisons are included to define the technical achievements of the systems and to assess their potential relevance for future maritime waste heat recovery applications.

The section titled *Latent heat thermal energy storage prototype* presents the device developed by *The University of Birmingham (UoB)* for the recovery, storage, and subsequent release of waste heat at low and medium temperature levels. The latent heat thermal energy storage (LHTES) prototype integrates a phase change material (PCM) with a heat exchanger comprising ten pillow plates, in which water circulates as the heat transfer fluid (HTF) of the system. The selected configuration was obtained through a systematic design process combining one-dimensional analytical modelling and three-dimensional computational fluid dynamics simulations. The final prototype includes 367 kg of RT80HC and has a mass of approximately 710 kg in total. Under representative charging and discharging

D 5.5 | Technology benchmark and competitor analysis of ZHENIT WH2X systems

conditions, with inlet water temperatures of 90°C and 70°C, respectively, the system achieves an energy storage capacity of 26.51 kWh, an energy storage density of 54.76 kWh/m³, and a thermal power between 2.54 kW and 3.17 kW for mass flow rates between 0.2 kg/s and 1.2 kg/s of water. The prototype was experimentally tested in laboratory conditions resembling the hot water demand typically present on board vessels, validating its successful functioning. The device has reached a technology readiness level (TRL) equal to 4, and further experimental validation in more representative operating environments would support its progression towards TRL 5 in the future.

The section named *Organic Rankine cycle prototype* describes the integrated system developed by the *National Technical University of Athens (NTUA)* for the conversion of waste heat into electricity, heating, and cooling. The prototype is designed to operate with hot water from waste heat at 140°C and with 100 kW_{th} of thermal input. Four operating modes are considered, comprising the delivery of electricity only through a recuperative organic Rankine cycle (ORC), combined heat and power provision through an ORC without recuperation, combined cooling and electrical power supply with ORC–ejector–vapour compression cooling (EVCC) functioning, and operation dedicated exclusively to cooling through the heat pump integrated with the ejector. At the design point, the system provides a net electrical output of 10.30 kW_e in the mode for electricity supply and 7.68 kW_e in combined heat and power mode, with heating output of 88.97 kW_{th} as the corresponding value. The device provides cooling outputs in the range from 2 kW_c to 3 kW_c in the cooling modes. The developed ORC–EVCC prototype extends the conventional role of ORC systems from electricity production alone to multifunctional energy conversion, including electricity, heat, and cooling. The proposed configuration has a TRL between 3 and 4 and requires further investigations to improve its maturity.

The section entitled *Isobaric expansion engine prototype* reports on the technology developed by *Tecnalia* for the conversion of heat at low temperature values into useful mechanical output for maritime waste heat recovery. The device operates according to the principle of isobaric expansion, in which a working fluid with a low boiling point is evaporated by a heat source and expanded at approximately constant pressure to provide linear reciprocating work. This mechanical work is converted into hydraulic power through the expander system. The isobaric expansion engine (IEE) prototype uses R134a as the working fluid and is specifically oriented towards heat sources below 100°C, with particular relevance for low-grade thermal streams that are difficult to exploit through conventional power conversion systems. Experimental tests were conducted with temperatures of 80°C and 90°C on the hot side, temperatures between 14°C and 35°C on the cold side, and different levels of

D 5.5 | Technology benchmark and competitor analysis of ZHENIT WH2X systems

hydraulic resistance. The achieved hydraulic power output ranges between 200 W and 500 W, while the corresponding efficiency is between 2% and 5% over the investigated operating conditions. The technology readiness level is assessed as 4, since the integrated system has been designed, manufactured, and experimentally validated in a laboratory environment.

The section identified as *Sorption desalination and cooling prototype* presents the system developed by the *Institute of Advanced Technologies for Energy (ITAE)* of the *Consiglio Nazionale delle Ricerche (CNR)* and by *Sorption Technologies GmbH (SorTech)* for the simultaneous production of desalinated water and chilled water by recovering waste heat at low and medium temperature levels. Two physical prototypes were designed and fabricated within the project, one for controlled testing at the laboratory of *Tecnalia* and the other for testing on board the vessel *Teseo I* of *Tringali S.r.l.* under real navigation conditions. The system operates according to a closed adsorption cycle using water as the refrigerant and an advanced solid sorbent as the adsorbent. The sorption desalination and cooling (SDC) prototype has a nominal cooling capacity of 10 kW_{th,cold} and is conceived for waste heat driving temperatures between 60°C and 100°C, with 80°C defined as the design point. The target thermal coefficient of performance for the cooling mode is between 0.6 and 0.7, while the expected improvement in specific daily water production is at least 30% with respect to silica gel. The technology progressed from TRL 3 before the project to TRL 4 by means of integrated laboratory testing, while the on-board installation supports the progression towards TRL 5 through the ongoing experimental campaign.

The section dedicated to the *Conclusions* summarises the main results achieved with the four innovative prototypes and the outcomes of the technology benchmark and competitor analysis. The results confirm that the developed systems address complementary functions within a broader maritime waste heat recovery framework, including thermal energy storage, conversion of waste heat into electricity, heating and cooling, provision of mechanical or hydraulic output from waste heat, and simultaneous generation of chilled water and desalinated freshwater. Furthermore, the implementation of these emerging technologies into an integrated waste heat recovery system could significantly increase energy efficiency and reduce fuel consumption by recovering heat from exhaust gases, scavenge air, jacket water, and lubricating oil. The analysis also indicates that the prototypes occupy distinct technological positions with respect to existing solutions, either by adapting emerging technologies to maritime operating conditions or by extending the functionality of established concepts towards integrated and multifunctional energy systems. At the same time, the conclusions identify the main remaining challenges, which are primarily associated with further experimental validation, performance

D 5.5 | Technology benchmark and competitor analysis of ZHENIT WH2X systems

optimisation, system integration, and progression towards higher technology readiness levels in environments more representative of real vessel operation.

2 Introduction

Maritime transport plays a fundamental role in the global economy and remains indispensable for international trade and tourism. At the same time, its environmental impact has become an increasingly important concern, particularly in view of the need to reduce fuel consumption and greenhouse gas emissions. Indeed, the sector is responsible for a relevant share of global emissions, accounting for 2.9% of total global greenhouse gas emissions [1]. In the absence of effective mitigation measures, these emissions are expected to rise significantly by the middle of the current century [2]. This situation has led to progressively stricter regulatory targets. In particular, the *International Maritime Organization (IMO)* has introduced measures aimed at improving energy efficiency and reducing carbon intensity, with the objective of achieving net-zero greenhouse gas emissions within this timeframe [3]. In this context, technological innovation is essential to support the decarbonisation of shipping and to improve the overall sustainability of vessel energy systems.

Current efforts to enhance the environmental performance of ships focus on several complementary directions. These include the optimisation of propulsion systems, the adoption of cleaner fuels, the integration of renewable energy sources, and the deployment of advanced waste heat recovery technologies [4, 5]. The maritime sector still relies predominantly on Diesel engines to power vessels, with more than half of the fuel energy commonly dissipated as waste heat during operation [6]. At the same time, the need to reduce greenhouse gas emissions has intensified the transition towards alternative fuels such as liquefied natural gas, methanol, hydrogen, ammonia, and biofuels [5, 7, 8], together with the investigation of propulsion technologies based on wind [7, 9, 10]. In parallel, the use of photovoltaic systems, hybrid solutions, and advanced strategies of energy management can contribute to reducing the load on auxiliary engines and, consequently, the overall fuel demand [11, 12]. Since a relevant fraction of the fuel input is still dissipated as thermal energy, waste heat recovery remains one of the most direct and promising ways of increasing efficiency and lowering emissions [5].

The relevance of waste heat recovery in maritime transport is directly connected to the limited thermal efficiency of marine engines. In large two-stroke Diesel engines, which dominate the propulsion of civilian ships above 100 tons, around 50% of the fuel input may be rejected as heat through exhaust

D 5.5 | Technology benchmark and competitor analysis of ZHENIT WH2X systems

gases and cooling streams [5]. Although several waste heat sources are available within on-board energy systems, the most relevant are generally associated with the propulsion and auxiliary systems. Exhaust gases from main and auxiliary engines usually represent the largest recoverable source, accounting for approximately between 15% and 28% of the fuel energy, with temperatures in the range from about 190°C to 370°C under representative operating conditions. Another important source is scavenge air, which also offers significant potential for heat recovery and may contribute between 11% and 16% of the fuel energy, at temperatures between 85°C and 210°C as a typical interval. Lower-temperature sources are represented by lubricating oil and jacket water. Lubricating oil may account for between 5% and 8% of the fuel energy, usually at temperatures between 60°C and 90°C, whereas jacket water typically contributes between 3% and 6%, with temperatures ranging from 33°C to 93°C in general [13, 14]. These differences in thermal level and recoverable energy content strongly affect the suitability of the different waste heat recovery technologies and make integrated solutions particularly attractive.

Available estimates indicate that, through more effective recovery and utilisation of the thermal energy available on board ships, total engine efficiency could potentially rise from approximately 50% to 60%, while fuel savings in the range of 4% to 16% may be attainable [5]. More generally, the literature reports that waste heat recovery can reduce fuel consumption by an amount between 3% and 15% for typical ship configurations [15]. Some technologies, such as waste heat boilers and turbocharging systems, are already well established in marine applications. However, a broader set of solutions originally developed for terrestrial use has recently attracted increasing attention because of their potential to further improve vessel energy performance, especially in relation to heat sources at low and medium temperatures [5, 16]. The main challenges to overcome are maximising the use of recoverable thermal energy, especially at low and intermediate temperatures, and mitigating the discontinuous nature of waste heat availability [5, 16]. In this framework, innovative technologies such as thermal energy storage systems, organic Rankine cycles, isobaric expansion engines, and sorption desalination and cooling systems have the potential to recover waste heat and contribute to satisfying on-board energy demand. The implementation of an integrated waste heat recovery (WHR) system incorporating these emerging technologies could increase energy efficiency by 7.5% and reduce fuel consumption by 13% through the recovery of heat from exhaust gases, scavenge air, jacket water, and lubricating oil [17].

The availability of waste thermal energy and the related quantity and quality depend on the typology of the ship and its operation along the route. Cargo vessels, such as container ships and bulk carriers, are generally equipped with large main engines that release substantial quantities of waste thermal energy

D 5.5 | Technology benchmark and competitor analysis of ZHENIT WH2X systems

through the exhaust gases. The high temperature of these gases provides waste heat of high thermal quality, while the elevated propulsion power required by these vessels, particularly in the case of large container ships, results in a significant overall amount of recoverable heat. The availability of this waste heat is usually relatively stable during long sea voyages, although it may become intermittent during loading and unloading operations in port [5].

Passenger vessels, encompassing cruise ships and ferries, tend to incorporate elaborate energy systems comprising multiple engines and boilers, which together yield a broad spectrum of thermal energy at high, medium, and low temperature levels. Beyond propulsion, a significant part of the waste heat originates from the auxiliary infrastructure required to sustain on-board living standards, covering heating, cooling, and cooking functions. This dual dependency on propulsion systems and accommodation services favours a relatively continuous availability of thermal energy, regardless of whether the vessel is navigating or in port [5, 15].

The thermal energy profile of fishing vessels differs markedly from that of larger ships. Relatively modest engine sizes, combined with the auxiliary machinery deployed for on-board catch handling, tend to reduce both the temperature and the overall amount of recoverable heat. Nonetheless, during periods of active fishing, the rejected thermal energy is not negligible. The availability of waste heat can be highly variable, depending on fishing activities and periods of idling or low-speed cruising [5].

Naval vessels have advanced propulsion and power generation systems, which often release high-quality thermal energy. These vessels generally provide large amounts of waste heat owing to the relevant power demands for propelling them and supplying their auxiliary systems. The availability of waste heat significantly depends on the specific mission, with peaks during high-speed manoeuvres and lower availability during patrol or standby periods [5].

The nature of the voyage also significantly affects waste heat characteristics. Long-distance voyages tend to provide high-quality waste heat due to the continuous operation of main engines at high loads, resulting in large quantities of thermal power over extended periods. The availability of waste heat during such voyages is consistent, making them ideal for integration with WHR systems. Conversely, short-distance and coastal voyages have mixed waste heat quality due to frequent engine start-stop cycles and varying loads. Consequently, these journeys provide lower quantities of waste heat, with intermittent availability that necessitates systems capable of handling variable input. Operations involving variable speed profiles supply variable quality waste heat due to changing engine loads,

resulting in fluctuating quantities of waste heat. The availability of waste heat in these scenarios is highly variable, necessitating robust waste heat recovery and storage solutions.

3 Latent heat thermal energy storage prototype

Latent heat thermal energy storage systems represent one of the most promising solutions for the accumulation of excess thermal energy when heat availability is high and for its subsequent delivery when demand increases across a broad range of technical applications. This capability is provided by the use of phase change materials, which are subject to phase transformations while absorbing or releasing substantial quantities of latent heat at an almost constant temperature. In most cases, the transition takes place between the solid and liquid phases, although transformations from solid to solid may also be exploited. The energy stored is mainly determined by the latent heat of fusion of the phase change material and by the sensible heat contribution due to the temperature difference between the heat transfer fluid and the melting point of the storage material [18]. Thus, these systems can convert and valorise waste heat, while mitigating the fluctuations in the thermal energy availability in energy systems, thereby improving energy efficiency and reducing the use of fossil fuels [19].

3.1 Configuration of the LHTES prototype

The latent heat thermal energy storage prototype developed by *The University of Birmingham* is shown in Figure 1. The device comprises a tank closed by a removable lid, within which ten pillow plates are arranged vertically and installed in parallel along their minor axis. The plates are connected to three base stands that provide vertical support and to four structural brackets, one located on each side and two at the top of the plate assembly, which enhance the mechanical stability of the structure. Four spacers are mounted on the upper brackets to prevent horizontal displacement of the plate bundle. All plates are connected through dedicated piping to the inlet and outlet manifolds, which are in turn linked to the main inlet and outlet pipes. The manifolds function as distribution chambers, promoting uniform flow conditions for the heat transfer fluid. These components are welded into an integrated structure, referred to as the pillow plate bundle. The space surrounding the plates is filled with a phase change material as the thermal energy storage medium. The tank and lid are thermally insulated to minimise heat losses to the environment. The lid is equipped with fifteen thermocouples, vertically adjustable to measure the temperature distribution within the storage material. The tank includes a pipe located at the bottom of one side wall, which is normally sealed with a drain cap. This connection allows the

D 5.5 | Technology benchmark and competitor analysis of ZHENIT WH2X systems

removal of the storage material by replacing the cap with a drain valve and melting the PCM to facilitate its extraction from the tank. Moreover, the tank base has two forklift openings to enable the safe movement of the device [19].



Figure 1 – Photograph of the latent heat thermal energy storage prototype developed by *The University of Birmingham*.

The tank walls are made of stainless steel grade 1.4301 and have a thickness of 3 mm, while the removable lid has a thickness of 2 mm to withstand the expected mechanical loads. The insulation consists of a layer of 50 mm of fibreglass enclosed within aluminium cladding with a thickness of 0.9 mm, which together provide thermal protection and mechanical shielding [19].

The heat exchanger comprises pillow plates formed by two stainless steel sheets of uniform thickness, joined by linear and spot welds and expanded to create internal flow channels [20]. This produces a corrugated geometry that increases stiffness and heat transfer area, while the weld spots maintain sheet separation and induce local turbulence in the heat transfer fluid. The internal weld pattern defines the flow passages, thereby controlling fluid distribution within the plates [21]. In the present design, the fluid follows a serpentine path that directs it first toward the lower region and then through successive horizontal passes upward along the plate. This configuration enhances temperature uniformity within the phase change material while limiting pressure losses in the hydraulic circuit.

3.2 Geometry of the LHTES prototype

The geometry of the LHTES prototype is primarily defined by the configuration and dimensions of the pillow plates and by the placement of the plate bundle within the tank. The pillow plates have a welding spot diameter of 6 mm, a longitudinal pitch of 33.5 mm, a transverse pitch of 67 mm, a maximum inner channel height of 8 mm, a maximum plate distance of 48 mm, and a metal sheet thickness of 1 mm per layer. The minimum spacing between adjacent plates was selected as 40 mm, corresponding to the minimum separation achievable using standard manufacturing practices for pillow plates with rigid manifolds and piping. Subsequently, the distance between the pillow plate bundle and the inner surfaces of the tank side walls was set to 40 mm to achieve geometric consistency with the spacing between adjacent plates. This clearance ensures the symmetric positioning of the bundle within the tank and a uniform distribution of the PCM around the surfaces of the heat exchanger. The height of the three supporting stands was set at 30 mm based on standard dimensions. This parameter defines the vertical spacing between the lower edges of the plates and the inner surface of the tank base, ensuring sufficient PCM volume beneath the plate bundle while preventing direct contact between the heat exchanger structure and the tank base [19].

After establishing the aforementioned geometric parameters, the plate length L , plate height H , and the number of plates N were determined through a parametric analysis conducted with the one-dimensional analytical model developed. The model and the analysis are described in detail in Deliverable 3.3 of the ZHENIT project, while in this document, the main achievements are summarised. The length, height, and number of plates determine the volume of phase change material contained in the tank and the total heat transfer surface available, and therefore directly influence the storage capacity, energy density, and overall dimensions of the prototype. The analysis aimed to identify configurations achieving the design targets of a storage capacity exceeding 25 kWh and an energy storage density greater than 50 kWh/m³, while limiting the mass to approximately 700 kg in total. Three values of plate number equal to 8, 10, and 12 were considered, and the plate length and height were examined within the interval from 0.50 m to 1.50 m, while all the other geometric quantities were maintained constant. The configuration with ten plates, a plate length of 1.00 m, and a plate height of 0.80 m, with a corresponding plate bundle width of 0.46 m, was selected because it provides the most suitable compromise between energy storage capacity and density, mass, and expected thermal response. The larger dimension was assigned to the plate length, whereas the smaller was assigned to

D 5.5 | Technology benchmark and competitor analysis of ZHENIT WH2X systems

the height to limit the structural load transmitted per unit area of the supporting surface, in accordance with the installation constraints at the laboratory of *Tecnalia*, where the prototype was tested [19].

The rendering of the latent heat thermal energy storage system developed in this research is presented in Figure 2, which illustrates its overall structure and the arrangement of its principal components.

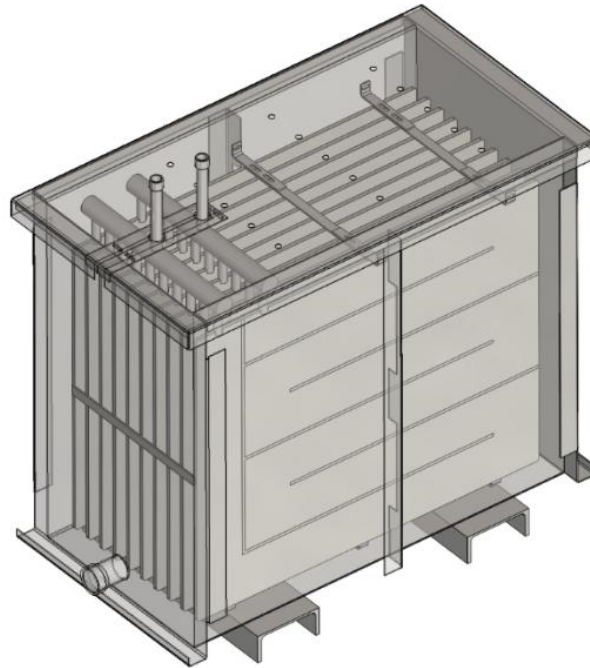


Figure 2 – Rendering of the LHTES prototype revealing its external structure and the internal arrangement of its principal components.

3.3 Working principle of the LHTES prototype

The functioning of the LHTES system is based on the interaction between a heat exchanger formed by pillow plates and a phase change material acting as the storage medium. The heat transfer fluid enters the device through the inlet pipe of the heat exchanger, then passes through the pillow plates and exits from the outlet pipe, while exchanging thermal energy with the phase change material, either releasing or absorbing heat depending on the operating phase. During the charging period, the HTF flows through the system at a temperature higher than the melting point of the PCM, which therefore absorbs thermal energy and undergoes melting. In this manner, the heat transfer fluid behaves as a heat source, and the PCM as a heat sink. Conversely, during the discharging phase, the HTF temperature is lower than that of the PCM, which releases the stored heat to the heat transfer fluid and solidifies [18].

D 5.5 | Technology benchmark and competitor analysis of ZHENIT WH2X systems

The design of heat exchangers based on pillow plates blends scalability, strength, and simplicity. This favours their applicability to various energy systems. In applications characterised by repeated charging and discharging processes, pillow plates also provide adequate durability, resistance to thermal cycling, and favourable heat transfer performance. This technology has been selected for its fundamental fluid-dynamic and thermodynamic characteristics, and for its reliable design and proven operation in different industrial applications. In the specific case of thermal energy storage, pillow plates offer advantages in terms of heat transfer, mechanical robustness, and geometric flexibility. Their modular and scalable nature allows the adaptation of both dimensions and the number of layers, which makes them suitable for systems ranging from the small scale to the large scale. All these features make them particularly attractive for thermal energy storage systems based on phase change materials for applications on board maritime vessels [19].

3.4 Principal components of the LHTES prototype

The bill of materials of the prototype designed and assembled by *The University of Birmingham* is reported in Table 1. An extended description of the components and materials of the device is provided in Deliverable 3.3, while this document summarises the main features of the principal components.

Table 1 – Bill of materials of the LHTES prototype designed and assembled by *The University of Birmingham*.

Component	Quantity, -	Material, -
Tank	1	Stainless steel 1.4301
Drain cap	1	Stainless steel 1.4301
Lid	1	Stainless steel 1.4301
Finger plates	2	Stainless steel 1.4301
Finger plate screws	4	Stainless steel 1.4301
Thermal insulation	1	Fibreglass
Cladding	1	Aluminium
Silicone	1	Polysiloxane
Rivets	77	Stainless steel 1.4301
Pillow plates	10	Stainless steel 1.4301
Manifolds	2	Stainless steel 1.4301
Long pipes	2	Stainless steel 1.4301

D 5.5 | Technology benchmark and competitor analysis of ZHENIT WH2X systems

Short pipes	20	Stainless steel 1.4301
Stands	3	Stainless steel 1.4301
Brackets	4	Stainless steel 1.4301
Spacers	4	Stainless steel 1.4301
Spacer bolts	8	Zinc plated steel
Spacer washers	8	Zinc plated steel
Spacer nuts	8	Zinc plated steel
PCM	1	RT80HC
HTF	1	Tap water
Thermocouples	15	Alloy 600, chromel, alumel, and graphene sheets-filled thermoplastic
Thermocouple sockets	15	Chromel, alumel, and graphene sheets-filled thermoplastic
Thermocouple cable	1	Chromel, alumel, and heat-resistant polyvinyl chloride
Thermocouple plugs	15	Chromel, alumel, and graphene sheets-filled thermoplastic
Compression fitting bodies	15	Brass
Compression fitting ferrules	15	Brass
Compression fitting nuts	15	Brass
Compression fitting body locknuts	15	Brass

The LHTES prototype can be equipped with a drain valve made of stainless steel 1.4301 after removing the drain cap to facilitate draining the PCM from the tank when necessary. The drain cap can be unscrewed and replaced with the drain valve while the PCM is in the solid phase. Once the PCM has fully melted, it can be drained by opening the valve [19].

The main components of the prototype and the drain valve are shown in Figure 3, including the tank and lid with thermal insulation and external cladding, the pillow plate bundle with spacers, the phase change material, the thermocouples and wiring, and the compression fittings used for their installation.

D 5.5 | Technology benchmark and competitor analysis of ZHENIT
WH2X systems



Figure 3 – Photograph of the thermally insulated tank and lid, the drain valve with washer, the bundle of pillow plates with the spacers, the PCM, and the thermocouples with the dedicated wire and compression fittings.

3.4.1 Tank and lid

The tank designed to contain both the pillow plate bundle and the PCM is illustrated in Figure 4, where the forklift openings and the drain pipe fitted with its cap can be identified in the lower part. The tank, lid, and associated components were supplied by *KGD Enterprises Ltd* based on the design provided by *The University of Birmingham* for the specific device [19]. Stainless steel 1.4301 was utilised to fabricate the tank, drain cap, lid, and finger plates, together with their bolts, nuts, and rivets.



Figure 4 – Photographs of the thermally insulated tank: (left) isometric view and (right) side view.

D 5.5 | Technology benchmark and competitor analysis of ZHENIT WH2X systems

The thermal insulation made of fibreglass, the external cladding made of aluminium, and the heat-resistant polysiloxane silicone, utilised to minimise the heat losses from the tank, are depicted in Figure 5. The images also reveal the inner part of the tank, including its internal and external side walls, as well as the drain opening, its pipe, and its cap.



Figure 5 – Photographs of the thermal insulation, aluminium cladding, and heat-resistant silicone of the tank: (left) isometric view and (right) close-up of the side walls.

The top view of the lid covering the tank is provided in Figure 6, where the two finger plates can be observed together with the openings intended for the inlet and outlet pipes of the pillow plate bundle and the fifteen holes designed to accommodate the compression fittings. Moreover, the lid includes four handholds to facilitate its handling. The finger plates allow the tank to be covered and uncovered by the lid while avoiding the disconnection of the inlet and outlet pipes of the pillow plate bundle.

D 5.5 | Technology benchmark and competitor analysis of ZHENIT
WH2X systems

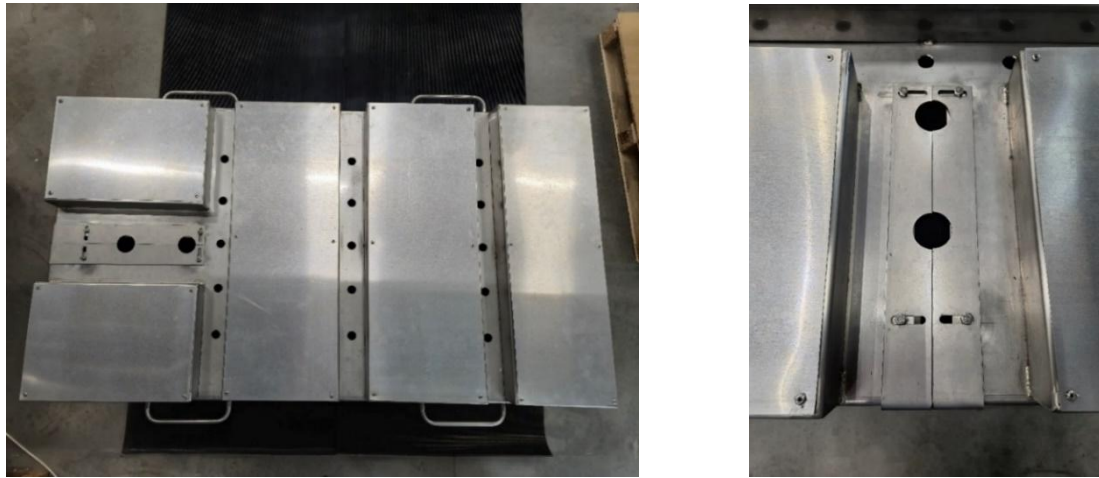


Figure 6 – Photographs of the tank: (left) top view of the lid mounted on the tank and (right) closed configuration of the two finger plates.

3.4.2 Pillow plates

The pillow plates and the related bundle configuration in Figure 7 were designed by *The University of Birmingham* based on the simulations performed with the analytical and computational fluid dynamics models developed [19].

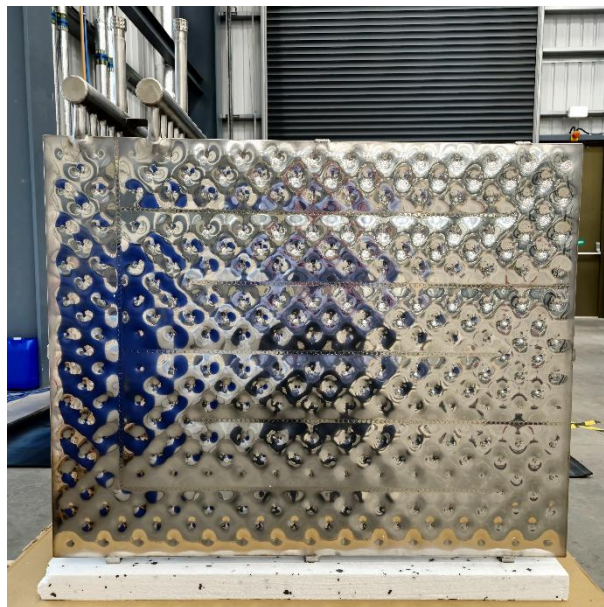


Figure 7 – Side view photograph of the pillow plate bundle, showing the plates, pipes, manifolds, brackets, and stands, with the test rig in the background.

The pillow plate bundle produced by *GMF Equipment Ltd* is illustrated in Figure 8. It comprises pillow plates, manifolds, pipes, stands, and brackets made of stainless steel 1.4301, as well as spacers fastened

D 5.5 | Technology benchmark and competitor analysis of ZHENIT WH2X systems

to the upper brackets. The bolts, washers, and nuts utilised to connect the brackets and spacers are made of steel with a zinc-plated coating to enhance durability and corrosion resistance.

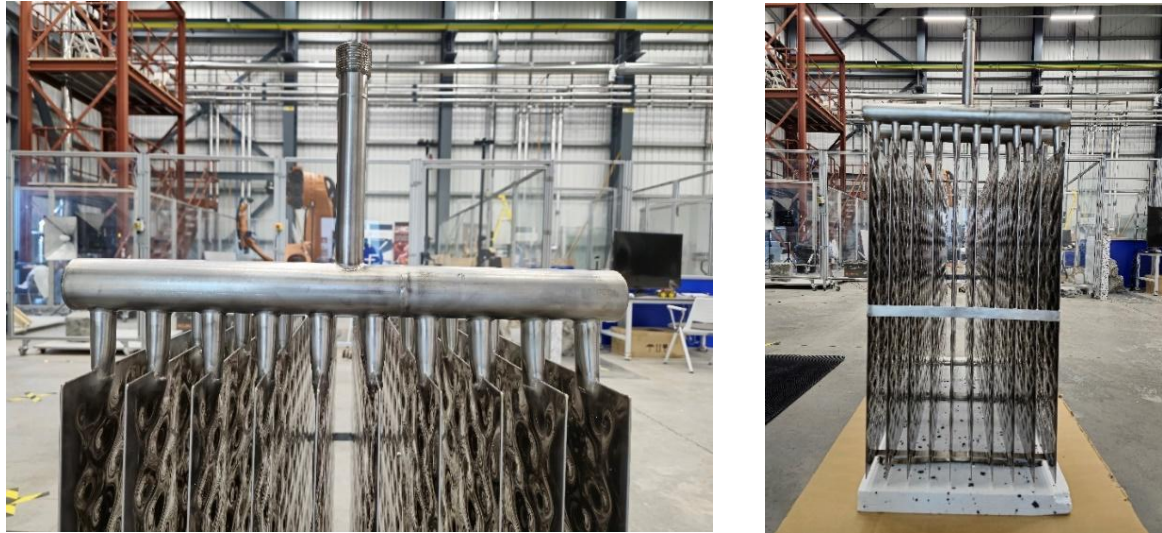


Figure 8 – Photographs of the pillow plate bundle depicting the plates, pipes, manifolds, brackets, and stands: (left) close-up of the pipes and manifold and (right) front view of the region close to the pipes.

The spacers are secured using eight high-tensile M8 bolts with a length of 20 mm, eight M8 flat washers with a diameter of 25 mm, and eight hexagon nuts.

3.4.3 Phase change material

The phase change material RT80HC, shown in Figure 9 and produced by *Rubitherm Technologies GmbH*, was selected to store thermal energy in the developed LHTES prototype [22].

D 5.5 | Technology benchmark and competitor analysis of ZHENIT
WH2X systems



Figure 9 – Photographs of the sacks containing the phase change material RT80HC: (left) side view and (right) top view.

A total mass of 367 kg of RT80HC was inserted into the tank, where it surrounds the bundle of pillow plates [19]. The side view of the tank incorporating the phase change material and the plate bundle, together with the close-up of the pipes, manifold, and PCM, is provided in Figure 10.



Figure 10 – Photographs of the tank containing the phase change material RT80HC and the pillow plate bundle: (left) side view and (right) close-up of the pipes, manifold, and storage medium.

3.4.4 Thermal sensors

The LHTES prototype was equipped with fifteen thermocouples, the corresponding fifteen sockets, insulated cables, and miniature thermocouple plugs, all designed specifically for type K thermocouples.

D 5.5 | Technology benchmark and competitor analysis of ZHENIT WH2X systems

These components were utilised to measure the temperature of the phase change material and the surrounding environment. The set of eight thermocouples with sockets, the insulated thermocouple cable, and the eight miniature thermocouple plugs utilised to prepare the measurement instrumentation for the commissioning tests performed at the *Tyseley Energy Park* of *The University of Birmingham* are shown in Figure 11.

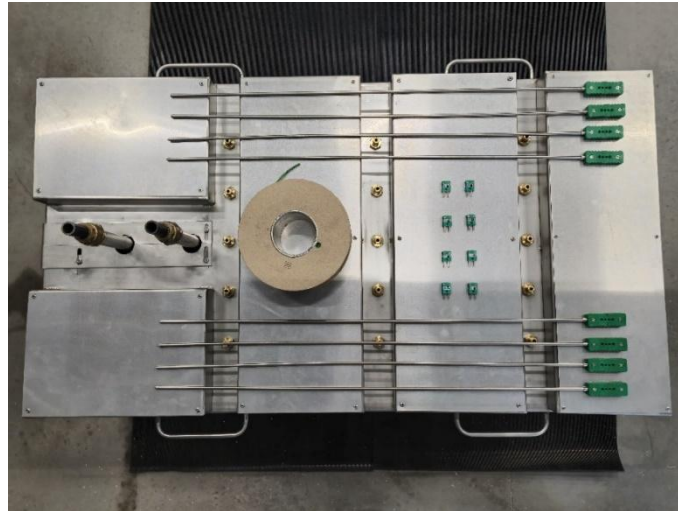


Figure 11 – Top view photograph of the eight thermocouples with sockets, the insulated thermocouple cable, and the miniature thermocouple plugs utilised for the commissioning tests.

In the experiments conducted at the *Thermal Systems and Energy Efficiency Laboratory* of *Tecnalia*, all fifteen thermocouples were utilised to measure the temperature of the phase change material.

Compression fitting glands were selected to hold the thermocouples in a vertical position. Each compression fitting consists of a body with an in-line G3/8" male compression thread, a ferrule, a compression nut, and a locknut for fastening. All these components are made of brass. The miniature thermocouple plugs were supplied by *RS Components Ltd*, while all the other components were provided by *KGD Enterprises Ltd*, based on the specifications defined by *UoB* during prototype design.

3.5 Design choices, novel features, and technology readiness level of the LHTES prototype

The LHTES prototype developed in the present research is the outcome of a systematic design process aimed at identifying the most suitable configuration for the recovery and utilisation of waste heat at low and medium temperatures on board maritime vessels. The selected solution is characterised by specific design choices and innovative characteristics associated with the integration of a pillow-plate heat

D 5.5 | Technology benchmark and competitor analysis of ZHENIT WH2X systems

exchanger with a phase change material. The maturity level of the developed prototype is also assessed, and the actions for its future improvement are outlined.

3.5.1 Main design choices for the LHTES prototype

The main design choices are associated with the identification of the most suitable prototype configuration based on the integration of a pillow-plate heat exchanger with a phase change material as the storage medium and water as the heat transfer fluid for the recovery of otherwise unutilised thermal energy from sources at low and medium temperatures on board ships. The initial design stage consisted of the selection of the most favourable commercial phase change material in accordance with the targets of the project and the operating conditions, which resemble the typical water demand present in these applications [22-26]. The phase change material RT80HC was chosen using the analytical model as it provides the most favourable combination of energy storage capacity and energy storage density for a given PCM mass, along with a balanced charging and discharging response. In this process, the constraints related to the geometry, mass, and operation of the device were taken into account [19]. Subsequently, a parametric investigation was performed with a one-dimensional analytical model to determine the effects of plate length, plate height, and number of plates on the performance of LHTES systems and to identify the configurations providing the most favourable combination of system mass, thermal energy storage capacity, and thermal energy storage density. The results were then utilised to support the selection of the final prototype dimensions. On this basis, the selected configuration consists of a heat exchanger formed by ten pillow plates with a length of 1.00 m and a height of 0.80 m for each of them. The prototype has a total mass of approximately 710 kg and contains 367 kg of RT80HC as the phase change material [19]. The design was then refined through the use of the three-dimensional computational fluid dynamics (CFD) model developed, which enabled a more detailed assessment of the fluid-dynamic and heat transfer phenomena occurring within the system during operation [19, 27]. Following the numerical design phase, the components of the prototype were manufactured, and the system was assembled according to the selected specifications [19]. Finally, the prototype was experimentally tested to assess its operation and verify the correct functioning of the assembled device.

The materials and the operating conditions of the LHTES prototype were chosen to limit the requirements for its safe assembly and functioning in laboratory environments. The list of the principal

D 5.5 | Technology benchmark and competitor analysis of ZHENIT WH2X systems

materials composing the prototype and their Chemical Abstracts Service (CAS) numbers is reported in Table 2, together with the hazard number of the phase change material.

Table 2 – Main materials constituting the LHTES prototype with their Chemical Abstracts Service numbers, and the hazard number of the selected phase change material.

Material	CAS numbers	Hazard number
Steel	12597-69-2	-
RT80HC	61788-66-7	H302, H312, and H332
Tap water	7732-18-5	-

3.5.2 Novel features of the LHTES prototype

The principal innovation of the developed prototype is represented by the integration of pillow plates as the heat exchange structure in a latent heat thermal energy storage device with phase change material for maritime waste heat recovery. This configuration enables a compact storage concept suitable for the operating constraints typically present on board vessels. A further significant aspect is the methodology applied for the development of the system, in which analytical modelling, computational fluid dynamics simulations, and experimental testing were combined to support the identification of the target configuration and to provide an initial verification of the correct functioning of the device under typical maritime conditions [19]. This approach enabled the identification of the most suitable design and operating parameters and improved the understanding of the fluid-dynamic and thermodynamic behaviour of the system. The prototype is a promising and technically relevant solution for utilising waste heat sources at low and medium temperatures, which remain only partially exploited in ship energy systems. Moreover, the device supports a more effective temporal matching between thermal energy availability and on-board demand. The main achievements are presented and discussed in Subsection 3.6 and represent the main advantages provided by the developed technology.

The latent heat thermal energy storage prototype was designed to operate both as a stand-alone device and as an integrated device coupled with the isobaric expansion engine prototype or the sorption desalination and cooling prototype. In this integrated configuration, the LHTES prototype acts as a thermal management system, storing recovered heat when it is available and releasing it when the waste heat source is temporarily unavailable or excessively fluctuating. This function supports stable operation of the coupled technologies by providing the thermal input required to maintain their intended operating conditions.

3.5.3 Technology readiness level of the LHTES prototype

The LHTES prototype has been verified through laboratory analyses under operating conditions intended to replicate the hot water demand generally present on board maritime vessels. The essential technological components have been assembled to demonstrate their effective operation as an integrated unit, resulting in an early representation of the intended full-scale system. Preliminary experimental analyses were performed at the *Tyseley Energy Park of The University of Birmingham*, thereby confirming the correct functioning of the prototype and providing valuable insights into its fluid dynamics and thermodynamics. The results obtained are presented and discussed in detail in Deliverable 3.3 for the various testing configurations and operating conditions investigated. Furthermore, an extensive experimental campaign has been conducted at the *Thermal Systems and Energy Efficiency Laboratory of Tecnia* in order to obtain a more detailed understanding of its fluid-dynamic and thermodynamic behaviour under various operating conditions. The related results are included in Deliverable 4.4 for the extensive set of cases considered.

The current technology readiness level of the LHTES prototype is classified as 4, which is consistent with the target of the project. A further extension of the experimental campaign would support the progression of the prototype towards TRL 5 by expanding its validation to a broader range of operating conditions and to an application context more closely aligned with real on-board operation.

3.6 Operating conditions and performance of the LHTES prototype

The LHTES prototype was developed to operate under the conditions reported in Table 3, which were defined to reproduce the hot water demand typically present on board a vessel. For the analytical and CFD models, the reference operating conditions correspond to water mass flow rates between 0.3 kg/s and 0.9 kg/s in both the charging and discharging phases, with inlet temperatures of 90°C during charging and 70°C during discharging. In addition, an extended range of operating conditions was considered, with mass flow rates between 0.2 kg/s and 1.2 kg/s and inlet temperatures between 90°C and 95°C during charging and between 30°C and 70°C during discharging. For the experimental campaign conducted at the laboratory of *Tecnia*, the prototype was operated with water volume flow rates between 1.0 m³/h and 3.5 m³/h, while the corresponding inlet temperatures were 90°C during charging and 70°C during discharging as principal values, with extended intervals between 90°C and 95°C for charging and between 30°C and 70°C for discharging. The maximum temperature was set to

D 5.5 | Technology benchmark and competitor analysis of ZHENIT
WH2X systems

95°C, which corresponds to the upper limit permitted for the safe operation of the device. The water pressure was kept below a threshold of 2.5 atm during operation [19].

Table 3 – Inlet water conditions considered for the design of the LHTES prototype with the analytical and CFD models and applied in the experiments performed at the laboratory of *Tecnalia*.

Model type	Parameter	Charging phase		Discharging phase	
		Principal values	Extended values	Principal values	Extended values
Analytical and CFD models	Mass flow rate, kg/s	0.3 – 0.9	0.2 – 1.2	0.3 – 0.9	0.2 – 1.2
	Temperature, °C	90	90 – 95	70	30 – 70
Experimental model	Volume flow rate, m ³ /h	1.0 – 3.5	1.0 – 3.5	1.0 – 3.5	1.0 – 3.5
	Temperature, °C	90	90 – 95	70	30 – 70

The results are presented for the final configuration of the latent heat thermal energy storage prototype, which comprises ten pillow plates with a length of 1.00 m and a height of 0.80 m and contains 367 kg of the phase change material RT80HC, for a mass of approximately 710 kg in total [19].

The results reported in this document refer to representative operating conditions and are intended to characterise the main performance characteristics of the developed LHTES prototype. In all these cases, the inlet water temperature was set to 90°C during charging and to 70°C during discharging [19].

The operation of the system is based on the phase transition of the storage material determined by its thermal interaction with the heat transfer fluid. The dynamic behaviour of the liquid mass fraction and the static temperature of the phase change material in the entire domain for various water mass flow rates is shown in Figure 12 for the results of the analytical model [19].

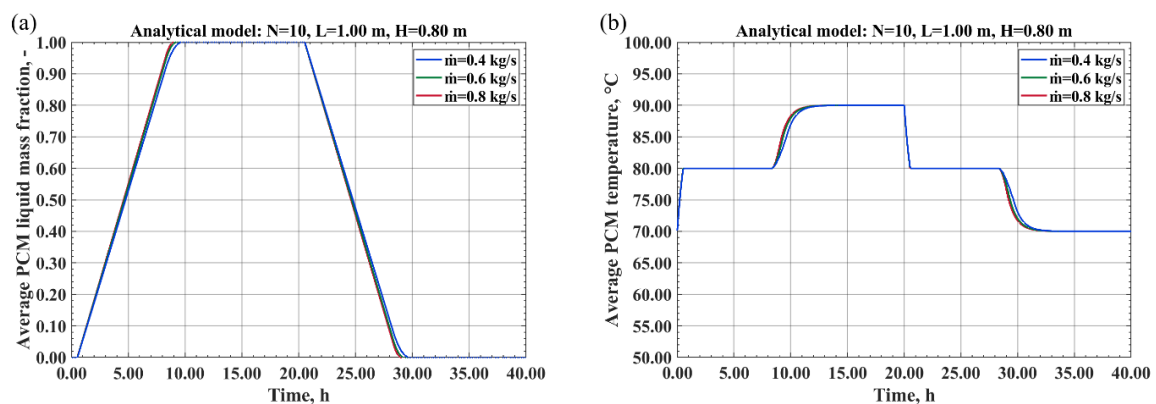


Figure 12 – Time series of (a) the liquid mass fraction and (b) the average static temperature of RT80HC determined with the analytical model for different water mass flow rates.

D 5.5 | Technology benchmark and competitor analysis of ZHENIT
WH2X systems

The time series of the outlet temperature of the water and its average value, calculated with the analytical model, are illustrated in Figure 13, highlighting the effects of the water mass flow rate [19].

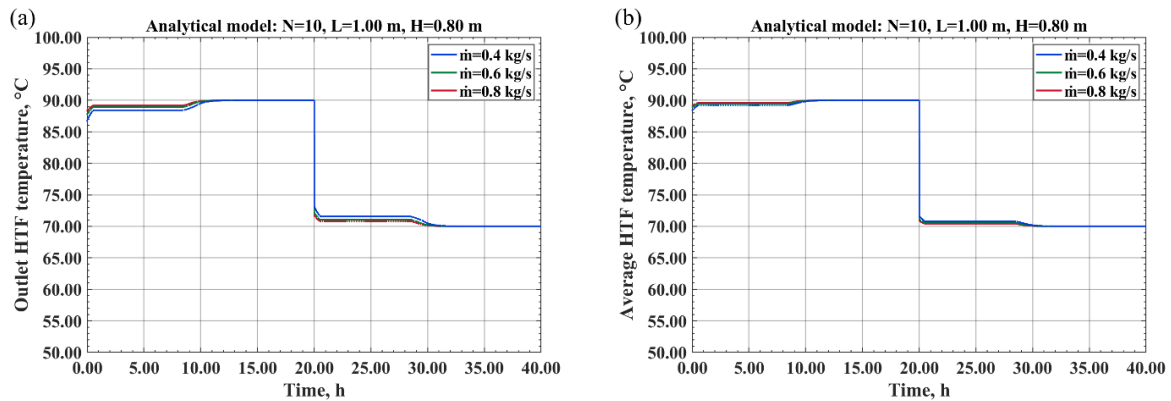


Figure 13 – Time series of (a) the outlet temperature of the water and (b) its average static temperature determined with the analytical model for different water mass flow rates.

The time evolution of the main thermodynamic parameters was also determined with the CFD model to extend the assessment of prototype performance. The progression of the liquid mass fraction and the static temperature of RT80HC over time is presented in Figure 14 for the results of this model [19].

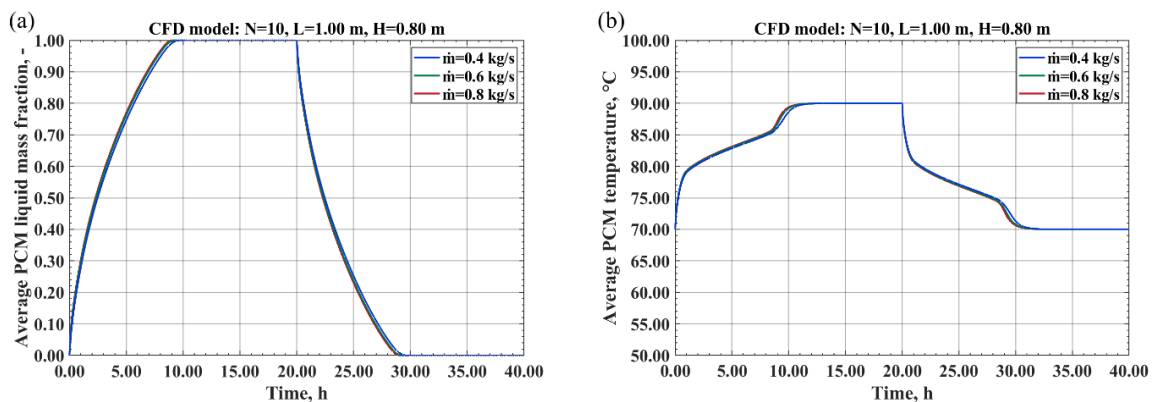


Figure 14 – Time series of (a) the liquid mass fraction and (b) the average static temperature of RT80HC determined with the CFD model for different water mass flow rates.

The outlet and average values of the water temperature obtained with the CFD model are shown in Figure 15 for different operating values of the water mass flow rate [19].

D 5.5 | Technology benchmark and competitor analysis of ZHENIT
WH2X systems

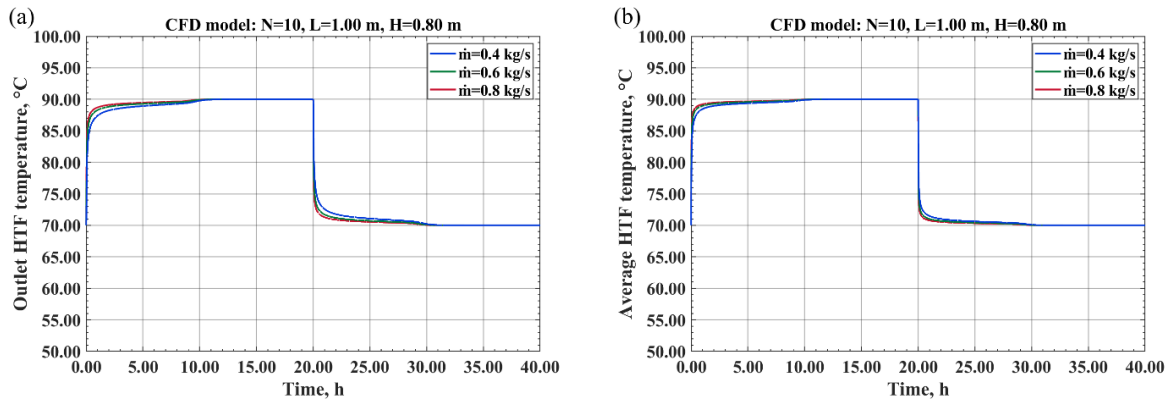


Figure 15 – Time series of (a) the outlet temperature of the water and (b) its average static temperature determined with the CFD model for different water mass flow rates.

For both the analytical and CFD models, when the water flow rate increases, the duration of the phase change process decreases because the temperature gradients at the interface with the storage material become stronger, thereby enhancing heat transfer and accelerating the propagation of the phase front. The corresponding thermal evolution is therefore faster, with a more rapid transition between sensible and latent heat exchange. At the same time, the shorter residence time of the water within the heat exchanger limits its thermal equilibration with the phase change material, which results in lower outlet temperatures despite the higher heat transfer rate. In particular, the water flow rate affects the water temperature at the outlet, which determines the temperature profile of the output delivered. The design of LHTES systems must therefore achieve an appropriate compromise between the reduction of charging and discharging times and the preservation of sufficiently high outlet water temperatures. Within the subset of water flow rates presented, the overall variations in the main thermodynamic response are limited, and all the profiles are satisfactory. More pronounced differences emerge particularly at values closer to the lower operating limit of the prototype.

The key performance indicators of the LHTES prototype operating with an inlet water temperature of 90°C during charging and 70°C during discharging, and with values of water mass flow rate between 0.2 kg/s and 1.2 kg/s, are reported in Table 4 for the predictions of the analytical and CFD models. The prototype achieves a thermal energy storage capacity of 26.51 kWh with a thermal power between 2.54 kW and 3.17 kW in these operating conditions. The energy storage density of 54.76 kWh/m³ refers to the volume occupied by the plates and the PCM inside the tank, as it identifies the core region of heat transfer for the device. The related global value of energy storage density is equal to 31.58 kWh/m³ when the total device volume is considered [19].

D 5.5 | Technology benchmark and competitor analysis of ZHENIT
WH2X systems

Table 4 – Key performance indicators of the LHTES prototype determined with the analytical and CFD models.

Parameter	Analytical model	CFD model
Energy storage capacity, kWh	26.51	26.51
Energy storage density, kWh/m ³	54.76	54.76
Charging or discharging time, h	8.51 – 10.46	8.37 – 10.04
Thermal power, kW	2.54 – 3.11	2.64 – 3.17

The results of relevant experimental tests conducted on the LHTES prototype at the laboratory of *Tecnalia* are presented in Figure 16 illustrating the transient response of the average temperature of the phase change material.

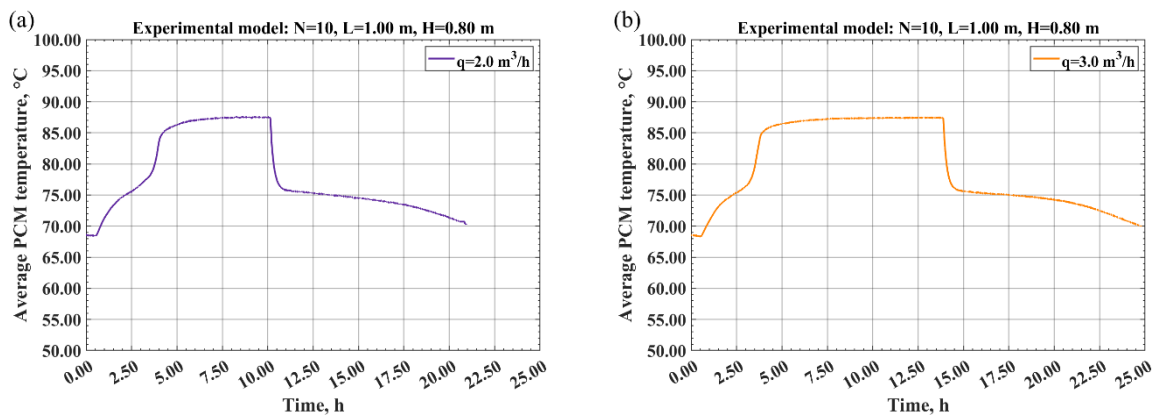


Figure 16 – Time series of the average static temperature of RT80HC measured during the experiments performed with water volume flow rates of (a) 2 m³/h and (b) 3 m³/h imposed at the inlet.

The measurements were made at the central height of the domain of the RT80HC using the fifteen thermocouples. During the tests, uniform values of the volume flow rate of 2 m³/h or 3 m³/h were imposed throughout the circuit, and inlet water temperatures were set to 90°C during charging and to 70°C during discharging. The achieved results show the progression of sensible heat exchange and latent heat transfer during the melting and solidification processes occurring during the charging and discharging phases. Comparing the two phases, the temperature evolution exhibits a complementary thermal response, even though they are not completely symmetric.

3.7 Cost overview for the LHTES prototype

The cost of the LHTES prototype is reported in Table 5 for all the main subassemblies or components that constitute it. The item cost, the packaging, shipping, and customs expenses, and the total cost including value-added tax are specified.

D 5.5 | Technology benchmark and competitor analysis of ZHENIT
WH2X systems

Table 5 – List of component and subassembly costs, packaging, shipping, and customs expenses, and total costs inclusive of value-added tax for the LHTES prototype.

Component	Item cost without value-added tax, £	Packaging, shipping, and customs cost, £	Item cost with value-added tax, £	Supplier
Tank	7500.00	400.00	12324.00	<i>KGD Enterprises Ltd</i>
Drain cap				
Drain valve				
Lid				
Finger plates				
Finger plate screws				
Thermal insulation				
Cladding				
Silicone				
Rivets				
Thermocouples	2370.00			
Thermocouple sockets				
Thermocouple cable				
Thermocouple plugs				
Compression fitting bodies				
Compression fitting ferrules				
Compression fitting nuts				
Compression fitting body locknuts				
Thermocouple plugs	49.05	0.00	58.86	<i>RS Components Ltd</i>
Pillow plates	8384.00	591.00	10770.00	<i>GMF Equipment Ltd</i>
Manifolds				
Long pipes				
Short pipes				

D 5.5 | Technology benchmark and competitor analysis of ZHENIT
WH2X systems

Stands				
Brackets				
Spacers				
Spacer bolts				
Spacer washers				
Spacer nuts				
PCM RT80HC	4204.66	259.23	5356.67	Rubitherm Technologies GmbH
Total	22507.71	1250.23	28509.53	-

3.8 Thermal energy storage technologies for maritime applications

Thermal energy storage systems have a key role in improving the overall efficiency of on-board energy systems and in supporting the effective utilisation of thermal streams originating from Diesel engine exhaust gases, lubricating oil, scavenge air, jacket water, and other recoverable sources, often in synergy with dedicated waste heat recovery technologies.

There are three main classes of thermal energy storage (TES) devices classified according to the physical mechanism by which thermal energy is stored. Sensible heat thermal energy storage (SHTES) systems rely on the variation in temperature of the storage medium. Typical media used for this purpose include water, rocks, sand, concrete, molten salts, and metals [28]. Latent heat thermal energy storage systems exploit the enthalpy of phase transition of a phase change material, which occurs at nearly constant temperature [29]. Thermochemical storage (TCS) systems are based on enthalpy changes connected with reversible endothermic and exothermic reactions, including sorption processes, salt hydration, carbonation, and oxidation–reduction mechanisms [30].

Sensible heat thermal energy storage systems can be utilised over temperature levels extending from a few tens of degrees Celsius to several hundred degrees Celsius [31-33]. This category is mainly characterised by relatively low cost, the possibility of using a wide variety of materials suitable for different operating temperature intervals, and a straightforward design, as the heat transfer fluid commonly exchanges heat directly with the storage material [34]. However, these systems are generally characterised by comparatively low energy storage density, significant variations in thermal power

D 5.5 | Technology benchmark and competitor analysis of ZHENIT
WH2X systems

during the discharge process, and significant heat losses. The materials most frequently used in SHTES applications, together with their main thermophysical properties, are reported in Table 6.

Table 6 – Properties of materials commonly used in sensible heat thermal energy storage systems [32].

Material	Type	Density, kg/m ³	Thermal conductivity, W/m/K	Specific heat, kJ/kg/K
Water at 10°C	Liquid	1000	0.6	4.19
Oil	Liquid	880	0.14	1.88
Ethanol	Liquid	790	0.171	2.4
Propanol	Liquid	800	0.161	2.5
Butanol	Liquid	809	0.167	2.4
Ceramic brick	Solid	1800	0.73	0.92
Rock	Solid	2800 – 1500	3.5 – 0.85	1
Concrete	Solid	2000	1.35	1
Wood	Solid	700 – 450	0.12 – 0.18	1.6
Aluminium	Solid	2707	204	0.896
Copper	Solid	8954	385	0.383
Granite	Solid	2640	4.0 – 1.7	0.82
Sand and gravel	Solid	2200 – 1700	2	1.18 – 0.91
Clay or silt	Solid	1800 – 1200	1.5	2.5 – 1.67
Limestone	Solid	2600 – 1600	2.30 – 0.85	1
Cement mortar	Solid	1800	1	1
Brick	Solid	1600	1.2	0.84
Marble	Solid	2500	2	0.88
Plastic board	Solid	1050	0.5	0.837

For latent heat thermal energy storage systems, the phase change material is chosen according to the characteristics of the thermal source from a set of media suitable for the required operating conditions [35-39]. The primary advantage of this system type is the utilisation of latent heat associated with phase change, which allows substantially greater storage density. However, the main disadvantage is the low thermal conductivity of the medium. Thus, performance enhancement measures are often required, including the use of composite media or the enlargement of the heat exchange area; these measures tend to increase system size and, in turn, lower the overall storage density at the device level.

D 5.5 | Technology benchmark and competitor analysis of ZHENIT WH2X systems

Representative phase change materials considered for waste heat recovery from internal combustion engines are listed in Table 7.

Table 7 – Properties of phase change materials typically utilised for waste heat recovery in internal combustion engines [38].

PCM compound	PCM type	Melting temperature, °C	Specific heat of fusion, kJ/kg	Thermal conductivity, W/m/K	Density, kg/m ³
Na ₂ SO ₄ ·10H ₂ O	Inorganic	32.4	254	0.544	1485
Na ₂ HPO ₄ ·12H ₂ O	Inorganic	36	265	-	1522
Lauric Acid	Organic	41 – 44.2	211.6	0.192	1007
Stearic Acid	Organic	55.1	160	0.172	848
NaOH·H ₂ O	Inorganic	58	-	-	-
Paraffin wax	Organic	58 – 60	214	0.167	790
Climsel C70	Inorganic	70	144	0.65	1700
D-Sorbitol	Organic	89 – 95	185	-	1525
Xylitol	Organic	92 – 94	256	-	1530
Na	Inorganic	91	113	85	930
Erythritol	Organic	117.6	339.8	0.72	1480
73%NaOH/23%NaNO ₃	Eutectic	237	280	0.63	2241
59%LiCl/41%KCl	Eutectic	352.7	251.5	-	1880
NaNO ₃	Inorganic	307	172	0.5	2257

Thermochemical storage systems are able to function over a range of operating temperatures determined by the selected reaction process, while also providing minimal thermal losses and the highest energy storage density among thermal energy storage technologies. Their main limitations are the still low level of technological development and the considerable complexity of the systems required for their control and operation [40]. The materials utilised in these systems, together with their main properties, are listed in Table 8.

Table 8 – Properties of materials commonly used in thermochemical storage systems [40].

Reaction type	Thermochemical material type	Energy storage density	Temperature range, °C
Sorption	Zeolites	136 – 200 kWh/m ³	25 – 230
	Silica Gels	31 – 41 kWh/m ³	130 – 150
	Metal-Organic Framework	0.17 kWh/kg	30 – 100
	Aluminophosphates	0.13 kWh/kg	30 – 277
	Salt Hydrates	361 – 867 kWh/m ³	24 – 214

D 5.5 | Technology benchmark and competitor analysis of ZHENIT WH2X systems

	Composites	166 – 308 kWh/m ³	30 – 250
Reaction	Ammonia Based	< 830 kWh/m ³	350 – 750
	Metal Based	803 – 2050 kWh/m ³	300 – 1400
	Carbonates	300 – 889 kWh/m ³	500 – 1730

The identification of the most appropriate thermal energy storage solutions for maritime use requires an assessment of the compatibility between the main thermal energy storage technologies, the corresponding storage media, and the constraints imposed by on-board integration. This is necessary because the suitability of a storage concept for on-board waste heat recovery depends not only on its intrinsic thermal performance, but also on its technological maturity, compatibility with the available temperature levels, volumetric energy storage capability, and adaptability to the limited space and weight margins that characterise marine systems.

Regarding technological development, sensible heat thermal energy storage currently represents the most mature TES typology, with a technology readiness level in the range from 7 to 8 for industrial applications [41]. Latent heat thermal energy storage has a technology readiness level between 6 and 8 for industrial applications [41]. By contrast, thermochemical storage is still at an earlier stage, since its development is predominantly restricted to laboratory investigations [40]. In addition to its low maturity, thermochemical storage is also affected by substantial complexity at both material and system levels, together with the limited number of successful demonstrations in complete energy systems [40]. On this basis, thermochemical storage cannot currently be considered an appropriate solution for maritime installations in the near future. These values of TRL refer to the general maturity of the corresponding TES technologies and not to their specific readiness for on-board maritime applications, which is currently significantly lower. On this basis, the latent heat thermal energy storage prototype developed in the present work is consistently classified at TRL 4, since it has been validated in laboratory conditions as an integrated unit relevant to the intended application, but it has not yet been demonstrated in an environment sufficiently representative of on-board operation.

A further element governing TES selection is the temperature range of the recoverable waste heat sources available on board vessels. In marine applications, the propulsion system is normally the main source of recoverable thermal energy and is generally based on two-stroke or four-stroke Diesel engines [42, 43]. Under such conditions, the temperature of the exhaust gases is typically around 285°C, while scavenge air is available at about 150°C in general. Other relevant waste heat streams, including

D 5.5 | Technology benchmark and competitor analysis of ZHENIT WH2X systems

lubricating oil, jacket water, cooling water, and seawater, are associated with temperatures between 30 and 90°C as typical references [42, 43]. These values are not constant, however, because on-board waste heat generation depends strongly on the operating profile of the ship. The corresponding temperature levels may vary according to vessel type, engine load, geographical route, ambient air conditions, and seawater temperature [42, 43]. Although this variability complicates the design of thermal storage systems, it does not prevent their use on board various typologies of vessels.

A major limitation related to the implementation of thermal energy storage technologies on board ships is the severe restriction on available volume. Consequently, storage systems intended for maritime waste heat recovery should provide a high volumetric energy storage density. In this context, a value greater than 50 kWh/m³ can be considered appropriate for the on-board installation of TES systems. Although it is possible in principle to raise the temperature of waste heat streams by introducing auxiliary solutions, these are not practically feasible due to increased volume occupancy and decreased energy density [7]. Based on the analysis conducted in Deliverable 3.3 and the requirements of the specific application, a list of promising pure materials is provided in Table 9 based on the data included in Table 6, Table 7, and Table 8, and considering the highest parameter values where intervals are reported. Additionally, a temperature difference of 30°C between the charging and discharging fluid and the TES medium was considered for the SHTES system to calculate energy density. This temperature difference was set to ensure that the temperature variation of the medium remains at 65°C, assuming an exhaust gas temperature of 285°C and a lower limit of 85°C, which are the boundary levels for absorption chiller applications. In this regard, a possible further improvement of the developed LHTES prototype consists of reducing its overall volume through the removal of the features specifically required for the installation and adjustment of the thermocouples during the experimental campaign.

Table 9 – Thermal energy storage typologies and media suited for on-board applications.

TES typology	Material	Energy storage density, kWh/m ³	Limiting factor
SHTES	Water at 10°C	75.65	-
	Oil	29.87	Too low energy density
	Ethanol	34.23	
	Propanol	36.11	
	Butanol	35.06	
	Ceramic brick	29.90	
	Rock	50.55	-

D 5.5 | Technology benchmark and competitor analysis of ZHENIT
WH2X systems

	Concrete	36.11	Too low energy density
	Wood	20.22	
	Aluminium	43.79	
	Copper	61.91	-
	Granite	39.09	Too low energy density
	Sand and gravel	46.87	
	Clay or silt	81.25	-
	Limestone	46.94	Too low energy density
	Cement mortar	32.50	
	Brick	24.27	
	Marble	39.72	
	Plastic board	15.87	
LHTES	Na ₂ SO ₄ ·10H ₂ O	104.78	-
	Na ₂ HPO ₄ ·12H ₂ O	112.04	
	Lauric Acid	59.19	
	Stearic Acid	37.69	Too low energy density
	Paraffin wax	46.96	
	Climsel C70	68.00	-
	D-Sorbitol	78.37	
	Xylitol	108.80	
	Na	29.19	Too low energy density
	Erythritol	139.70	-
	73%NaOH/23%NaNO ₃	174.30	Too high melting temperature
	59%LiCl/41%KCl	131.34	
NaNO ₃	107.83		

The use of latent heat systems is constrained by the thermal conductivity of phase change materials, which is generally below 1 W/m/K, and this represents one of their main limitations [39]. This characteristic tends to reduce the thermal power exchanged during both charging and discharging and therefore becomes a key factor in the sizing of the storage system. In order to mitigate this limitation, particular attention is dedicated to the selection of the heat transfer fluid, the geometric arrangement of the storage medium, and the possible encapsulation material, as these factors strongly influence the

D 5.5 | Technology benchmark and competitor analysis of ZHENIT WH2X systems

thermal transmittance and the final dimensions of the device. The materials considered for latent heat storage include organic paraffins, organic non-paraffins, inorganic compounds, and eutectic mixtures, considering both transitions between solid and liquid and between solid and solid [29].

In this context, TES technologies do not directly provide mechanical or electrical output, nor do they inherently supply other useful effects such as cooling or desalination. Their functions are to accumulate and release thermal energy and to improve the temporal and spatial matching between variable waste heat availability and on-board thermal demand [44]. For this reason, TES devices should be regarded as components of a broader energy system rather than as isolated technologies. This system-level perspective is particularly relevant in marine applications, where several waste heat streams coexist at different temperature values, from slightly more than 30°C for jacket water up to around 370°C for exhaust gases [42, 43], whereas each storage material is normally effective only within a comparatively limited temperature interval. One possible strategy to address the presence of multiple on-board thermal sources is to use a cascade of storage materials with progressively lower melting temperatures, operating at different temperature levels [45]. Such a solution is potentially attractive because it could extend the portion of on-board waste heat that can be exploited. In this regard, the use of a latent heat cascade with multiple PCMs has been analysed, and a possible recovery of fuel energy in the range between 1% and 10% has been reported in the literature [45]. However, this possible layout has been mainly studied theoretically, while experimental evidence is limited to demonstrators at the laboratory scale [46]. In addition, such systems have not yet been sufficiently refined for operation under the strongly dynamic waste heat profiles typical of real ships. As a consequence, most TES concepts developed for marine applications continue to focus on individual on-board locations, where a specific waste heat stream can be coupled to a particular thermal demand or to a dedicated waste heat recovery technology [46].

After the TES concept and the storage medium have been selected, the definition of the storage structure becomes necessary. For sensible and latent heat storage at low and medium temperature levels, the storage medium is generally placed within a thermally insulated structure in order to reduce thermal losses during the storage period. The most common configurations used for this purpose are layouts relying on tanks, packed-bed structures, and arrangements with heat exchangers [28]. With reference to systems using tanks, the most common options are the two-tank configuration and the thermocline layout [34]. The former is associated with a relatively simple operating principle, but also with a large physical footprint, which leads to a comparatively low volumetric energy density at the

D 5.5 | Technology benchmark and competitor analysis of ZHENIT WH2X systems

system scale. Instead, the latter is based on the formation of thermally stratified regions within a single tank and therefore provides a more compact solution capable of limiting the volumetric drawbacks of systems with two tanks [47]. For sensible heat storage in maritime applications, the thermocline configuration therefore appears to be the most favourable option when a reduction in occupied space is required [47]. Packed-bed arrangements represent another possible solution, particularly where design simplicity and the use of low-cost materials are desirable. In such systems, the heat transfer fluid passes directly through the void spaces of the bed. The corresponding void fraction must, however, be selected carefully to avoid excessive pressure drops and the associated increase in pumping power [47]. A further possibility is represented by layouts based on heat exchangers, which can be used for both sensible and latent heat storage [48]. In these configurations, the storage medium is encapsulated in cylindrical or rectangular elements, whereas the heat transfer fluid is circulated inside tubes or plates to avoid direct contact between the two media while allowing heat transfer. For latent heat storage, configurations with heat exchangers and configurations with packed beds are the most frequently applied solutions.

In this framework, the selection between sensible and latent heat storage depends primarily on the temperature level of the waste heat stream to be exploited, which in turn is governed by the operating condition of the ship [43]. Sensible heat storage benefits from a more advanced general technological maturity, but its comparatively low storage density may represent a major drawback where compactness is essential [41, 49]. Latent heat storage appears more advantageous in this respect because of its higher energy density and its suitability for heat sources at low and medium temperature levels [28]. At the same time, it requires specific design measures aimed at increasing heat transfer rates and limiting the growth in device volume associated with the heat exchange surfaces and with the encapsulation structure. The identification of the optimal storage size should include not only thermal considerations, but also economic aspects, such as capital expenditure and operating expenditure, which depend on the technology, the material selection, the adopted system configuration, and the operating behaviour of the ship propulsion plant [7, 50].

At present, commercially available compact TES devices are still mainly represented by sensible heat storage systems. Among the most relevant examples are the modular *Thermal Battery* developed by *EnergyNest*, which can be charged at temperatures up to 400°C [48], the *EcoStock* system developed by *Eco-Tech Ceramics*, which is suitable for temperatures up to 1000°C [51], and the steel-based storage system proposed by *Lumenion* [52]. These devices were, however, developed primarily for industrial

D 5.5 | Technology benchmark and competitor analysis of ZHENIT WH2X systems

contexts, solar-thermal installations, or applications converting mechanical power into thermal power, and their suitability for on-board maritime waste heat recovery remains uncertain, especially in view of the strong constraints related to footprint and weight [7]. In contrast, fewer commercial LHTES devices suitable for marine applications are available, one being the thermal battery named *Central Bank* produced by *Sunamp* [53].

In the framework of research activities on thermal energy storage systems for maritime applications, the available literature has mainly investigated sensible heat storage solutions for integration with ship energy systems. Among these analyses, Baldi et al. investigated the possible application of thermal storage to merchant ships using diathermic oil as the storage medium. The study considered the system from both energetic and economic perspectives by varying the storage capacity, operating temperature, heat exchanger surface, and mass flow rate. The results indicated that a storage volume of 1000 m³ could reduce by approximately 80% the fuel consumption of auxiliary boilers. This outcome highlighted the potential role of TES as a buffering technology able to increase the utilisation of recoverable heat and reduce the dependence on auxiliary thermal generation [54]. Ancona et al. subsequently studied the optimisation of a cruise ship energy system operating in the Baltic Sea, where thermal demand is strongly influenced by space heating and domestic hot water requirements. Their analysis considered load allocation strategies and the integration of thermal storage as part of the overall energy management of the vessel. The results showed that appropriate storage sizing could allow the auxiliary boilers to be shut down in the configurations investigated. In the optimised case, the reduction in dissipated thermal energy exceeded 14 GWh per year, corresponding to approximately 57% compared with the reference configuration [55]. The use of thermal storage in ships supplied by electricity was examined by Huang et al., who treated thermal storage and controllable thermal loads as a virtual energy storage system. In this approach, thermal energy storage was considered as an element of the operational optimisation of the vessel. The study analysed voyage scheduling, thermal demand management, and economic dispatch of the on-board power transformation system. For the representative cruise selected, the coordinated strategy produced a reduction of 17.4% in operating costs and 23.6% in greenhouse gas emissions with respect to conventional operation [56]. Ouyang et al. proposed a different integrated concept for marine natural gas engines, in which waste heat recovery was combined with the recovery of cold energy released during liquefied natural gas regasification. The system incorporated organic Rankine cycles and supercritical Brayton cycles to improve the exploitation of the available thermal and cryogenic streams. The resulting configuration increased the net power

D 5.5 | Technology benchmark and competitor analysis of ZHENIT WH2X systems

output by 214.5 kW and raised the thermal efficiency by 5.14% in total. The economic assessment indicated a payback period of 6.98 years, together with reductions in fuel consumption and carbon dioxide emissions [57]. A further solution based on thermal oil storage was analysed by Baldasso et al. to reduce emissions during ferry harbour stays. The proposed configuration combined an organic Rankine cycle, an exhaust gas boiler, and a TES device filled with Therminol 66, which was selected because it can operate at temperatures up to 345°C without pressurisation. Two storage layouts were compared, consisting of a stratified single tank and an arrangement with two tanks. The analysis identified a required storage volume of nearly 82 m³ and showed that the layout with a single tank could reduce the volume of the storage system by about 40% compared with the configuration using two tanks. A total reduction of approximately 8% was estimated for carbon dioxide emissions [58]. The integration of sensible heat storage with combined electricity and cooling production was examined by Ouyang et al. in a system developed for marine engine waste heat utilisation. The proposed arrangement included an organic Rankine cycle, an absorption refrigeration subsystem, and a heat storage device. The storage unit was introduced to recover excess heat and to support cooling production when the absorption refrigeration system alone was not sufficient to meet the demand. Several solid storage materials were compared, and the analysis indicated that high density and high specific heat capacity are favourable properties for this application. The presence of the heat storage device improved the ability of the overall system to satisfy the cooling load and contributed to enhancing its economic performance [59]. More recently, Brækken et al. assessed the energy use associated with hotel functions on a cruise ship in a Nordic climate, where the thermal demand during port stays can be particularly significant. Among the energy efficiency measures considered, a hot water storage tank charged by engine waste heat during sailing was analysed as a means of reducing auxiliary boiler operation in port. The study showed that a tank volume of 200 m³ could reduce the heat supplied by boilers during port operation by 59%, while a volume of 600 m³ could satisfy 97% of the heating demand in the same operating condition [60]. Wang et al. investigated a Carnot battery concept for vessels operating on intercontinental routes based on the recovery of jacket water waste heat from the main engine. During navigation, the heat available from the cylinder liner water is extracted and stored through a heat pump cycle. During harbour stays, the stored thermal energy is then converted into electricity by an organic Rankine cycle. The case study referred to a vessel operating along the route connecting Shanghai and Rotterdam. Depending on the characteristics of the different port segments,

D 5.5 | Technology benchmark and competitor analysis of ZHENIT WH2X systems

the optimised system was able to cover between 35.5% and 100% of the ship electrical demand during harbour operation [61].

Furthermore, Frazzica et al. designed a hybrid storage device based on both sensible and latent heat for the supply of domestic hot water on board ships by exploiting heat recovered from jacket cooling water. The system used the PCM S58, characterised by a melting temperature of 58°C, and consisted of 20 polypropylene tubes containing 40 dm³ of macro-encapsulated PCM placed in a cylindrical tank with a total volume of 100 dm³ and made of stainless steel. The corresponding unit was able to provide hot water between 65°C and 85°C, with a power ranging between 15 and 20 kW during the discharging phase [62].

For latent heat thermal energy storage systems, the research activity specifically focused on maritime applications has not yet been extensively developed. Manzan et al. examined the introduction of thermal storage in the hot potable water system of cruise ships, with specific attention to the reduction of the additional heat input required during port stays. This condition is critical because the contribution from the engine cooling circuit becomes limited when the vessel is not navigating. The analysis was performed through dynamic simulations of the distribution system and compared alternative storage arrangements. The study also considered PCM S58S to improve the thermal response of the storage tank. The results showed that the required heating power for hot water preparation could be reduced by up to 39%. In addition, the phase change material contributed to maintaining higher temperatures in the upper part of the tank during periods of elevated demand, thereby improving the useful thermal availability of the stored energy [63]. Catapano et al. subsequently investigated a laboratory system representative of naval waste heat recovery applications, integrating a Diesel engine, a Stirling engine, an organic Rankine cycle device, and a latent heat thermal storage device. The storage system is charged by thermal energy recovered from the engine cooling circuit and can subsequently deliver heat for domestic hot water production or provide thermal input to the ORC system for additional electricity generation. The experimental activity reproduced a representative cruise ship operation at laboratory scale. The results confirmed the capability of latent heat storage to support domestic hot water demand and to reduce the need for auxiliary boiler operation [64]. Another approach was proposed by Zhang et al., who analysed a waste heat recovery layout for maritime vessels combining a transcritical carbon dioxide Rankine cycle with cascade latent thermal energy storage. The storage of thermal energy was based on three phase change materials selected to operate at progressively different temperature levels, which are LiNO₃-NaCl, D-mannitol, and oxalic acid. This configuration was introduced to reduce

D 5.5 | Technology benchmark and competitor analysis of ZHENIT WH2X systems

the detrimental effect of exhaust gas variability on the recovery system and to support more stable operation during the voyage. Under design conditions, the system delivered 223.2 kW of net power and 289.9 kW of heating output. When the cascade storage unit was used as the thermal source for the recovery process, the corresponding values were 168.0 kW and 231.5 kW, respectively. Over a daily route, the integrated configuration increased the total net work output and the supplied heating by 19.1% and 7.9%, respectively, compared with a conventional waste heat recovery arrangement [65]. More recently, Ouyang et al. investigated a combined cooling, heating, power, and storage system for a large marine vessel. The proposed architecture couples an organic Rankine cycle, an absorption refrigeration cycle, and a phase change heat storage unit to improve the coordination between waste heat recovery and the electrical and thermal requirements of the ship. The study included working fluid selection, sensitivity analysis, multi-objective optimisation, and the evaluation of the interaction between the storage unit and the Diesel generators along a representative operating profile. Under the optimal configuration, the system reached a thermal efficiency of 30.07%, with a payback period of 6.22 years, yearly fuel savings of 2791.74 m³, and an annual carbon dioxide emission reduction of 8910.49 t in total. The use of phase change storage increased the thermal efficiency by 12.88% and improved both fuel savings and carbon dioxide emission reduction by 25.48% compared to the analogous system without storage [66].

Moreover, the implementation of optimised control strategies may significantly improve the matching between waste heat availability and on-board demand under variable operating conditions. This aspect could significantly contribute to the achievement of the targets defined by the *IMO* to improve energy efficiency and reduce carbon intensity. Indeed, recent studies on multi-energy microgrids for ships have shown that thermal storage can increase the operational flexibility of on-board energy systems when it is coordinated with power generation units, thermal loads, voyage scheduling, and energy conversion devices [67-69]. In these configurations, the storage device contributes to the redistribution of thermal energy over time, while the supervisory control strategy determines how the available heat should be stored, converted, or supplied to the on-board users. This approach is particularly relevant for vessels operating under variable profiles, where propulsion demand, hotel loads, weather conditions, and renewable energy availability may change significantly during the route. The study of Li et al. addressed the robust coordination of a hybrid microgrid for an on-board application, combining alternating current and direct current networks with flexible voyage and thermal loads. In addition to Diesel generators and battery storage, the system included photovoltaic generation, a combined cooling, heating, and power

D 5.5 | Technology benchmark and competitor analysis of ZHENIT WH2X systems

unit, thermal storage, and devices for the conversion of electrical power into thermal power. The proposed method coordinated the on-board units while accounting for uncertainties associated with renewable energy generation, on-board power loads, and outdoor temperature. This study further confirmed that the benefits of TES devices depend strongly on their integration within the overall control system of the vessel, and not only on the storage material or device size [67]. Afterwards, Xu et al. investigated the simultaneous scheduling of electric and thermal energy in a hybrid power ship system. The proposed configuration included Diesel generators, photovoltaic generation, electric energy storage, thermal energy storage, and electric boilers, while an adaptive optimisation strategy was developed to reduce operating costs and greenhouse gas emissions. The results supported the relevance of coordinated electrical and thermal energy management for improving the economic and environmental performance of ship energy systems [68].

Within this context, increasing attention has been focused on latent heat storage concepts based on pillow-plate heat exchangers [70, 71]. These studies have shown that the integration of pillow plates within latent heat thermal energy storage systems can support the development of compact configurations characterised by enhanced heat transfer, shorter charging and discharging times, and improved suitability for the stringent space constraints of maritime applications [18]. In particular, the application potential and technical and economic characteristics of a latent heat thermal energy storage concept based on pillow-plate heat exchangers and phase change materials for the recovery of waste heat at medium temperature levels in maritime systems have been investigated [14].

Overall, the implementation of TES on board ships is still progressing through the research and development stages. The main issues to solve concern the design of systems specifically tailored to maritime requirements, their integration with existing on-board systems and complementary waste heat recovery technologies, the maximisation of energy storage density at the system scale, the reduction of footprint and related costs, and the optimisation of charging and discharging durations under realistic operating conditions [62].

4 Organic Rankine cycle prototype

The prototype developed by the *National Technical University of Athens* is a heat pump combining an organic Rankine cycle and an ejector. It is designed to recover thermal energy from a hot-water waste heat stream at 140°C with a nominal thermal input of 100 kW_{th}, in order to provide electricity, heating,

D 5.5 | Technology benchmark and competitor analysis of ZHENIT WH2X systems

and cooling. The envisaged operating modes are four and include an electricity-only mode based on a recuperative organic Rankine cycle, a combined heat and power mode based on a non-recuperative ORC, a combined power and cooling mode based on the simultaneous operation of an ORC and an ejector-integrated heat pump, and a cooling-only mode based on the operation of the ejector-integrated heat pump alone.

The maximum cycle temperature was set to 130°C for the prototype. At the design point, the net power output of the system is 10.30 kW_e in electricity-only mode and 7.68 kW_e in combined heat and power (CHP) mode. In the mode combining heat and power, the heating output is around 88.97 kW_{th} overall. In the two cooling modes, electricity and cooling are produced simultaneously by the ORC and the vapour compression cooling (VCC) cycle, respectively. The cooling output is in the interval between 2 kW_e and 3 kW_e for these two cases.

A complete piping and instrumentation diagram of the ORC prototype is shown in Figure 17, where all components are illustrated together with their main interconnections. The prototype is driven by hot water supplied to the common heat exchanger, which functions as the ORC evaporator during power production and as the generator of the ejector cooling cycle during cooling operation. This heat exchanger will hereafter be named the generator for brevity. Heat is rejected from the prototype in a condenser cooled with water. The cooling effect is delivered by chilled water flowing through the cooling evaporator heat exchanger. For brevity, this latter heat exchanger will hereafter be named the evaporator. The prototype also includes a recuperator, which is operated in the ORC electricity-only mode to improve thermal efficiency. Finally, the prototype includes a subcooler to prevent pump cavitation issues in all operating modes. Electricity is produced by two parallel open-drive expanders, each coupled to a generator. Moreover, the prototype includes two semi-hermetic compressors, which are used to drive the compression process in the modes based on vapour compression.

D 5.5 | Technology benchmark and competitor analysis of ZHENIT WH2X systems

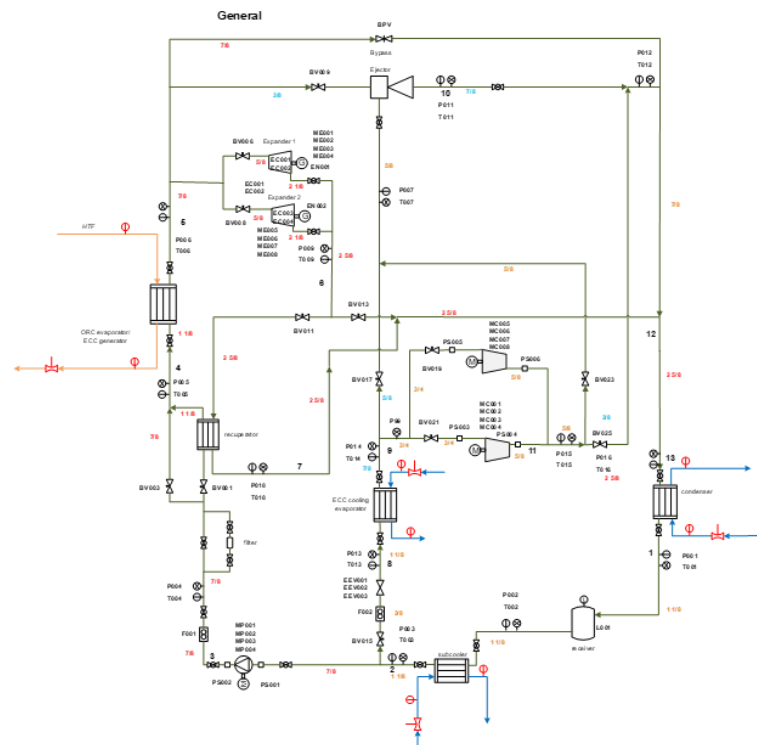


Figure 17 – Piping and instrumentation diagram of the ORC–ejector integrated heat pump prototype developed by the National Technical University of Athens.

4.1 Working principle of the ORC prototype

The prototype developed by *NTUA* is based on an innovative integration of an organic Rankine cycle and an ejector–vapour compression cooling cycle.

4.1.1 Organic Rankine cycle – Electricity production modes

Organic Rankine cycle systems are power generation cycles implemented for the conversion of thermal energy into electricity at relatively low temperatures, typically lower than 300°C, and at power capacities below 2 MW_e in general. The main feature of these devices is the use of organic substances, such as alkanes, hydrofluorocarbons, hydrofluoroolefins, and siloxanes, as working fluids instead of water and steam. In an ORC system, the saturated liquid organic working fluid, which is the refrigerant, exits the condenser and is subcooled and pressurised in a pump and subsequently heated by the heat source in a heat exchanger, which is the evaporator, where it is converted into saturated or superheated vapour. Subsequently, the pressurised hot vapour exiting the evaporator is driven to an expander, where it expands to produce mechanical power, which is then converted into electricity through a

D 5.5 | Technology benchmark and competitor analysis of ZHENIT WH2X systems

generator. The working fluid leaving the expander can then be used for preheating the liquid refrigerant leaving the pump through an internal heat exchanger, which is the recuperator. Finally, it is driven to the condenser, where it is cooled down by a cooling fluid and condensed before being recirculated into the pump to repeat the processes. The liquid refrigerant subcooler in the ORC, as well as in all other subsequent cycles and configurations presented in this document, does not constitute a fundamental process of the thermodynamic cycle. However, subcooling is necessary as a measure to prevent cavitation from occurring in the refrigerant pump by providing a sufficient net positive suction head, which is a common issue in similar micro-scale ORC systems.

4.1.2 Ejector cooling cycle – Cooling mode

The ejector cooling cycle (ECC) is a thermally driven cooling cycle utilised to provide cooling through the utilisation of thermal energy. The ECC is similar to the conventional VCC, but in this case, the mechanical compression process of the latter is replaced by a dynamic compression process occurring within an ejector device.

More specifically, in an ECC, the liquid working fluid exiting the condenser is divided into two flows, which are a primary flow at high pressure and a secondary flow at low pressure. The primary flow is pressurised in a pump and subsequently heated by the heat source stream in a heat exchanger, which is called the generator, where it is converted, as in the case of the ORC, into saturated or superheated hot vapour at high pressure. The secondary flow is throttled to low pressure and temperature in an expansion valve and then supplied to a heat exchanger, which is the evaporator, where it evaporates to provide cooling. Both the primary and the secondary flows enter the ejector device through different ports. The primary flow is accelerated to supersonic velocity in a converging-diverging nozzle inside the ejector and entrains the low-pressure secondary flow exiting the evaporator. The two flows are then mixed and leave the ejector device at an intermediate pressure. The mixed stream is subsequently driven to the condenser, where it is cooled down and condensed, thereby releasing heat. Under normal operation of the ejector, both the primary and the secondary flows are choked as they enter the device.

The main advantage of the ejector cooling cycle compared to the vapour compression cooling is the significantly lower electricity consumption, since the power absorbed by the liquid pump is considerably lower than that required by a vapour compressor. Nevertheless, ejector cooling cycles still need to be driven by a heat source at a relatively high temperature, and their cooling capacity is strongly dependent

D 5.5 | Technology benchmark and competitor analysis of ZHENIT WH2X systems

on the properties of the heat source, such as temperature and thermal capacity, and is therefore constrained by them.

4.1.3 Ejector-vapour compression cycle configuration – Cooling mode

The configurations with ejector cooling cycles exhibit significantly lower electricity consumption than conventional configurations with vapour compression cooling. However, their cooling capacity is strongly dependent on the temperature and thermal capacity of the driving heat source, as well as on the temperature of the heat sink, which in this case is represented by the cooling water in the condenser. One possible approach to overcome this limitation is the integration of an ECC with a VCC into an ejector vapour compression cycle. This type of cycle can provide higher cooling capacities, which may be advantageous depending on the cooling demand. Nevertheless, it is associated with higher electricity consumption than simple thermally driven ECCs, thereby representing a compromise between the two technologies. Two main configurations can be identified for the integration of a VCC with an ECC, which are the parallel and serial arrangements. In the prototype developed by *NTUA*, both parallel and serial EVCC configurations can be implemented.

4.1.4 Parallel ORC–EVCC configuration

In the parallel ORC–EVCC configuration, the ORC and the EVCC are physically interconnected in parallel and operate with the same working fluid. From a thermodynamic perspective, this configuration is equivalent to two separate systems, represented by an ORC and an EVCC, which operate with the same working fluid, are driven by the same heat source, and release heat to the same heat sink. Heat is supplied to the whole system by the heat source in a heat exchanger that simultaneously functions as the ORC evaporator and the ECC generator. The superheated vapour is then divided into two streams. The first stream is supplied to the ejector as the primary flow for cooling production in the EVCC, whereas the second stream is supplied to the expander in the ORC to supply electricity. The proportion of heat supplied to the ORC and the EVCC can be adjusted using valves for flow regulation. Finally, the superheated vapour exiting the ejector or the compressor, together with the expanded vapour leaving the expander in the non-recuperative ORC or the recuperator in the recuperative ORC, is mixed and directed to a single condenser.

4.2 Principal components of the ORC–ejector integrated heat pump prototype

The fully developed layout of the parallel ORC–EVCC prototype realised by the *National Technical University of Athens* is shown in Figure 18.



Figure 18 – Photograph of the ORC–ejector integrated heat pump prototype installed at the *National Technical University of Athens*.

The key components of the ORC prototype are the heat exchangers, the pump, the expanders and motors, the compressors, the ejector, the expansion valve, the sensors, and the control hardware and cabinet.

4.2.1 Heat exchangers

The ORC prototype includes several heat exchangers with different functions. The ORC evaporator/ECC generator is the heat exchanger in which thermal energy is supplied from the heat source, represented by hot water, to the working fluid, which is the refrigerant. The condenser is the component in which heat is released from the working fluid to the cooling water. The subcooler provides slight subcooling of the working fluid before it enters the pump, thereby preventing cavitation. The evaporator is the heat exchanger in which the working fluid cools down a stream of chilled water. Finally, the recuperator operates as an internal heat exchanger, in which the hot vapour leaving the expanders is utilised to preheat the liquid working fluid before it enters the ORC evaporator/ECC generator, thus improving the thermal efficiency.

D 5.5 | Technology benchmark and competitor analysis of ZHENIT WH2X systems

4.2.2 Pump and motor

The prototype is equipped with a volumetric pump selected for its capability to provide straightforward control of the refrigerant flow rate independently of the pressure difference across the pump. The pump specifications were determined according to the design choices presented in Deliverable 2.3 of the ZHENIT project. The pump and motor installed on the prototype are illustrated in Figure 19.



Figure 19 – Photograph of the working fluid pump and motor installed on the ORC–ejector integrated heat pump prototype.

4.2.3 Expanders and motors

The selection of the expander for a micro-scale ORC system is particularly challenging, as commercially available products cannot be readily procured for this purpose. Instead, a common practice in micro-scale ORC prototypes is to modify commercially available compressors in order to enable their operation in reverse as expanders. These modifications typically require the removal of the check valve located at the compressor discharge port.

For micro-scale systems, the compressor typologies most commonly considered for this purpose are scroll and screw compressors. Screw compressors are generally utilised for very high volumetric capacities, which exceed by a wide margin those presented in Deliverable 2.3 for the ORC–ejector heat pump prototype. By contrast, scroll compressors are applied for volumetric capacities that are compatible with the design requirements of the developed prototype. The expanders and motors installed in the ORC prototype are shown in Figure 20.

D 5.5 | Technology benchmark and competitor analysis of ZHENIT WH2X systems



Figure 20 – Photograph of the expanders and motors installed on the ORC–ejector integrated heat pump prototype.

4.2.4 Compressors

The selection of the compressor models was carried out according to three main factors, which are the required refrigerant pressure difference, the pressure ratio, and the volumetric flow rate at the suction. Owing to the novel character of refrigerant R1233zd(E), the identification of a suitable compressor model was particularly challenging, since commercially available compressors are generally not certified for operation with this working fluid. An additional point of concern was represented by the extremely small pressure difference between the compressor suction and discharge. Under these conditions, and following consultation with the manufacturer *Copeland*, it was decided to adopt the piston compressor depicted in Figure 21.

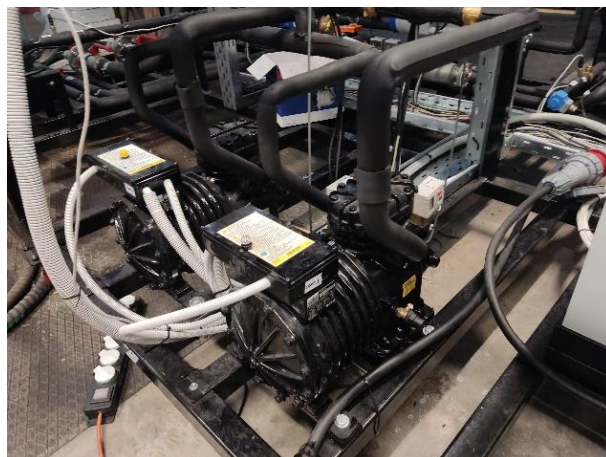


Figure 21 – Photograph of the compressors installed on the ORC–ejector integrated heat pump prototype.

D 5.5 | Technology benchmark and competitor analysis of ZHENIT
WH2X systems

4.2.5 Ejector

The ejector is a key component of the ORC–ejector integrated heat pump prototype. An ejector prototype was designed and manufactured by the *National Technical University of Athens* on the basis of the modelling approach presented in Deliverable 2.3, which was applied to determine its main dimensions. The standard view of the computer-aided design (CAD) model of the ejector is shown in Figure 22.

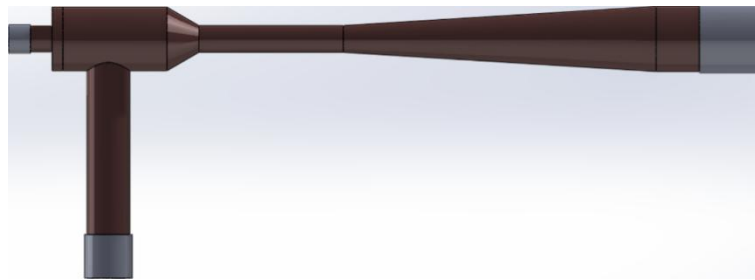


Figure 22 – Rendering of the standard view of the ejector designed for its application in the ORC–ejector integrated heat pump prototype.

The internal arrangement of the ejector components is illustrated in the sectional view of the CAD model illustrated in Figure 23.

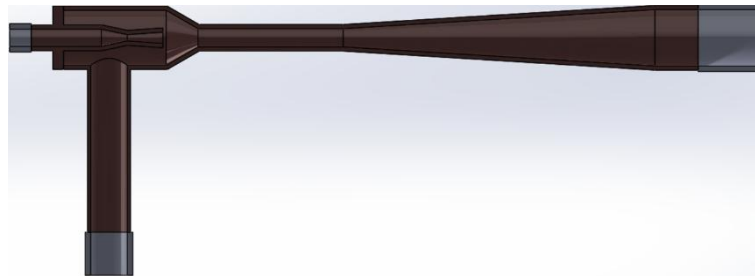


Figure 23 – Rendering of the sectional view of the ejector designed for its application in the ORC–ejector integrated heat pump prototype.

The ejector and its thermal insulation are illustrated in Figure 24, where they are installed in the final configuration of the ORC–ejector integrated heat pump prototype.

D 5.5 | Technology benchmark and competitor analysis of ZHENIT WH2X systems



Figure 24 – Photograph of the thermally insulated ejector installed on the ORC–ejector integrated heat pump prototype.

4.2.6 Expansion valve

The expansion valve is a key component of the EVCC section of the ORC–ejector integrated heat pump. Its selection was carried out on the basis of the operating conditions associated with the different operating modes of the prototype. The electronic expansion valve model *AKV10P6* manufactured by Danfoss was selected for the developed prototype.

4.2.7 Sensors

The refrigerant circuit of the ORC prototype includes three main types of sensors. Temperature sensors are installed to measure the temperature of the refrigerant and water streams, and a total of twenty-four *PT100 Class A* sensors are present in the prototype. Pressure sensors are utilised to measure the refrigerant pressure and include ten *SPKT0013P* sensors, suitable for the measurement of absolute pressures below 1 atm in the low-pressure section of the system, together with seven *SPKT00F3P* transducers for the refrigerant pressure in the sections at medium and high pressure levels. All these sensors were manufactured and provided by *Carel*. Flow meters are installed to measure the refrigerant flow rate, and for this purpose, two identical Coriolis flow meters, model *OPTIMASS 1400C–S15*, manufactured by *Krohne*, are utilised.

The temperature and pressure sensors are distributed throughout the refrigerant sections of the prototype to enable the calculation of the energy balances in the heat exchangers. In addition, they are positioned where needed to allow the characterisation of expander performance, for example, through the determination of volumetric and adiabatic efficiencies, as well as the characterisation of pump

D 5.5 | Technology benchmark and competitor analysis of ZHENIT WH2X systems

performance in terms of the same parameters. Further sensors are installed at the inlet and outlet of the ejector in order to evaluate its entrainment ratio and to support the validation of the models presented in Deliverable 2.3 for the developed system.

With regard to the flow meters, two Coriolis flow meters were procured to measure the refrigerant mass flow rate at the discharge of the pump and at the outlet of the evaporator. These measurements enable the characterisation of the prototype in terms of electrical efficiency in the ORC operating modes, as well as thermal and electrical coefficient of performance in all the cooling modes. The Coriolis flow meters installed on the prototype are illustrated in Figure 25.



Figure 25 – Photograph of the Coriolis flow meters installed on the ORC–ejector integrated heat pump prototype.

Finally, four pressure switches were installed in the system. Two are located around the pump, one upstream and one downstream, in order to protect it from excessively low suction pressure and from excessive pressure in the high-pressure line. The other two are installed in the cooling circuit, one before and one after the compressors, in order to protect both the circuit and the compressors from excessively low and excessively high pressures.

4.2.8 Control hardware and cabinet

An essential component of the implementation of the test rig is the control cabinet, which is also responsible for power distribution. Its purpose is to contain all power and voltage distribution devices used to monitor and control the test rig, while also protecting these components from leaks and potential short circuits.

4.3 Design choices, novel features, and technology readiness level of the ORC prototype

The ORC prototype was designed to exploit waste heat sources at high temperatures typical of maritime vessels. The selected solution is characterised by specific design choices, novel features related to the integration of the ORC and EVCC technologies, and a maturity level that still requires further experimental validation.

4.3.1 Main design choices for the ORC prototype

During the design process, several possible configurations of the ORC and ejector heat pump systems were considered, as described in detail in Deliverable 2.3 of the ZHENIT project. Some configurations were excluded a priori from further consideration due to technical or thermodynamic infeasibility, or because of critical drawbacks. The remaining options were then investigated through numerical modelling. Ultimately, a parallel ORC–parallel EVCC configuration driven by high-temperature waste heat of 140°C was identified as the most suitable solution in terms of thermodynamic performance, simplicity, space and weight requirements, and cost. The main characteristics of this configuration are the physical integration of the ORC and the ejector heat pump, which function with the same working fluid, and their connection in a parallel arrangement. The selected working fluid for the system is hydrofluoroolefin R1233zd(E), which was chosen owing to its safe use, commercial availability, and favourable environmental properties.

First, it should be noted that the maximum prototype temperature of 140°C was imposed by technical constraints related to the use of lubricating oils in the refrigerant circuits of the scroll expanders, as well as by the operating limits of the scroll expanders themselves.

The cooling water used in the prototype is representative of seawater; therefore, its temperature strongly depends on seawater conditions. In the North Sea and Mediterranean Sea, seawater temperature generally varies from a minimum of 4°C in the North Sea during February and March to a maximum of 25°C in the Mediterranean Sea in August. However, in practice, the seawater temperature within a piping network of a maritime vessel supplying energy systems is typically higher than the temperature of the surrounding sea and can reach 40°C as the upper limit. For this reason, even higher cooling-water temperatures were considered in the thermodynamic optimisation. Furthermore, temperatures above 40°C were also considered for the combined heat and power mode.

D 5.5 | Technology benchmark and competitor analysis of ZHENIT WH2X systems

Only subcritical ORCs were considered for the prototype. In addition, maximum cycle pressures approaching the critical point were excluded because the abrupt changes in fluid properties near critical conditions can result in unstable system behaviour. The critical temperature of R1233zd(E) is 165°C, which is significantly higher than the value of 130°C, representing the global upper limit. Therefore, for this working fluid, a maximum cycle temperature of 130°C, equal to the global upper limit, is acceptable.

An additional design parameter for the EVCC cooling modes is the temperature of the chilled water supplied to the cooling evaporator. This variable is not independent, as it is determined in practice by the cooling demand of the vessel. This value was varied between 12°C and 18°C in the present analysis.

4.3.2 Novel features of the ORC prototype

The first novel aspect of the prototype is represented by the EVCC concept, which is based on the integration of a vapour compression cycle and an ejector cooling cycle into a hybrid system driven by both electrical and thermal energy. In the EVCC, an external heat source is utilised to supply the primary flow of the ejector. This flow enables the partial compression of the working fluid exiting the cooling evaporator, thereby reducing the specific power consumption of the mechanical compressor in the VCC. In contrast to the widely investigated ejector-expansion vapour compression cycle (EXVCC) concept, in the EVCC, the ejector is introduced to realise an ECC for the purpose of recovering and utilising thermal energy from an external heat source. As a result, the EVCC constitutes a hybrid system driven by both heat and electricity, whereas EXVCC systems are driven exclusively by electricity.

The second novel aspect of the prototype concerns both the EVCC concept itself and the assessment of its integration potential with an ORC. Although the integration of ejectors into VCCs according to the ejector-expansion vapour compression cycle concept has been widely investigated, research on EVCC systems remains limited. Accordingly, the present prototype contributes to the advancement of knowledge in this area by evaluating the feasibility and potential benefits of EVCC–ORC integration.

The main advantages of the prototype are its operational flexibility and ability to operate in multiple modes, including electricity generation, cooling production, and heating supply, using the same set of components. At the same time, further design optimisation is required to improve compactness and facilitate integration within the constrained spaces typically available on board vessels.

The ORC–ejector prototype can also operate in cascade with the sorption desalination and cooling prototype developed by *CNR–ITAE* and *SorTech* when necessary. In this arrangement, the thermal

D 5.5 | Technology benchmark and competitor analysis of ZHENIT WH2X systems

energy rejected at the lower temperature level by the ORC desuperheater can be supplied to the SDC prototype as driving heat. This integration enables the residual thermal output of the ORC–ejector system to be further exploited for chilled water and freshwater production, thereby extending the functionality of the prototype from stand-alone waste heat recovery to operation within a more integrated on-board energy configuration representative of maritime applications.

4.3.3 Technology readiness level of the ORC prototype

Organic Rankine cycle systems for waste heat recovery in maritime applications are already commercially available. However, their integration with EVCC technology is still at an early stage of development. For this reason, the overall prototype should be considered at a technology readiness level between 3 and 4, corresponding to a relatively low maturity level. At this stage of development, the design of the integrated system has been established on the basis of thermodynamic analysis, component selection, and system-level engineering considerations, demonstrating the technical feasibility of the proposed concept. The main operating principles of the combined ORC–EVCC architecture have therefore been identified and assessed, and the expected functionality of the system has been substantiated through modelling and design activities.

The integrated configuration of the ORC–EVCC prototype has not yet reached the level of maturity associated with a fully validated system under representative operating conditions. In particular, although the individual subsystems rely on known technologies, the innovation is represented by their combination within a single architecture for maritime waste heat recovery, cooling, and power generation. This integration introduces additional design and operational challenges related to component interaction, control strategy, thermal matching, and overall system stability, which still require verification through laboratory-scale implementation and testing. The system can therefore be considered to have progressed beyond the purely conceptual stage. However, it still requires experimental validation in a controlled environment before moving towards higher readiness levels.

4.4 Operating conditions and performance of the ORC prototype

The prototype of the organic Rankine cycle with EVCC technology was designed by considering four main operating modes. The device can operate in the ORC mode for electricity production, in the ORC mode for combined heat and power, in the ORC–parallel EVCC mode for combined cooling and power production, and in the ORC–serial EVCC mode for combined cooling and power production.

D 5.5 | Technology benchmark and competitor analysis of ZHENIT
WH2X systems

The design assumptions for the ORC modes for electricity production and CHP are summarised in Table 10 for the developed prototype.

Table 10 – Design assumptions applied for the electricity production and CHP modes of the ORC prototype.

Group	Parameter	Value
Heat source	Composition	Water
	Pressure	5 bar
	Temperature at ORC evaporator inlet	140°C
	Temperature at ORC evaporator outlet	130°C
	Heat input to ORC	100 kW _{th}
Components	Expander isentropic efficiency	65%
	Pump isentropic efficiency	65%
	Expander generator efficiency	96%
	Pump motor efficiency	85%
Heat exchangers	Cooling water temperature at the condenser and subcooler inlet	20°C – 50°C
	Cooling water temperature increase in the condenser and subcooler	5 K
	Minimum pinch point in ORC evaporator	10 K
	Pinch point in the condenser	3 K
	Pinch point in recuperator or recuperative ORC in electricity-only mode	10 K
Cycle design parameters	ORC maximum cycle temperature	90°C – 130°C R1233zd(E): 130°C
	Superheating in the evaporator	5 K
	Subcooling in the subcooler	5 K
	Condensation pressure	Calculated to comply with the pinch point in the condenser

The detailed results for the design points of the ORC under electricity-only mode, which is recuperative, and the CHP mode, which is non-recuperative, are shown in Table 11.

Table 11 – Results obtained for the electricity-only mode and the combined heat and power mode of the ORC prototype.

D 5.5 | Technology benchmark and competitor analysis of ZHENIT
WH2X systems

Parameter	Electricity-only	CHP
Hot water mass flow rate	2.341 kg/s	2.341 kg/s
Hot water temperature at ORC evaporator inlet	140°C	140°C
Hot water temperature at ORC evaporator outlet	130°C	130°C
Heat input to ORC	100 kW _{th}	100 kW _{th}
Working fluid	R1233zd(E)	R1233zd(E)
Working fluid temperature at the expander inlet	130°C	130°C
Evaporation pressure	17.35 bar	17.35 bar
Evaporation temperature	125°C	125°C
Cooling water temperature	35°C	50°C
Cold stream temperature rise in the recuperator	18.97°C	-
Condensation temperature	42.80°C	57.29°C
Condensation pressure	2.35 bar	3.62 bar
Expander hydraulic power	11.79 kW	8.97 kW
Expander generator power output	11.32 kW _e	8.61 kW _e
Pump hydraulic power	0.86 kW	0.79 kW
Pump motor power consumption	1.02 kW _e	0.93 kW _e
Net electric power output	10.30 kW _e	7.68 kW _e
Condenser heat duty	86.21 kW _{th}	88.97 kW _{th}
Subcooler heat duty	2.87 kW _{th}	2.86 kW _{th}
Recuperator heat duty	10.95 kW _{th}	0 kW _{th}
Working fluid mass flow rate	0.461 kg/s	0.450 kg/s
Condenser cooling water mass flow rate	4.126 kg/s	4.255 kg/s
Subcooler cooling water mass flow rate	0.137 kg/s	0.137 kg/s
ORC electric efficiency	0.103	0.077

The design assumptions applied during the design process for the parallel ORC–EVCC configuration are summarised in Table 12.

Table 12 – Design assumptions applied for the parallel ORC–EVCC configuration of the ORC prototype.

Parameter	Value
-----------	-------

D 5.5 | Technology benchmark and competitor analysis of ZHENIT WH2X systems

Heat source	Composition	Water
	Pressure	5 bar
	Temperature at evaporator inlet	140°C
	Temperature at evaporator outlet	130°C
	Heat input to ORC–EVCC	100 kW _{th}
	ORC/EVCC working fluid	R1233zd(E)
Components	Expander isentropic efficiency	65%
	Pump isentropic efficiency	65%
	Expander generator efficiency	96%
	Compressor motor efficiency	85%
	Pump motor efficiency	85%
Heat exchangers	Cooling water temperature at the condenser and subcooler inlet	30°C, 35°C, and 40°C
	Cooling water temperature increase in the condenser and subcooler	5 K
	Pinch point in the condenser	3 K
	Chilled water temperature at the EVCC evaporator inlet for cooling	15°C
	Chilled water temperature drop in the EVCC evaporator for cooling	5 K
	Pinch point in the EVCC evaporator for cooling	3 K
	Pinch point in the recuperator	10 K
Ejector	Area ratio range	1.05 – 15.00
	Primary flow isentropic efficiency	0.95
	Secondary flow isentropic efficiency	0.85
Cycle design parameters	Thermal split fraction	0.8 – 0.9
	ORC/EVCC maximum cycle temperature	130°C
	Superheating in ORC evaporator/ECC generator	5 K
	Subcooling in the subcooler	5 K
	Superheating in the EVCC evaporator for cooling	5 K

D 5.5 | Technology benchmark and competitor analysis of ZHENIT
WH2X systems

	Condensation pressure	Calculated to satisfy the pinch point in the condenser
	Reduced intermediate pressure p^* for serial EVCC-2	0.05 – 0.50
	Reduced compressor mass flow rate for parallel EVCC	0.05 – 2.00

The final design specifications of the ORC–EVCC under the ORC-parallel EVCC mode and ORC-serial EVCC mode are listed in Table 13 including the values of the coefficient of performance (COP) achieved for both configurations.

Table 13 – Results of the ORC–EVCC combined cooling and power production modes of the ORC prototype.

Parameter	ORC-parallel EVCC	ORC-serial EVCC-2
Hot water mass flow rate	2.34 kg/s	2.34 kg/s
Hot water temperature at ORC evaporator inlet	140°C	140°C
Hot water temperature at ORC evaporator outlet	130°C	130°C
Heat input to ORC	100 kW _{th}	100 kW _{th}
Working fluid	R1233zd(E)	R1233zd(E)
Working fluid temperature at expander inlet	130°C	130°C
Evaporation pressure	17.35 bar	17.35 bar
Evaporation temperature	125°C	125°C
Thermal split fraction	0.1	0.1
Reduced compressor mass flow rate	1	-
Reduced intermediate pressure	-	0.13
Cold stream temperature rise in the recuperator	17.12 K	-
Cooling water temperature	35°C	40°C
Condensation temperature	42.7°C	47.7°C
Condensation pressure	2.35 bar	2.74 bar
Evaporation temperature	7°C	7°C
Evaporation pressure	0.65 bar	0.65 bar
Expander hydraulic power	10.51 kW	9.91 kW
Expander generator power output	10.09 kW _e	9.51 kW _e
Pump hydraulic power	0.85 kW	0.86 kW

D 5.5 | Technology benchmark and competitor analysis of ZHENIT
WH2X systems

Pump motor power consumption	1.00 kW _e	1.01 kW _e
Compressor hydraulic power	0.32 kW	0.28 kW
Compressor motor power consumption	0.37 kW _e	0.32 kW _e
Compressor volumetric capacity	9.1 m ³ /h	13.5 m ³ /h
Net electric power output	8.71 kW _e	8.18 kW _e
Condenser heat duty	90.80 kW _{th}	90.44 kW _{th}
Subcooler heat duty	2.95 kW _{th}	3.01 kW _{th}
Recuperator heat duty	9.76 kW _{th}	9.35 kW _{th}
EVCC evaporator heat duty	3.1 kW _c	2.2 kW _c
Working fluid mass flow rate in the ORC evaporator and EVCC generator	0.456 kg/s	0.466 kg/s
Working fluid mass flow rate in the EVCC evaporator	0.019 kg/s	0.014 kg/s
Working fluid mass flow rate in the condenser and subcooler	0.475 kg/s	0.480 kg/s
Working fluid mass flow rate in the compressor	0.009 kg/s	0.014 kg/s
Ejector secondary mass flow rate	0.009 kg/s	0.014 kg/s
Condenser cooling water mass flow rate	4.346 kg/s	4.328 kg/s
Subcooler cooling water mass flow rate	0.141 kg/s	0.144 kg/s
EVCC evaporator cooling water mass flow rate	0.147 kg/s	0.106 kg/s
ORC electric efficiency	0.10	0.08
Ejector throat diameter	2.9 mm	2.9 mm
Ejector CDN outlet diameter	4.1 mm	4.1 mm
Ejector constant area section diameter	8.4 mm	8.6 mm
Ejector area ratio	8.46	8.54
Ejector entrainment ratio	0.203	0.297
EVCC electrical COP	6.56	5.23

4.5 Organic Rankine cycle technologies for maritime applications

The available literature shows that the organic Rankine cycle technology has attracted considerable attention for waste heat recovery in both terrestrial systems and on-board applications [72-74]. Among the studies dedicated to maritime use, Song et al. analysed a system with a rated power of 100 kW

D 5.5 | Technology benchmark and competitor analysis of ZHENIT WH2X systems

supplied by waste heat streams at different temperature levels, including the contribution of jacket cooling water for preheating [75]. Afterwards, Lion et al. reported a thermodynamic assessment of a closely related concept, thereby broadening the understanding of the subject [76]. Moreover, Casisi et al. examined several layouts for vessel waste heat recovery, with the aim of exploiting the characteristics of the on-board thermal sources, including high-temperature cooling water used upstream of the evaporator [77]. Alongside these scientific analyses, ORC technology has long been offered commercially for biomass systems, combined heat and power plants, geothermal applications, and industrial waste heat recovery by companies such as *General Electric*, *Turboden*, and *Ormat* [78, 79]. More recent developments have also led to initial proposals of ORC products for use on board vessels. These include the *Efficiency Pack* of *Orcan-Energy* [80], the *E-Power Pack* of *Alfa Laval* [87], and the *Hydrocurrent Organic Rankine Cycle Module 125EJW* developed through the partnership between *Calnetix Technologies* and *Mitsubishi Heavy Industries* [81, 82].

Representative performance data for ORC systems intended for marine waste heat recovery have been collected by Fisher et al. and are reported in Table 14.

Table 14 – Configuration, temperature levels, and performance of organic Rankine cycle systems for marine applications [7].

Configuration	Working fluid	Heat source temperature, °C	Net power output, kW	Efficiency, %	Development level
Basic cycle	R-245ca	82.8 / 51.9	427	7.39	Theoretical
Dual heat sources	Cyclohexane	300 / 90	96	20.75	Theoretical
Parallel devices	R245fa	300	101	10.20	Theoretical
Regenerated cycle	Toluene	190	482	20.90	Theoretical
Regenerated cycle	Benzene	293.15	396	22.00	Theoretical
Basic cycle	R123	315	625	16.38	Theoretical
-	-	Up to 550	150	10 – 20	Commercial
Basic cycle	R236fa / R245fa	160	994	8.43	Theoretical
Dual Loop	Water (high temperature) /	300 / 90	115	11.60	Theoretical

D 5.5 | Technology benchmark and competitor analysis of ZHENIT
WH2X systems

	R236fa (low temperature)				
Basic cycle	R245fa	80	125	6.20	Prototype
Regenerated cycle	Toluene	145	684	26.70	Theoretical
Four heat sources	R134a	240 / 140 / 89 / 65	3399	41.10	Theoretical
Dual loop	Wet steam ((high temperature) / R236fa (low temperature)	207 / 97	115	11.95	Commercial

The available economic analysis by Fisher et al. indicates a clear trend toward economies of scale for both conventional ORCs and marine ORC systems for on-board waste heat recovery when specific cost is considered. In particular, the specific investment cost decreases as the system size increases, showing that larger units are generally more economically favourable. In addition, the estimates reported for on-board ORC systems appear to be broadly consistent with those associated with terrestrial applications. This suggests that the economic behaviour of terrestrial ORCs can provide a representative benchmark for maritime systems, while also supporting the reliability of the available cost estimates for naval applications. More specifically, organic Rankine cycle devices for maritime applications with net electrical outputs in the range from 100 kW to 1000 kW are associated with specific costs decreasing from approximately 10000 €/kW to about 5000 €/kW in general [7].

A further relevant reference is provided by the ENGIMMONIA project, a sister project of ZHENIT, in which an ORC system was adapted to on-board applications for waste heat recovery and electricity provision. Within this framework, the ORC system was designed, fabricated, and tested under variable conditions for the heat source, including jacket cooling water and direct steam. More specifically, an *ORCAN Efficiency Pack eP M 150.200* was considered for maritime waste heat recovery on a long-distance vessel. A compact ORC system was designed to convert between 1000 kW_{th} and 2100 kW_{th} of thermal input into up to 200 kW_e of electrical power, with a reported footprint of 3.9 m² to limit the required installation space. The integration concept relies on two heat source levels, which are a hot water loop in the range from 110°C to 145°C and a warm water loop in the range from 75°C to 109°C, while the cooling loop can operate with inlet temperatures between -5°C and 40°C under the operating conditions considered. In the proposed configuration, excess steam from the exhaust gas boiler is

D 5.5 | Technology benchmark and competitor analysis of ZHENIT WH2X systems

transferred to the ORC through an intermediate hot water loop, whereas jacket cooling water provides the lower temperature contribution for preheating the working fluid. The same study also identifies the main adaptations required for maritime implementation, including compact assembly, vibration decoupling through compensators, automated response to heat source fluctuations, class compliance, heat rejection based on seawater, and the adoption of an intermediate heat transfer loop to protect and standardise the ORC device [83]. In the context of the ENGIMMONIA project, Stainchaouer et al. analysed the potential integration of recuperative ORC systems on a very large crude carrier using long-term operational data from the main engine and Diesel generator sets. The study evaluated the use of exhaust gas waste heat from the main engine alone and in combination with the exhaust gases of the generator sets, considering R245fa and R1233zd(E) as working fluids. The results showed that, at mean engine load, the net electrical output of the recuperative ORC can range from 381 kW_e to 532 kW_e, with thermal efficiencies between 13% and 15% when only the main engine exhaust gases are utilised. The net electrical power output can increase up to 653 kW_e with R245fa and 741 kW_e with R1233zd(E), while the thermal efficiency can reach values up to approximately 17% when the exhaust gases of the generator sets are also considered. The same analysis estimated annual carbon dioxide emission reductions in the range from about 4% to 7%, depending on the waste heat evaluation method and on the exhaust gas streams included [84].

Overall, although ORC systems are already successfully deployed in conventional WHR applications, their adaptation to maritime operations is still incomplete. The principal aspects that still require further development concern dedicated design for vessel use, experimental verification of the related prototypes, integration within the ship energy system, reduction of capital expenditure, and compliance with maritime regulatory requirements [72-74].

The benchmarking indicates that the ORC–EVCC prototype developed in the project occupies a different technological position with respect to the ORC systems reported in the literature. Whereas the majority of the available solutions are primarily oriented towards electricity generation from on-board waste heat, the ORC prototype is conceived as a more integrated system with a broader functional role within the energy systems of ships. A further distinction concerns the degree of integration of the developed prototype. Several ORC concepts available in the literature rely on modified thermodynamic layouts and on the exploitation of multiple heat sources to improve cycle performance [75-77]. Instead, the ORC–EVCC prototype combines the ORC with an ejector–vapour compression cooling cycle, thereby extending the conventional concept of a stand-alone ORC unit and increasing its operational flexibility.

D 5.5 | Technology benchmark and competitor analysis of ZHENIT WH2X systems

The comparison with commercially available systems leads to a similar conclusion, as they are mainly focused on power production [80-82, 85]. This also applies to the *ORCAN* module of the *ENGIMMONIA* project, which is conceived to supply electrical power to the on-board grid from recovered heat, despite the presence of multiple thermal streams and several maritime-specific integration measures [83]. The study based on long-term operational data further confirms that the principal performance indicator of conventional maritime ORC systems remains the net electrical output achievable from the available waste heat streams [84]. The prototype developed in the project is instead directed towards multifunctional operation, which may position it more favourably for vessel applications characterised by coupled electrical, thermal, and cooling demands.

5 Isobaric expansion engine prototype

The isobaric expansion engine is an innovative technology utilised to obtain mechanical power from heat at low temperature levels. The corresponding heat sources have temperatures up to about 100°C and, in some cases, may be as low as 40°C with limited thermal gradients of around 30°C in general. These devices are particularly suited to applications at small and medium scales, typically below 500 kW, where conventional heat engines or organic Rankine cycle devices may be economically or technically unattractive because of their low efficiency under such operating conditions.

Unlike conventional engines, in which expansion is commonly associated with a pressure drop, isobaric expansion engines operate according to a different thermodynamic principle: expansion occurs at approximately constant high pressure, while compression takes place at approximately constant low pressure. This isobaric operation can reduce thermal and mechanical losses, improve efficiency, and simplify the overall system architecture.

The main applications of IEEs include waste heat recovery from industrial processes, exhaust gases, and other low-temperature heat sources, as well as decentralised and miniature power generation systems. They may also be suitable for pumping and compression duties requiring specific speed and torque characteristics.

Historically, the same fundamental principle has appeared in several mechanical arrangements, including the Savery, Newcomen, and Watt pumping systems, followed by later developments such as the Worthington direct-acting steam engine and the Bush thermo-compressor. Among these, the Worthington arrangement is generally the most relevant reference for maritime waste heat recovery

D 5.5 | Technology benchmark and competitor analysis of ZHENIT WH2X systems

applications. Developed in the nineteenth century, it utilised high-pressure steam to directly drive a piston connected to a pumping cylinder, with self-acting valves regulating the flow of steam and liquid. Although primarily applied for water pumping, its expansion process at constant pressure makes it an important historical precursor to modern isobaric expansion engine technology.

5.1 Working principle of the IEE prototype

Isobaric expansion engines are energy conversion devices that provide useful work through an expansion process occurring inside a reciprocating chamber under conditions close to constant pressure. Their operation is based on the thermodynamic principle of isobaric expansion, whereby a working fluid is evaporated by recovering low-grade heat and subsequently expanded at approximately constant pressure to supply mechanical work. The basic cycle comprises four main stages. First, a low-boiling-point refrigerant is heated and evaporated by means of a low-temperature heat source, such as industrial waste heat or geothermal energy. The vapourised refrigerant then expands in the isobaric expander while the pressure remains essentially constant throughout the expansion stroke, thereby providing linear mechanical work through a piston mechanism. After expansion, the refrigerant transfers part of its residual thermal energy in a recuperator to preheat the pressurised liquid stream before it enters the evaporator. This internal heat recovery reduces the external heat input required in the evaporator and improves the thermal utilisation of the cycle. The refrigerant is then condensed by means of a cooling medium, such as water or ambient air. Finally, the condensed refrigerant is pumped back to the evaporator, thus completing the cycle.

The mechanical work delivered during the expansion process takes the form of linear reciprocating motion, which is then converted into hydraulic power through a double-acting piston integrated into the rod system of the expander. This hydraulic power can then be exploited in two main ways. It may be used directly in hydraulic applications, such as hydraulic actuators and lifting mechanisms, or converted into rotational mechanical power by means of a hydraulic motor, thereby enabling the system to drive conventional machinery or electric generators.

The simplified piping and instrumentation diagram of the isobaric expansion engine prototype is illustrated in Figure 26 and identifies the main components of the system and their interconnections.

D 5.5 | Technology benchmark and competitor analysis of ZHENIT
WH2X systems

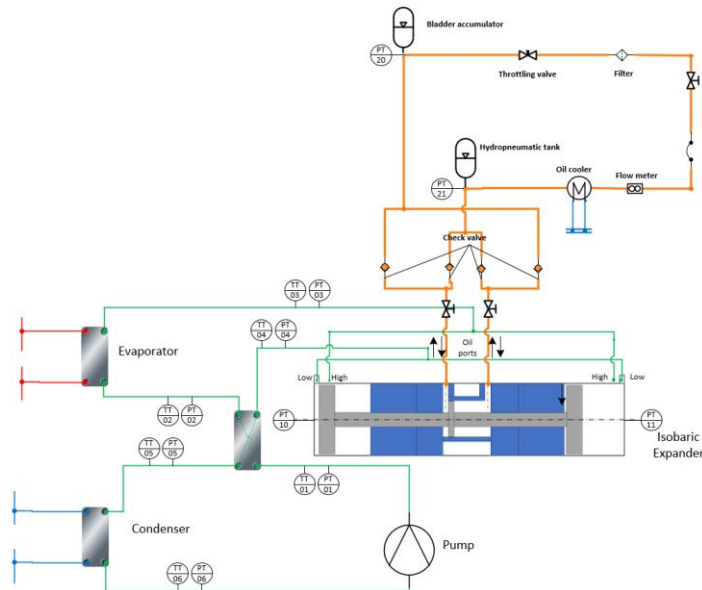


Figure 26 – Simplified piping and instrumentation diagram of the isobaric expansion engine prototype.

The evaporator is the heat exchanger in which the refrigerant is heated and vaporised using the low-grade heat source. The isobaric expander is the core component in which the vaporised refrigerant expands at constant pressure, thereby generating mechanical work. The recuperator is the internal heat exchanger in which the expanded refrigerant stream releases heat to the pressurised refrigerant before evaporation, thereby decreasing the heat duty imposed on the external heat source. The condenser is the heat exchanger in which the expanded vapour is cooled and condensed, whereas the pump is used to pressurise the condensed refrigerant and return it towards the recuperator and then to the evaporator. The hydraulic power conversion unit includes a double-acting piston and a hydraulic motor to convert the linear motion into hydraulic or rotational power. Control valves and sensors are also included in the system to regulate the flow, pressure, and temperature at the critical points of the cycle. Overall, the simplified piping and instrumentation diagram provides a clear representation of the flow paths, control strategies, and instrumentation required to ensure the safe and efficient operation of the isobaric expansion engine.

5.2 Principal components of the IEE prototype

The isobaric expansion engine comprises a set of core and auxiliary components that operate together to convert heat from a source at a low temperature level into mechanical work.

D 5.5 | Technology benchmark and competitor analysis of ZHENIT WH2X systems

5.2.1 Core components of the IEE prototype

The core components of the isobaric expansion engine prototype are the isobaric expander, the refrigerant feed pump, and the heat exchangers. The isobaric expander illustrated in Figure 27 is the central unit of the IEE prototype, where the refrigerant expands at constant pressure to provide mechanical work.

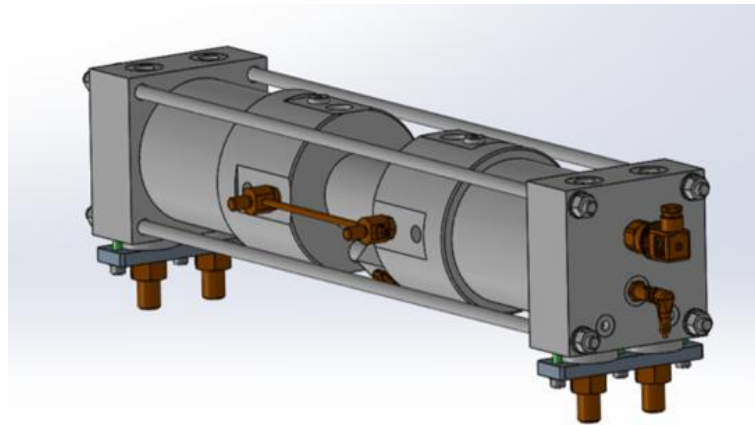


Figure 27 – Isometric view of the assembly of the expander of the IEE prototype.

The expander comprises three main chambers, which are the refrigerant chambers A and B, where the refrigerant R134a expands, and the hydraulic chamber, where the oil is pressurised. It features carbon steel cylinders and pistons. The diameter measures 120 mm for the refrigerant piston, while it has a diameter of 60 mm for the oil piston.

The refrigerant feed pump is a reciprocating pump designed to pressurise the refrigerant before entering the evaporator. It has a refrigerant piston diameter of 120 mm, while 65 mm is the dimension of the oil piston diameter. The prototype comprises the three heat exchangers indicated in Table 15 where their principal specifications are reported.

Table 15 – Technical specifications of the heat exchangers installed in the IEE prototype.

Parameter	Condenser	Regenerator	Evaporator
Manufacturer	SWEP	SWEP	SWEP
Model	B85Hx80/1P	B10THx50/1P	B80ASHx26/1P
Fluid on side 1	R134a	R134a	R134a
Fluid on side 2	Water	R134a	Water
Heat load	30.7 kW	4.86 kW	26.1 kW

D 5.5 | Technology benchmark and competitor analysis of ZHENIT
WH2X systems

Inlet temperature	40.0°C	60.0°C	41.0°C
Outlet temperature	17.0°C	26.6°C	89.0°C
Flow rate	0.15 kg/s	0.15 kg/s	0.15 kg/s
Total heat transfer area	4.68 m ²	1.49 m ²	1.44 m ²
Total pressure drop	2650 Pa	7010 Pa	6840 Pa
Number of plates	80	50	26
Total mass	13.70 kg	6.19 kg	6.88 kg

5.2.2 Auxiliary components of the IEE prototype

The auxiliary components utilised for the proper functioning of the isobaric expansion engine are check valves operating at low and high pressure, a high-pressure accumulator, a low-pressure accumulator, a needle valve, an oil filter, a flow meter, an oil cooler, and a sight glass for inspection of the hydraulic oil.

The high-pressure check valves FPR 1/2 and the low-pressure check valves VYC 179 are installed to prevent backflow in the hydraulic circuit. In particular, the low-pressure valves were selected to avoid cavitation under low-pressure conditions. The structure of a VYC 179 valve is presented in Figure 28.



Figure 28 – Photograph of a low-pressure check valve VYC 179 installed in the IEE prototype.

The high-pressure accumulator *H4000R* depicted in Figure 29 is a bladder-type accumulator utilised to stabilise pressure and absorb shocks in the high-pressure line.

D 5.5 | Technology benchmark and competitor analysis of ZHENIT
WH2X systems



Figure 29 – Photograph of the high-pressure accumulator *H4000R* utilised in the IEE prototype.

The low-pressure accumulator *CCT63-100* shown in Figure 30 is a hydropneumatic converter utilised to maintain a minimum operating pressure in the low-pressure line, thereby preventing cavitation.



Figure 30 – Photograph of the hydro-pneumatic converter *CCT63-100* included in the IEE prototype.

The needle valve *FT251U08* is a component that regulates the pressure differential within the system and enables throttling of the hydraulic flow. The oil filter *Dicsa F160XD100G10AB5DSZ30* is utilised to filter the hydraulic oil, ensuring the protection of the flow meter and the hydraulic motor from contamination. The flow meter *Profimess VM-01.2.1* presented in Figure 31 is a gearwheel volumetric sensor utilised to measure the flow rate of the hydraulic oil for system monitoring.

D 5.5 | Technology benchmark and competitor analysis of ZHENIT
WH2X systems



Figure 31 – Photograph of the gearwheel volume sensor *Profimess VM-01.2.1* used in the IEE prototype.

The oil cooler *Hrale B3-12-10* is a plate-type heat exchanger made of copper-brazed stainless steel, utilised to cool the hydraulic oil by means of water at approximately 20°C, thereby maintaining the hydraulic oil within the intended operating temperature range of the hydraulic circuit.

The sight glass was installed to enable visual inspection of the hydraulic oil level and flow, as well as to detect possible contamination or air entrainment. The schematic of the structure of the isobaric expansion engine prototype is presented in Figure 32, where the frame dimensions are specified.

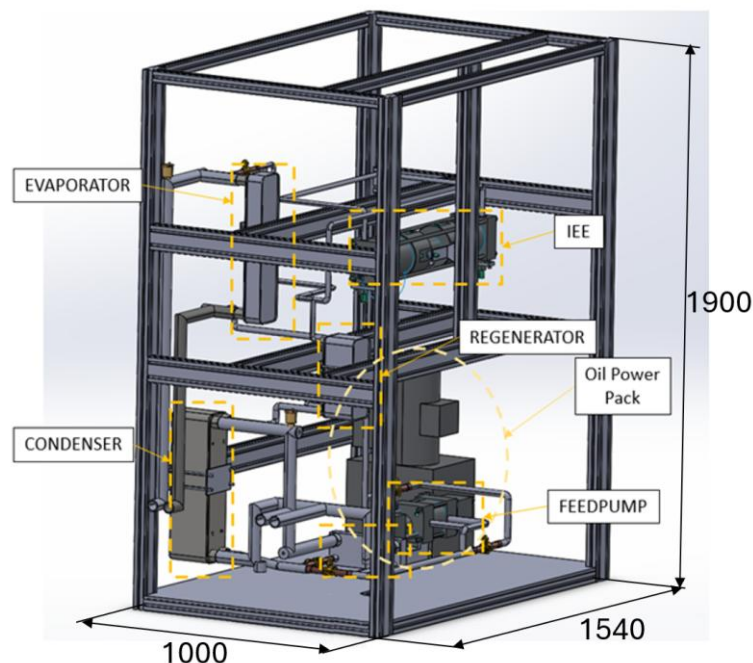


Figure 32 – Schematic of the structure of the IEE prototype with indication of the frame dimensions.

5.3 Design choices, novel features, and technology readiness level of the IEE prototype

This section presents the main design choices applied in the development of the isobaric expansion engine prototype, the distinctive features introduced into the system, and its current technology readiness level.

5.3.1 Main design choices for the IEE prototype

The isobaric expansion engine prototype was developed according to a modular approach based on its three main subsystems: the isobaric expansion engine module, the hydraulic oil module, and the fuel injection module. This design enables flexible testing and validation, while also allowing the separate fabrication, assessment, and subsequent integration of each subsystem. The overall concept is based on the isobaric expansion principle of the Worthington machine, which enables the generation of mechanical work under constant pressure conditions at both low and high levels.

A key design choice concerns the indirect utilisation of the mechanical work provided by the isobaric expansion engine. Instead of directly compressing fuel, which would introduce additional complexity, operational constraints, and safety concerns, the system was designed to pump high-pressure hydraulic oil. This solution enables the direct measurement of the mechanical output during laboratory testing and allows the power to be converted into shaft power by means of a hydraulic motor. The resulting shaft power can then be utilised to drive a marine Diesel fuel injection system or other mechanical processes.

5.3.2 Novel features of the IEE prototype

The prototype is specifically conceived for low-grade heat recovery, operating with R134a and targeting heat sources below 100°C, and focusing on those in the interval between 40°C and 50°C in particular. This extends the applicability of the IEE technology to conditions in which conventional power conversion systems are often technically or economically not convenient.

Another distinctive feature is the expander configuration with double effect, which enables useful work to be delivered during both piston strokes. Auxiliary chambers are also incorporated for piston lubrication and leakage collection, contributing to improved reliability, operational stability, and safety.

D 5.5 | Technology benchmark and competitor analysis of ZHENIT WH2X systems

The prototype further integrates pressure transducers and proximity sensors for real-time monitoring of pressure and piston position. These measurements support the optimisation of the operating frequency and improve the characterisation of the engine during experimental testing.

Finally, plate-type heat exchangers were selected based on detailed simulations and sensitivity analyses to ensure effective heat transfer within a compact system layout.

The isobaric expansion engine prototype can be integrated with the latent heat thermal energy storage prototype developed by *The University of Birmingham* to improve the continuity of the thermal input supplied to the expander. In this configuration, the LHTES unit can store waste heat during periods of availability and subsequently release it when the heat source becomes intermittent or temporarily unavailable. The stability of the thermal conditions imposed on the evaporator is particularly relevant for the IEE prototype because its mechanical and hydraulic output depends on them. Therefore, the integration with latent heat storage can support a more regular operation of the expander and extend its applicability from stand-alone heat recovery to a broader on-board waste heat recovery arrangement.

5.3.3 Technology readiness level of the IEE prototype

The technology readiness level of the isobaric expansion engine prototype is assessed as 4 because the system has been validated in a laboratory environment and its key components have been designed, manufactured, and tested under controlled operating conditions. This classification is consistent with the current stage of development of the prototype, which has progressed beyond conceptual design and numerical analysis to the realisation of an integrated experimental system.

5.4 Operating conditions and performance of the IEE prototype

During the design phase of the isobaric expansion engine, a set of operating conditions was defined to assess the performance of the system under representative thermal and hydraulic scenarios. These conditions were selected to resemble typical waste heat recovery applications at low temperature levels, in which the heat source is available at 80°C or 90°C, and the cooling medium is supplied at 14°C, 20°C, 30°C, or 35°C as representative reference values.

The experimental campaign was conducted under three different levels of hydraulic back-pressure, corresponding to the maximum, intermediate, and minimum opening conditions of the throttling valve, which were used to reproduce different load conditions on the hydraulic motor. The pump speed setting was maintained at 30% throughout the investigation so that the tests were conducted under equal refrigerant mass flow conditions, thereby ensuring consistency across the different operating points.

D 5.5 | Technology benchmark and competitor analysis of ZHENIT
WH2X systems

Overall, twenty-four operating points were examined, covering the full combination of the selected operating parameters.

The key performance indicators calculated for each operating condition are the hydraulic power output and the efficiency. The hydraulic power output is given by the product of the oil pressure difference Δp_{oil} and the volume flow rate of the oil measured in the hydraulic circuit. The thermal power introduced by the heat source is determined from the mass flow rate of the fluid acting as the heat source, its specific heat capacity, and the temperature difference measured between the inlet and outlet of the evaporator. The efficiency is determined by dividing the hydraulic power output by the thermal power input. The auxiliary power required by the pump for the working fluid is not subtracted from this value. If this contribution is included, the corresponding net efficiency should be calculated as the difference between the hydraulic power output and the pump power, divided by the external thermal power input supplied to the system.

Since the operation of isobaric expansion engines depends on the interaction between the thermodynamic boundary conditions and the active control settings imposed on the system, the operating point must be defined by both external thermal conditions and controlled variables. In the present experimental investigation, the operating conditions were determined by the temperature of the hot source, the temperature of the cold source, the refrigerant flow rate, and the oil load, the latter depending on the throttling conditions applied in the hydraulic module. The pump speed setting and the throttling valve position were controlled during the tests to impose repeatable operating conditions and to evaluate the response of the prototype under different hydraulic load levels. The specific parameters considered in the tests conducted on the prototype are summarised in Table 16.

Table 16 – Operating conditions of the isobaric expansion engine applied at the laboratory of *Tecnalia* during experimental testing.

Condition label	Cold-side temperature, °C	Hot-side temperature, °C	Refrigerant volume flow rate, L/min	Throttling level
T _i 14T _h 80	14	80	2.7	Minimum, medium, and maximum
T _i 20T _h 80	20			
T _i 30T _h 80	30			
T _i 35T _h 80	35			
T _i 14T _h 90	14	90	2.7	Minimum, medium, and maximum
T _i 20T _h 90	20			
T _i 30T _h 90	30			
T _i 35T _h 90	35			

The overall performance of the IEE prototype is determined on the basis of the two key performance indicators defined for the conditions specified in Table 16 and evaluated throughout the experimental campaign. In Figure 33, the distributions of the hydraulic power output and thermal efficiency as functions of the oil pressure difference at different temperatures of the cold side are presented, considering a fixed temperature of 90°C on the hot side.

D 5.5 | Technology benchmark and competitor analysis of ZHENIT
WH2X systems

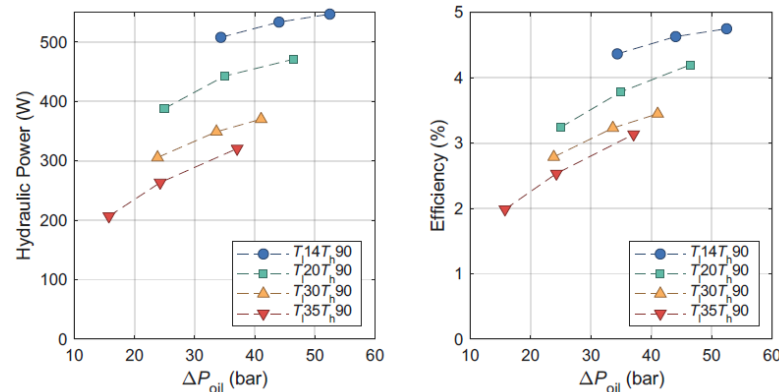


Figure 33 – Hydraulic power output and thermal efficiency as functions of the oil pressure difference at various temperatures of the cold side, for a fixed temperature of 90°C on the hot side.

In Figure 34, the outcomes of the experiments conducted with a fixed temperature of 80°C on the hot side show the distributions of the hydraulic power output and thermal efficiency as functions of the oil pressure difference at different temperatures of the cold side.

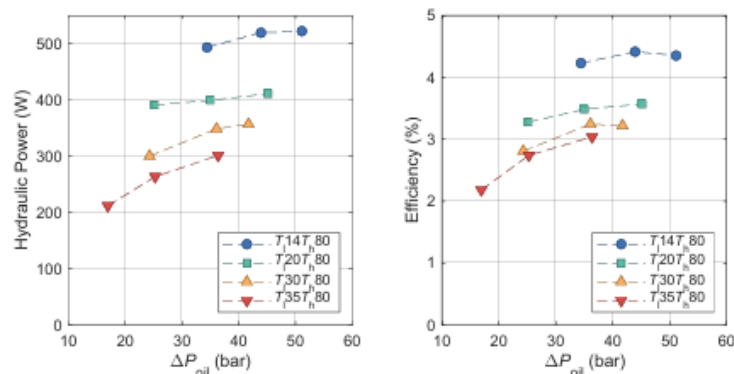


Figure 34 – Hydraulic power output and thermal efficiency as functions of the oil pressure difference at various temperatures of the cold side, for a fixed temperature of 80°C on the hot side.

Both the hydraulic power output and the thermal efficiency increase with rising temperature difference between the reservoirs at high and low temperatures. These two performance indicators also increase as the resistance on the oil side rises because this causes the machine to operate at progressively lower speeds. However, when the hydraulic resistance exceeds the range considered in the present investigation, the system enters an excessively slow operating regime, which results in a reduction in both the hydraulic power developed and the thermal efficiency. This behaviour is clearly observed in tests $T_{14T_h, 80}$ and $T_{30T_h, 80}$, among others. The optimal operating point within the range investigated corresponds to 14°C as the temperature of the cold side and 90°C as the temperature of the hot side.

5.5 Cost overview for the IEE prototype

The overview of the cost related to the most relevant components of the isobaric expansion engine prototype realised by *Tecnalia* is specified in Table 17, which indicates the quantity, the unit cost, and the total cost of each of them.

Table 17 – List of the most relevant components and the related costs for the IEE prototype.

Component	Quantity	Unit cost, €	Total cost, €
Isobaric expander	1 piece	1800	1800
Feed pump	1 piece	800	800
Evaporator heat exchanger	4 pieces	325	1300
Check valves for the refrigerant	4 pieces	50	200
Check valves for the oil	4 pieces	50	200
Pressure sensors	4 pieces	30	120
Temperature sensors	8 pieces	30	240
Piping	10 kg	10	100
Connectors and fittings	1 kg	50	50
Refrigerant HFC-134a	5 kg	65	325
Lubricating oil	30 g	1.33	40
Power pack	1 piece	800	800
Hydraulic components	15 kg	60	900
Total	-	-	6875

5.6 Isobaric expansion engine technologies for maritime applications

Among the historical solutions, the Worthington direct-acting steam engine is generally regarded as the most relevant reference when discussing the possible application of IEE technology to maritime waste heat recovery [86]. This machine is driven by steam supplied through the recovery of heat from exhaust gases. The steam cylinder and the pumping cylinder each contain a piston, and the two pistons are rigidly linked through a common rod. Dedicated valves control steam admission and release, while separate valves regulate the intake and discharge of the pumped liquid. When steam is introduced into the steam cylinder, the corresponding piston is forced through its stroke and simultaneously drives the piston located in the pumping chamber. Because the steam supply remains open during this

D 5.5 | Technology benchmark and competitor analysis of ZHENIT
WH2X systems

displacement, expansion takes place with approximately constant pressure, which is the defining characteristic of the device. At the end of the stroke, steam admission is interrupted, the pumping chamber is refilled with liquid, and the steam contained in the steam cylinder is expelled during the reverse movement, thereby completing the cycle. Although the basic concept is mechanically simple, several modifications have been proposed to improve performance [7]. These include, for example, the use of recuperative heat exchangers and pistons designed with thermal barrier membranes. Another attractive feature of IEEs is the possibility of operating with different working fluids, including refrigerants with low boiling points and natural working fluids, which makes the concept adaptable to different thermal conditions. This is particularly relevant in ship energy systems, where recoverable heat is available from multiple streams characterised by different temperature levels. Although water and steam may be considered in principle, they are generally less practical for low-temperature waste heat recovery applications. Despite this flexibility, the performance of the isobaric expansion engine configurations most frequently discussed in the literature, which are the Worthington and Bush types, is modest. In particular, the reported efficiencies are about 5% at net power levels below 1 kW, as indicated in Table 18, where the operating conditions and performance of these isobaric expansion engines are compared with those of a thermal power pump.

Table 18 – Operating conditions and performance of isobaric expansion engines compared to a thermal power pump [7].

Parameter	Cylinder volume, L	Pressure difference, bar	Cylinder period, s	Mechanical power, W	Efficiency, %
Thermal power pump	1.8	2	200	1	0.5
IEE-Worthington	0.02	15	2.5	20	5.4
IEE-Bush	1	23	4	500	6.3

The present state of development of isobaric expansion engine technology remains relatively limited. Most of the activity reported during the last decade has remained confined to demonstrators and proof-of-concept systems developed under laboratory conditions. The available literature does not document installations of isobaric expansion engine systems on board vessels. However, the company *Encontech BV* has conducted studies on the integration of this technology into ship energy systems [87]. Although these studies have not yet resulted in documented on-board installations, several possible uses can be envisaged for the mechanical output supplied by IEEs in marine energy systems. Historically, direct-

D 5.5 | Technology benchmark and competitor analysis of ZHENIT WH2X systems

acting steam pumps have been applied as emergency pumps or boiler feed pumps on ships [88]. More recently, the same general principle has been considered to replace electrically driven compressors, including uses in systems based on compressed air and vapour compression cooling devices [89].

The exploitation of the useful output constitutes another important aspect of isobaric expansion engines [7]. One possible solution consists of the direct use of the reciprocating motion provided by the expander, for example, to operate engine fuel injection equipment or to drive other positive-displacement pumps. In this case, the linear displacement of the IEE piston is utilised directly, without intermediate conversion into electricity. An alternative solution is represented by the transformation of the same reciprocating motion into electrical power through coupling with a hydraulic circuit and a generator. This dual approach to energy utilisation is receiving increasing attention in projects aimed at the decarbonisation of marine vessels. A further attractive characteristic of isobaric expansion engines is the comparatively low temperature level required to deliver useful work [7]. For this reason, the technology could potentially be deployed downstream of another on-board WHR system, functioning as a bottoming cycle for the further exploitation of residual low-temperature heat. For example, a turbine cycle could be applied to recover energy from exhaust gases as they cool from 350°C to 200°C for steam production, while the IEE could subsequently harness the remaining thermal content of the stream as it decreases from about 200°C to the acid dew point, which is in the range between 140°C and 160°C in general. In this context, the delivered mechanical output may be utilised to operate pumps and compressors [88], to support water desalination systems [28], or to be converted into electricity through hydraulic and electromechanical coupling [88]. Other possibilities include direct coupling with the cooling water circuit of conventional Diesel engines. In this case, the temperature levels are coherent with the operational range of isobaric expansion engines. Furthermore, integration with novel sustainable propulsion systems based on proton exchange membrane fuel cells supplied with hydrogen and operating at low temperatures shows considerable potential. Since these fuel cells reject waste energy as low-grade heat at temperatures below 80°C, the isobaric expansion engine is a suitable technology to be considered for the recovery of this otherwise lost energy stream.

At present, further work is still required before isobaric expansion engines can be considered technologically mature for maritime deployment. The main priorities concern the development of the fundamental understanding needed to design systems specifically adapted to on-board applications. In particular, performance improvements are required to comply with the operational requirements and constraints of on-board usage. This includes the optimisation of design and operation to increase useful

D 5.5 | Technology benchmark and competitor analysis of ZHENIT WH2X systems

power output, improve fuel efficiency, reduce emissions, and ensure sufficient reliability and durability under demanding marine conditions [7]. Additional investigations should also address the compatibility of IEEs with alternative fuels and different thermal sources, thereby contributing to improved sustainability and environmental performance in the maritime transport sector [88].

The isobaric expansion engine prototype developed within the ZHENIT project represents a meaningful progression beyond the existing competitor technologies. The available references indicate that the technology is still mainly represented by historical concepts, early demonstrators, and preliminary experimental arrangements, with very limited evidence of development specifically oriented towards maritime integration [87, 88]. Instead, the project prototype was conceived directly for waste heat recovery at low temperatures in on-board applications. The exemplary applications of the Worthington and Bush configurations reported in Table 18 are associated with efficiencies of 5.4% and 6.3%, respectively, and with mechanical power outputs ranging from tens to several hundreds of watts. In this context, the performance achieved by the isobaric expansion engine prototype confirms that the developed system operates within the same technological order of magnitude, with hydraulic power outputs between 200 W and 500 W and efficiencies between 2% and 5% over a relevant range of operating conditions. These values correspond to oil pressure differences approximately ranging from 15 bar to 55 bar and to two fixed temperatures of 80°C and 90°C on the hot side. This indicates that the developed system is already competitive with the literature benchmark in terms of its key performance indicators, while operating under conditions representative of low-grade heat recovery on board ships. Moreover, the experiments conducted showed that increasing the oil pressure difference can improve both hydraulic power output and efficiency up to a certain limit, beyond which the machine enters an excessively slow operating regime, and performance deteriorates. At the same time, further efforts remain necessary in relation to validation, performance improvement, and system integration before the IEE technology can be considered ready for wider deployment in maritime applications.

6 Sorption desalination and cooling prototype

The sorption desalination and cooling prototype was designed by the *CNR-ITAE* and *SorTech* to simultaneously produce desalinated water and chilled water by recovering waste heat at low and medium temperature levels for installation on board marine vessels. This device is intended to provide a technical solution to a critical challenge in maritime energy management: the substantial amount of thermal energy released into the environment through engine cooling circuits and exhaust systems. The

D 5.5 | Technology benchmark and competitor analysis of ZHENIT WH2X systems

primary application of the prototype is for commercial and passenger maritime vessels, including cargo ships and container ships, ferries and roll-on and roll-off passenger ships, cruise ships with high freshwater demand, and vessels used for offshore support and service operations.

The prototype directly contributes to the objective of achieving a 25% reduction in the primary energy consumption of the vessel, with this sub-system specifically targeting energy savings in the range between 7% and 10% through the replacement of electrically driven reverse osmosis desalination and refrigeration loads for vapour compression. By means of adsorption technology, the prototype is expected to reduce the electrical energy demand associated with cooling and water production by an amount between 30% and 50% within the overall vessel energy balance.

6.1 Working principle of the SDC prototype

The sorption desalination and cooling prototype operates according to a closed-cycle adsorption principle, using water as the refrigerant and a solid sorbent material, based on an advanced metal-organic framework or composite sorbent, as the adsorbent. In contrast to conventional absorption chillers utilising liquid absorbents, the adsorption cycle relies on the interaction between solid and vapour. This feature improves the robustness of the system under ship motion and changing orientation conditions.

The thermodynamic cycle operates between two distinct pressure levels established within a hermetically sealed vessel, where the thermodynamic circuit operates without moving mechanical components. The low-pressure level in the evaporator corresponds to the saturation pressure of water at the evaporator temperature, typically in the range between 10°C and 20°C, which is equivalent to the interval from 12 mbar to 23 mbar in terms of pressure. Seawater is supplied to the evaporator, where its partial evaporation extracts thermal energy and thereby produces the cooling effect. The high-pressure level in the condenser corresponds to the saturation pressure of water at the heat-rejection temperature, typically between 30°C and 40°C, corresponding to the interval between 42 mbar and 74 mbar in terms of pressure. The vapour condensed under these conditions forms the desalinated water product.

Two sorption reactor modules, named reactor A and reactor B, operate in alternating half-cycles to provide a quasi-continuous supply of cooling and freshwater. During the adsorption half-cycle, reactor A operates under adsorption conditions, while reactor B operates simultaneously under desorption

D 5.5 | Technology benchmark and competitor analysis of ZHENIT WH2X systems

conditions. Reactor A, maintained at an adsorption temperature of approximately 30°C, is cooled by the seawater circuit. Under these conditions, water vapour obtained in the evaporator is continuously adsorbed by the sorbent bed, thereby maintaining the low-pressure conditions required in the evaporator. The heat released during the exothermic adsorption process is removed through the cooling water circuit. At the same time, reactor B, maintained at a desorption temperature of approximately 80°C, is heated by waste heat recovered from the vessel, for example, from jacket water or a heat exchanger recovering heat from exhaust gases. As a result, the water previously adsorbed in the sorbent bed is desorbed as vapour and conveyed to the condenser at the higher pressure level, where it condenses and forms the freshwater product.

During the desorption half-cycle, the roles of the two reactors are reversed. After a predefined cycle time, typically between 300 s and 600 s, the heat transfer fluid connections are switched by automated valves. Reactor A then receives waste heat and begins the desorption process, whereas reactor B is supplied with cooling water and starts the adsorption process. Before the main vapour transfer is established, a short pre-heating and pre-cooling period, generally corresponding to an interval between 10% and 15% of the total cycle time, is required to bring the sorbent beds to the appropriate temperature and pressure conditions.

Compared to conventional adsorption chillers, in which heat and mass transfer are commonly associated with contact in the vapour phase, the reactor of the prototype utilises a heat transfer fluid in the liquid phase circulating through internal heat exchanger plates installed within the sorbent bed. This configuration provides several advantages, including a higher heat transfer coefficient between the heat transfer fluid and the sorbent compared with arrangements operating in the vapour phase and using finned tubes, reduced thermal mass of the heat exchanger structure, with a consequent improvement in cycle efficiency, a more homogeneous temperature distribution within the sorbent bed, and compatibility with ship motion, as the liquid heat transfer fluid is confined within closed channels.

6.2 Principal components of the SDC prototype

Two sorption desalination and cooling prototypes have been designed and fabricated within the ZHENIT project. The two devices differ primarily in terms of their installation context and the extent of the instrumentation utilised. The bill of materials for the prototypes is provided in Table 19.

D 5.5 | Technology benchmark and competitor analysis of ZHENIT
WH2X systems

Table 19 – Bill of materials of the two developed sorption desalination and cooling prototypes.

Component	Quantity per device	Total quantity	Total cost, €
Sorption reactor housing module	2	4	8000
Silica gel	120 kg	240 kg	720
Plate evaporator	1	2	1000
Plate condenser	1	2	1000
System separation high-temperature loop	1	1	500
Seawater buffer tank	1	1	200
Desalinated product water tank	1	1	200
HTF circulation pump for the hot side	2	4	600
Seawater and coolant circulation pump	1	2	700
4-way HTF switching valve set	1 set	2 sets	1200
Vacuum butterfly valves	8	16	8000
Temperature sensors <i>PT1000</i>	20	40	1200
Pressure transducers	2	4	2600
Flow meters	4	8	3600
Programmable logic controller system	1	2	8000
Vacuum submersible pump	1	2	1300
Insulation for reactor modules and vessels	1 set	2 sets	1600
Structural skid and frame	1	2	4000
Pipework, fittings, and valves	1 lot	2 lots	1000
Wiring harness and cable tray	1 lot	2 lots	1000
Safety and relief devices	1 set	2 sets	200
Level sensor	1	2	2000
Vacuum pump for evacuation	1	1	800
Air compressor	1	1	500

The main characteristics of the two SDC prototypes, together with their respective test conditions and operating environments, are listed in Table 20. One prototype is installed at the laboratory of *Tecnalia* for controlled testing under representative boundary conditions, while the other is installed on board the vessel *Teseo I* of *Tringali S.r.l.* to assess system performance under real operating conditions at sea.

D 5.5 | Technology benchmark and competitor analysis of ZHENIT WH2X systems

Table 20 – Prototype characteristics, test conditions, and operating environments for the SDC prototypes installed at the laboratory of *Tecnalia* and on board the ship *Teseo I* of *Tringali S.r.l.* for testing.

Parameter	Prototype for <i>Tecnalia</i>	Prototype for <i>Tringali</i>
Nominal cooling capacity	10 kW _{th,cold}	10 kW _{th,cold}
Test duration	At least 500 h	At least 250 h
Location	Laboratory of <i>Tecnalia</i> , in Azpeitia, in Spain	On board <i>Teseo I</i> , in Augusta, in Italy
Heat source	Electric boiler	Vessel jacket-water circuit and exhaust-gas heat exchanger
Motion testing	Test rig of <i>CNR-ITAE</i>	Real sea conditions

The selected ship, shown in Figure 35, is a fishing vessel operating near Mazara del Vallo, in Sicily. The propulsion system consists of two independent Diesel powertrains, *FPT model N60 ENT M37*, each providing 398 kW at 2800 rpm as the maximum power output. The marine engines have six cylinders and a displacement of 6000 cm³ and are equipped with supercharging and intercooling. The engines are connected to the propeller shafts through inverter and reduction gear units, with one shaft line associated with each propulsion unit. The propulsion system is positioned in the stern area, in a dedicated compartment housing the two engines, the gearboxes, and their electronic control units. One of the powertrains drives a *Bosch 28 V, 10/80 A* alternator utilised to provide 24 V direct current.



Figure 35 – Photograph of the fishing vessel *Teseo I* of *Tringali S.r.l.* selected for the installation and testing of the sorption desalination and cooling prototype.

The CAD drawings illustrating the overall configuration of the two sorption desalination and cooling prototypes show the external dimensions of the frame and the internal arrangement of their principal components. The side view of the rendering of one SDC prototype is presented in Figure 36.

D 5.5 | Technology benchmark and competitor analysis of ZHENIT
WH2X systems

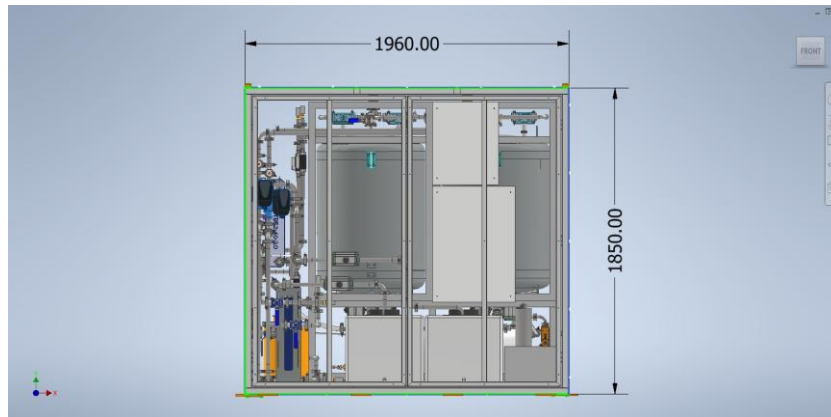


Figure 36 – Side view of the rendering of one SDC prototype illustrating the external dimensions and the internal arrangement of the principal components.

The top view of the rendering of the sorption desalination and cooling prototype that was developed and realised is provided in Figure 37.

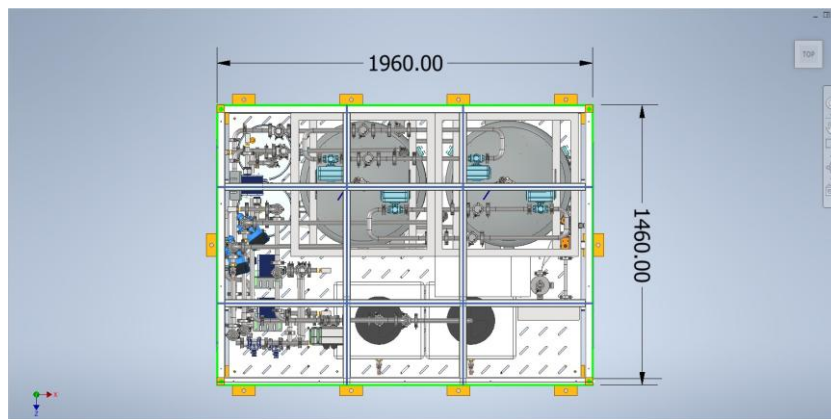


Figure 37 – Top view of the rendering of one SDC prototype illustrating the external dimensions and the internal arrangement of the principal components.

The main overall dimensions, footprint, and total mass of the sorption desalination and cooling prototype are listed in Table 21.

Table 21 – Principal dimensions, footprint, and total mass of one sorption desalination and cooling prototype.

Parameter	Value
Overall length	1960.00 mm
Overall width	1460.00 mm
Overall height	1850.00 mm
Footprint	2.86 m ²
Total mass	1500 kg

6.3 Design choices, novel features, and technology readiness level of the SDC prototype

The SDC prototype was designed to recover waste heat available within maritime vessels and utilise it for the combined production of desalinated water and cooling from thermal sources at low and medium temperature levels. The selected solution is characterised by specific design choices related to compact on-board integration and maritime operation, novel features associated with a system configuration based on sorption technology, and a maturity level that can be further improved through the ongoing experimental activities on board the selected vessel.

6.3.1 Main design choices for the SDC prototype

The main design choices of the sorption desalination and cooling prototype were defined to enable the recovery and utilisation of waste thermal energy from streams at low and medium temperatures available in ship energy systems for the combined supply of desalinated water and cooling.

The system layout was designed to ensure compactness and suitability for maritime applications. All the principal components, including the sorption reactors, seawater and desalinated water buffer tanks, plate heat exchangers for cooling provision and heat rejection, pumps, vacuum system, instrumentation, and control cabinet, were integrated into a single skid-mounted frame with a footprint below 3 m² in total. This integrated arrangement was defined to facilitate installation within the constrained spaces typically available in marine engine rooms.

Further design choices were specifically related to the maritime environment. The prototype configuration was developed to ensure reliable operation under ship motion, and dedicated dynamic testing was considered to assess hydraulic stability and sorbent performance under oscillatory conditions representative of vessel motion. In parallel, the materials and coatings of the components exposed to seawater were selected to limit corrosion, while the seawater pumping system and flow distribution were designed with attention to cavitation prevention and durability over the long term.

From the control and monitoring perspective, the prototype is equipped with an internal programmable logic controller, which communicates with the overall supervisory control and data acquisition system developed by SIGLA through *MODBUS TCP* and *Profinet* industrial protocols. In parallel, the monitoring platform of *KYMA* receives the operating data required for performance tracking and energy balance assessment.

6.3.2 Novel features of the SDC prototype

The sorption desalination and cooling prototype incorporates several novel features that distinguish it from more conventional cooling and desalination systems based on sorption processes and enhance its suitability for maritime waste heat recovery applications.

A first novel aspect concerns the application of a sorption technology driven by waste heat, rather than conventional desalination and refrigeration systems powered by electricity, in order to exploit waste heat availability in vessel energy systems.

A second important innovative feature is the selection and optimisation of the sorbent material. Advanced sorbents, including metal-organic frameworks and composite sorbents, were investigated to achieve efficient operation at driving temperatures between 60°C and 80°C under reference conditions. This operating interval is lower than that generally required by conventional microporous silica gel systems and is therefore more suitable for the thermal levels typically available in maritime WHR applications. The final selection was supported by a techno-economic assessment considering daily water production, cycling stability, and material cost.

Another distinctive feature concerns the reactor and heat transfer configuration. The prototype was developed according to the solutions introduced by *Sorption Technologies GmbH*, in which heat transfer between the sorbent and the refrigerant occurs in the liquid phase. This configuration was selected to enhance heat exchange effectiveness within the sorbent module and to improve the overall performance of the system under the intended operating conditions.

A further important innovative characteristic is the dual-mode operating capability of the prototype. The cycle architecture allows the independent or simultaneous production of chilled water and desalinated freshwater through appropriate adjustment of the operating boundary temperatures. This provides a level of functional flexibility that is particularly advantageous in maritime applications, where cooling and freshwater demands may vary significantly with operating conditions.

The sorption desalination and cooling prototype can be integrated with the latent heat thermal energy storage prototype developed by *The University of Birmingham* to enable load shifting during periods in which waste heat is temporarily unavailable. Additionally, the SDC prototype is thermally compatible with cascade operation together with the ORC–ejector prototype developed by the *National Technical University of Athens*, from which it can receive heat at the lower temperature level in the range from 70°C to 80°C from the ORC desuperheater. In this way, the prototype is suitable for operation both as a

D 5.5 | Technology benchmark and competitor analysis of ZHENIT WH2X systems

stand-alone device and in combination with a broader on-board energy system, under conditions representative of maritime operation.

6.3.3 Technology readiness level of the SDC prototype

The technology readiness level of the sorption desalination and cooling prototype has progressed significantly during the course of the project. Before the start of the project, *CNR-ITAE* and *SorTech* had designed and preliminarily validated a sorption module with a nominal capacity of 10 kW for desalination in a terrestrial desert application, driven by waste heat at 80°C, which was not yet adapted to marine operating conditions. This device was assessed at TRL 3, corresponding to an experimental proof of concept. During the project, the first configuration of the prototype for maritime applications was designed and fabricated, and subsequently tested at the laboratory of *Tecnalia* in an integrated system configuration. Thus, the prototype reached TRL 4, corresponding to technology validation in a laboratory environment. By the end of the project, the target is to achieve TRL 5, which corresponds to technology validation in a relevant environment. This progression is supported by the ongoing experimental campaign on the prototype installed on board the pilot fishing vessel *Teseo I* of *Tringali S.r.l.* in real navigation conditions, complemented by further extensive testing planned at the *CNR-ITAE* laboratory.

6.4 Operating conditions and performance of the SDC prototype

The sorption desalination and cooling prototype is designed to operate in integration with the main system-level interfaces generally available on board maritime vessels and compatible with the selected pilot vessel. The thermal driving source is represented by the waste heat recovery circuit, which may be based either on the engine jacket water, available at approximately 90°C, or on a boiler exhaust heat exchanger, operating in the range between 80°C and 100°C, as reference values. Under these conditions, the unit requires a supply of hot water delivered at the design temperature and corresponding flow rate to ensure the intended sorption operation. Heat release is achieved through a seawater cooling circuit connected to the condenser, including the related inlet strainer, circulation pump, and overboard return line. The cooling effect produced by the prototype is delivered through the hydraulic loop that supplies chilled water, which can serve either the on-board heating, ventilation, and air-conditioning system or the cooling loads associated with cargo refrigeration. At the same time, the

D 5.5 | Technology benchmark and competitor analysis of ZHENIT
WH2X systems

desalinated water provided by the system is discharged to the on-board freshwater storage and distribution network.

The design points and operational intervals of the conditions experimentally tested for the sorption desalination and cooling prototype are listed in Table 22.

Table 22 – Operating conditions of the sorption desalination and cooling prototype imposed during the experiments.

Parameter	Design point	Operational range
Waste heat driving temperature	80°C	60°C – 100°C
Adsorption and heat rejection temperature	30°C	25°C – 40°C
Evaporator temperature on the cooling side	15°C	10°C – 20°C
Nominal cooling capacity	10 kW _{th,cold}	3 kW _{th,cold} – 12 kW _{th,cold}
Nominal waste heat input	15 kW _{th} – 17 kW _{th}	Proportional to cooling capacity
Thermal COP for cooling	0.65	0.50 – 0.75
Half-cycle duration	400 s – 600 s	200 s – 800 s
Evaporator pressure	17 mbar with saturation at 15°C	12 mbar – 23 mbar
Condenser pressure	42 mbar with saturation at 30°C	32 mbar – 74 mbar
HTF flow rate per reactor	0.5 m ³ /h – 1.5 m ³ /h	Depending on the variable-frequency drive pump
Seawater flow rate	1 m ³ /h – 3 m ³ /h	Depending on the load
Ship roll for the on-board device	±5°	±15° at 0.1 Hz

The summary of the key performance indicators, acceptance criteria, and verification methods for the sorption desalination and cooling prototype, determined for representative operating conditions, is reported in Table 23.

Table 23 – Key performance indicators, target values, and verification methods for the SDC prototype.

Key performance indicator	Target value	Measurement method
Thermal COP for the cooling mode	0.6 – 0.7	Calorimetric measurement
Cooling capacity at the design point	10 kW _{th,cold}	Chilled-water heat-exchanger calorimetry

D 5.5 | Technology benchmark and competitor analysis of ZHENIT WH2X systems

Specific daily water production improvement over silica gel	≥ 30%	Product-water mass flow meter and sorbent mass measurement
Rolling penalty at ±15° with 0.1 Hz	< 10% decrease in COP and specific daily water production	Six-degree-of-freedom rolling-rig testing
Cycle time stability	< 5% drift over 10 cycles	Programmable logic controller cycle log and pressure-time profiles
On-board operation duration	≥ 250 hours	Supervisory control and data acquisition operating-hours log
Vacuum integrity in terms of leakage	< 1·10 ⁻⁵ mbar·L/s	Helium leak test and operating vacuum trend

6.5 Sorption desalination and cooling technologies for maritime applications

Technologies for cooling and freshwater production supplied by heat are receiving increasing attention in maritime energy systems because ships simultaneously require refrigeration and desalination while also releasing substantial amounts of recoverable thermal energy. Traditional refrigeration based on vapour compression has historically been the most relevant solution in maritime applications, especially for refrigerated cargo vessels and reefer systems, but its dependence on electrical power and conventional refrigerants has motivated the investigation of alternative systems better suited to waste heat utilisation [90]. In this context, the main technological routes of interest are absorption refrigeration, adsorption cooling and desalination, and hybrid configurations combining thermally driven cycles and mechanically driven cycles.

Absorption refrigeration is one of the most mature technologies based on thermal energy. Its operation relies on the evaporation of a refrigerant, often ammonia, to produce a cooling effect, followed by the absorption of the refrigerant vapour into a liquid solution. The resulting solution is then pressurised by a pump and supplied to a generator, where thermal input separates the refrigerant from the absorbent. The desorbed refrigerant is subsequently condensed and recirculated to the evaporator, thereby closing the cycle. In maritime waste heat recovery, the regeneration stage is commonly driven by hot water provided by the recovery of exhaust gases, while seawater typically functions as the sink for condensation [7]. Compared with conventional systems based on vapour compression, absorption

D 5.5 | Technology benchmark and competitor analysis of ZHENIT WH2X systems

devices require significantly less electrical power because the compressor is replaced by a liquid pump, and the refrigerant is regenerated thermally rather than mechanically.

Devices based on absorption refrigeration are already available commercially, but their direct adaptation to on-board use still requires validation in specific marine environments, satisfactory integration with existing ship energy systems, reduced capital and operating costs, and compliance with maritime regulations [91, 92]. A wide range of absorption cycle arrangements has been investigated to improve system performance, including two-stage systems, cascade configurations, and hybrid cycles combining absorption and compression processes. The resulting coefficients of performance and temperature levels depend significantly on the working pair and the cycle configuration considered [93]. For maritime applications, the most frequently utilised pairs are NH₃/H₂O and H₂O/LiBr, although other absorbent mixtures containing inorganic salts have also been proposed. The existing literature analyses generally involve generator temperatures from 80°C to 120°C, condenser temperatures between 20°C and 40°C, and absorber temperatures in the interval between 25°C and 30°C, which makes the reported cases reasonably comparable [7]. The predicted performance of on-board integrated systems determined in the literature is reported in Table 24 for reference cases. Under these conditions, the typical values of the coefficient of performance are between 0.4 and 0.7, while the cooling effect is commonly delivered at temperatures close to -5°C, although lower evaporation levels have also been reported in specific literature cases [7].

Table 24 – Working pairs, temperature levels, and performance of absorption refrigeration systems considered for integration on board ships [7].

Working pair	Generator temperature, °C	Condenser temperature, °C	Evaporator temperature, °C	Absorber temperature, °C	COP, -
NH ₃ /H ₂ O	90 – 120	20 – 40	20 – 40	25	0.60 – 0.70
NH ₃ /H ₂ O	80 – 110	20 – 30	-5 – 0	-	0.40 – 0.60
NH ₃ /H ₂ O	-	25 – 36	-30 – 0	-	0.45 – 0.55
H ₂ O/LiBr	65 – 90	30	-	30	0.70 – 0.90
NH ₃ /H ₂ O	80 – 110	20 – 40	-5	25	0.50 – 0.70
H ₂ O/LiBr	98 – 99	-	-	-	0.61 – 0.64

A second and more directly relevant category for the present project is constituted by cooling and desalination systems based on adsorption. In these technologies, the refrigerant vapour is not dissolved

D 5.5 | Technology benchmark and competitor analysis of ZHENIT WH2X systems

into a liquid phase, but is instead retained by a porous solid adsorbent. During regeneration, thermal energy is utilised to desorb the refrigerant and restore the sorbent capacity. Typical adsorbents include silica gel, although more advanced materials such as metal-organic frameworks have also attracted considerable attention. If seawater is used as the refrigerant, the same cycle can also provide freshwater, because the sequence of evaporation and condensation naturally separates water from dissolved salts. In this operating mode, however, the attainable cooling effect is generally limited to temperatures between 0°C and 5°C, which are typical of chilled water, due to the thermodynamic behaviour of seawater at low pressure levels [7]. The reference layout most often discussed in the literature is the two-bed configuration, but more complex three-bed systems and four-bed systems have also been examined to improve continuity of operation and capacity [94-96]. The reported cooling capacities are relatively modest, with maximum values typically around 100 kW, and the technology still has to be regarded as emerging.

The literature contains only a limited number of studies based on adsorption that are specifically relevant to maritime use. Palomba et al. examined a coupled sorption cooling and desalination system integrated with a conventional stage of vapour compression for a fishing vessel [97]. In that concept, the adsorption section meets the cooling requirement, whereas the subsystem for vapour compression provides lower refrigeration temperatures. The adsorption part of the system was associated with a coefficient of performance of approximately 0.06, while the specific cooling power varied significantly with the seawater temperature utilised as an external sink. Lu and Wang also investigated an adsorption refrigerator driven by engine exhaust gas and reported a coefficient of performance of 0.29 for seawater at 28°C as the temperature reference [98]. A further relevant contribution is provided by the ENGIMMONIA project, in which a 20 kW_c adsorption chiller was developed for maritime waste heat recovery and cooling provision. The device was conceived to recover thermal energy available on board ships and convert it into useful cooling, thereby reducing the demand associated with electrically driven refrigeration systems. The experimental validation also demonstrated stable operation under vessel rolling conditions, confirming the potential suitability of adsorption cooling technology for maritime environments characterised by dynamic motion and variable operating conditions. This result is particularly relevant because it provides evidence of validation in a maritime context for a thermally driven adsorption system, which remains limited in the available literature on cooling technologies for maritime applications [83]. Although these studies confirm the technical feasibility of thermally driven adsorption systems for ship applications, they also indicate that the technology is still at a research and

D 5.5 | Technology benchmark and competitor analysis of ZHENIT
WH2X systems

development stage. The main directions for improvement concern the development of better adsorbents, enhanced performance under variable conditions, higher reliability, improved scalability, and integration strategies capable of reducing both environmental impact and operational expenditure [99]. The cost information currently available is not clear, but the specific costs reported are generally between 1200 and 1300 €/kW for commercial adsorption chillers and prototypes [88-90]. The cooling power and specific cost of two commercially available adsorption chillers and one prototype are listed in Table 25 as references for the SDC prototype developed in this project.

Table 25 – Model, cooling power, specific cost, and advancement level of three reference adsorption chillers [7].

Device	Cooling power, kW	Specific cost, €/kW	Level of advancement
<i>SorTech eCoo 2.0 Silica Gel IP20</i>	16	1188	Commercial
<i>InvenSor LTC30 e plus</i>	10 – 35	1327	Commercial
Adsorber with silica gel and water	8	1331	Prototype

A third group of competing solutions is represented by hybrid refrigeration systems. Although they are less directly comparable with the sorption desalination and cooling prototype than absorption systems or adsorption systems, they are relevant within the context of cooling technologies driven by thermal energy for maritime applications. These systems combine two or more cooling technologies to exploit waste heat more effectively and reduce the electrical demand of refrigeration [7]. In the maritime sector, the principal examples are cascade configurations coupling an absorption cycle with a system relying on vapour compression. Garimella et al. investigated a hybrid unit in which an absorption chiller with LiBr/H₂O was integrated with a subcritical vapour compression cycle using carbon dioxide [100]. In that case, the heat released by the compression subsystem was partly reused to support the absorption section, and the resulting system was predicted to provide the same cooling duty with an electrical demand reduced by about 31% relative to a conventional solution with vapour compression. Cao et al. analysed another maritime hybrid concept for reefer vessels, in which an absorption subsystem driven by exhaust gases supplied chilled water that was then used to lower the condensing temperature of an existing device with vapour compression [101]. The outcomes indicated that the increase in on-board mass due to the additional components was limited and largely compensated by lower fuel consumption and a reduced requirement for auxiliary Diesel generation. Despite these promising results, hybrid refrigeration remains an option with a low level of maturity and is still far from widespread implementation on board ships [90, 102]. Therefore, the technology remains in the research and

D 5.5 | Technology benchmark and competitor analysis of ZHENIT WH2X systems

development stage. The main targets are the identification of system configurations capable of improving energy efficiency, the design of novel integrated arrangements combining different refrigeration and desalination processes, and the assessment of their environmental and economic performance relative to conventional stand-alone systems. In Table 26, the temperature levels, values of COP, and cooling power outputs are presented separately for the cooling section with vapour compression cooling, the absorption chilling section, and the overall integrated system for the two reference systems described.

Table 26 – Temperature levels, cooling power, coefficient of performance, and specific cost of reference hybrid refrigeration systems for maritime applications [7].

Device	Section	Temperature, °C	Cooling power, kW	COP, -	Specific cost, €/kW
LiBr/H ₂ O absorption chiller	Vapour compression cooling	5	82000	2.17	
	Absorption chilling	-40	51000	0.78	
	Total	-	133000	5.69	
Absorption subsystem driven by exhaust gases	Vapour compression cooling	7	108.41	1.92	4334
	Absorption chilling	-20	35.37	0.59	
	Total	-	143.78	2.00	

When comparing the sorption desalination and cooling prototype developed within the ZHENIT project with competitor technologies, absorption refrigeration systems constitute a relevant reference because they are also driven by thermal energy and are intended to reduce cooling loads supplied by electricity through waste heat utilisation. However, their physical principle differs substantially from that of the developed prototype, since they rely on liquid absorbent solutions and are generally oriented primarily towards cooling provision. Similarly, hybrid refrigeration systems are useful to define the broader context of cooling technologies driven by heat for maritime applications, but they are less directly comparable because they are based on the integration of heterogeneous cycles and on a higher level of system complexity. The most appropriate comparison is therefore represented by cooling and

D 5.5 | Technology benchmark and competitor analysis of ZHENIT WH2X systems

desalination systems based on adsorption. The literature is still mainly represented by theoretical studies, simplified demonstrators, and early prototypes, with only limited evidence of validation under conditions representative of on-board operation. In this respect, the developed SDC prototype occupies a more advanced position, as it was conceived specifically for maritime integration and was designed accordingly in terms of compactness, seawater compatibility, and operation under ship motion. In particular, it was designed to interface directly with the main on-board thermal and utility networks, including waste heat recovery from jacket water or heat exchangers recovering heat from exhaust gases, heat rejection based on seawater, delivery of chilled water for heating, ventilation, and air conditioning or cargo refrigeration, and freshwater discharge to the on-board storage and distribution system. A further distinction concerns the technological refinement of the developed system. Compared with conventional adsorption concepts, the prototype incorporates advanced sorbents selected for operation at driving temperatures in the range between 60°C and 80°C, a heat transfer arrangement based on liquid circulation within the reactor, and the capability to produce chilled water and desalinated freshwater either simultaneously or independently. The system has been designed for representative maritime boundary conditions, including waste heat driving temperatures between 60°C and 100°C, temperatures between 10°C and 20°C on the cooling side, and operation under ship roll. These features are particularly relevant because they extend adsorption operation to temperature levels more consistent with maritime waste heat availability, while also improving heat transfer effectiveness and operational flexibility.

The comparison is also favourable in terms of validation and technological maturity. Prior to the project, the underlying technology had only reached the level of an experimentally demonstrated concept for desalination in a terrestrial application. During the project, this basis was advanced to a first prototype designed, manufactured, and tested in an integrated laboratory configuration at *Tecnalia*, reaching TRL 4 for a maritime application. This progression is significant in relation to the literature, where dedicated validation under conditions representative of maritime operation remains limited, despite recent developments such as the adsorption chiller tested under vessel rolling conditions in the *ENGIMMONIA* project. Moreover, the installation of the second prototype on board the vessel *Teseo I* of *Tringali S.r.l.* and the current experimental campaign to measure system performance under real operating conditions at sea are supporting the transition towards TRL 5, which further reinforces this relevant technological progression.

7 Conclusions

The present research provides a detailed characterisation of the four innovative prototypes realised within the ZHENIT project and examines their position with respect to relevant benchmark and competitor technologies. The assessment considers the broader objective of improving waste heat recovery on board maritime vessels through technologies able to recover, store, convert, and utilise the thermal energy available from propulsion and auxiliary systems. The analysis indicates that the prototypes address complementary functions within an integrated maritime energy system, which are the temporal redistribution of waste heat, the conversion of thermal energy into electricity, heating, and cooling, the production of mechanical or hydraulic output from low-temperature heat, and the simultaneous provision of chilled water and desalinated freshwater.

The application context confirms that the relevance of these technologies is directly connected to the large amount of fuel energy released as excess heat in maritime propulsion systems. In conventional Diesel engine configurations, more than half of the fuel energy can be dissipated through exhaust gases, scavenge air, jacket water, lubricating oil, and other cooling streams. The temperature level, amount, and continuity of these waste heat sources vary with ship typology, route, operating condition, and energy demand distribution, thereby influencing the suitability of the different recovery, conversion, and storage technologies. Traditional solutions, such as waste heat boilers and turbocharging systems, already contribute to the utilisation of part of this recoverable energy. Furthermore, innovative technologies, including thermal energy storage systems, organic Rankine cycle systems, isobaric expansion engines, and sorption and desalination devices, can further extend the exploitation of waste heat sources at low and medium temperatures. In this regard, waste heat recovery can reduce fuel consumption by approximately 3% to 15%, depending on the vessel configuration and operating profile. These considerations confirm the need for technologies able to operate across different temperature intervals and to accommodate the temporal mismatch between heat availability and energy demand. For example, the implementation on board a cruise vessel of an integrated waste heat recovery system including these four emerging technologies could increase energy efficiency by 7.5% and reduce fuel consumption by 13% by exploiting thermal energy from exhaust gases, scavenge air, jacket water, and lubricating oil. These values confirm that the contribution of each prototype should not be interpreted only at device level, but also in relation to its role within a coordinated waste heat recovery architecture.

D 5.5 | Technology benchmark and competitor analysis of ZHENIT WH2X systems

The latent heat thermal energy storage prototype developed by *The University of Birmingham* represents a compact solution for the recovery, storage, and subsequent release of waste heat at low and medium temperature levels. The prototype integrates a heat exchanger comprising ten pillow plates with the phase change material RT80HC and uses water as the heat transfer fluid. The selected configuration was established through a systematic design procedure based on one-dimensional analytical modelling, three-dimensional computational fluid dynamics simulations, and experimental testing. The final device contains 367 kg of RT80HC and has a mass of approximately 710 kg in total. Under representative operating conditions, with inlet water temperatures of 90°C during charging and 70°C during discharging, the prototype achieves an energy storage capacity of 26.51 kWh, an energy storage density of 54.76 kWh/m³ referred to the core storage region, and a thermal power between 2.54 kW and 3.17 kW for water mass flow rates between 0.2 kg/s and 1.2 kg/s according to the estimations of the analytical and CFD models. The prototype was assembled and preliminarily tested at the *Tyseley Energy Park of The University of Birmingham*, after which an extended experimental campaign was conducted at the *Thermal Systems and Energy Efficiency Laboratory of Tecnalía* in conditions representative of the hot water requirements typically present on board maritime vessels. For the tests performed at the laboratory of *Tecnalía*, the prototype was operated with water volume flow rates between 1.0 m³/h and 3.5 m³/h, while the corresponding inlet temperatures were 90°C during charging and 70°C during discharging as principal values, with extended intervals between 90°C and 95°C for charging and from 30°C to 70°C for discharging. The comparison between the results of the analytical and computational fluid dynamics models indicates a coherent prediction of the main performance indicators and confirms the suitability of the modelling approach applied for the design of the system. Moreover, the experiments validate the correct functioning of the prototype in laboratory conditions and confirm the expected sequence of sensible heating, melting, sensible cooling, and solidification during charging and discharging. In relation to the state of the art, the system addresses a field in which sensible heat storage has been more frequently investigated for maritime applications, whereas latent heat storage offers a favourable combination of compactness, storage density, and thermal stability. The use of pillow plates is particularly significant because it enhances thermal exchange between the circulating water and the phase change material, supporting faster charging and discharging without requiring an excessively large storage volume. The device reached a technology readiness level equal to 4 during the project, while further validation in more representative maritime environments would support its progression towards TRL 5 in the future.

D 5.5 | Technology benchmark and competitor analysis of ZHENIT WH2X systems

The ORC–ejector integrated heat pump developed by the *National Technical University of Athens* is intended to exploit recovered thermal energy through a flexible conversion layout able to deliver different useful outputs according to the operating requirement. The prototype is designed to function with hot water from waste heat at 140°C and with 100 kW_{th} of thermal input. The system can operate in four configurations, which are electricity provision with recuperation in the organic Rankine cycle, combined delivery of heat and electrical power through the organic Rankine cycle operating without recuperation, simultaneous provision of cooling and electrical power through the ORC–EVCC arrangement, and exclusive cooling supply by means of the heat pump coupled with the ejector. At the design point, the system reaches a net electrical output of 10.30 kW_e in the mode dedicated to electricity provisioning and 7.68 kW_e in combined heat and power mode, with 88.97 kW_{th} as the corresponding heating output. The device provides cooling outputs in the range from 2 kW_c to 3 kW_c when operating in the cooling modes. The benchmark analysis indicates that organic Rankine cycle systems are already among the most mature technologies for waste heat recovery and have been widely considered for maritime applications. However, most existing systems are primarily designed only for electricity supply. The configuration developed in ZHENIT therefore differs from conventional ORC solutions because it combines electrical power, heat, and cooling functions within an integrated arrangement. The main contribution of the prototype is consequently related to functional flexibility and system integration, rather than to the optimisation of one isolated conversion mode. This feature increases the relevance of the system for vessels characterised by simultaneous and variable demands for electrical, thermal, and cooling services. At the same time, the specific integrated configuration remains less mature than conventional ORC systems because the interaction between the different operating modes, the control strategy, and the stability of the combined operation still require further verification. Consequently, the prototype is positioned at a technology readiness level between 3 and 4, and further experimental work is required to consolidate its operation and support its technological maturation.

The isobaric expansion engine prototype developed by *Tecnalia* addresses the recovery of waste heat at low temperatures through the provision of mechanical power and hydraulic output. This device is specifically designed to harness thermal sources below 100°C, where conventional power conversion technologies are generally less effective. Instead of relying on rotary expansion, the system exploits the evaporation and expansion at nearly constant pressure of R134a to provide reciprocating motion, which is then transferred to the hydraulic section of the device. In this way, low-temperature waste heat can

D 5.5 | Technology benchmark and competitor analysis of ZHENIT WH2X systems

be transformed into useful hydraulic output through a mechanically compact conversion architecture suitable for auxiliary actuation systems and hydraulic loads in maritime applications. Experimental tests were conducted with temperatures set at 80°C and 90°C on the hot side, temperatures ranging from 14°C to 35°C on the cold side, and different values of hydraulic resistance. The experimental campaign shows that hydraulic power output lies between 200 W and 500 W, while efficiency ranges from 2% to 5% across the investigated operating conditions. These results demonstrate that machine performance is governed not only by the available thermal gradient, but also by the hydraulic boundary conditions imposed on the expander. In particular, hydraulic resistance affects the cycle frequency and consequently influences both the useful hydraulic output and the energy conversion efficiency. An increase in oil pressure difference is beneficial only up to an intermediate range; when the resistance becomes excessive, the reciprocating motion slows down, and the performance decreases. Consequently, the hydraulic resistance should be regarded as a key parameter for both design and control. This aspect is particularly important for future optimisation, since the operating point of the expander must be selected by balancing pressure difference, cycle duration, hydraulic output, and efficiency. The benchmark comparison further indicates that the developed prototype achieves performance values aligned with the limited reference cases reported for isobaric expansion concepts, while offering a configuration more specifically oriented towards maritime waste heat recovery. The technology readiness level is assessed as 4, reflecting the design, manufacture, and experimental validation of the integrated system in a laboratory environment. Further work remains necessary to improve performance, reliability, durability, and integration within practical vessel energy systems.

The sorption desalination and cooling prototype developed by the *Institute of Advanced Technologies for Energy* of the *Consiglio Nazionale delle Ricerche* and by *Sorption Technologies GmbH* is conceived to convert waste heat available on board ships at low and medium temperature levels into chilled water and desalinated water. Two physical prototypes were realised within the project, one for controlled testing at the laboratory of *Tecnalia* and the other for testing on board the vessel *Teseo I* of *Tringali S.r.l.* under real navigation conditions. The process relies on a closed adsorption circuit, in which water functions as the refrigerant and an advanced solid sorbent provides the active material for water vapour adsorption and subsequent regeneration. The device is rated at 10 kW_{th,cold} in terms of nominal cooling capacity and is designed for thermal driving sources in the interval from 60°C to 100°C, with 80°C defined as the design point. In cooling operation, the target value of the thermal coefficient of performance is expected to remain between 0.6 and 0.7, while the expected improvement in specific

D 5.5 | Technology benchmark and competitor analysis of ZHENIT WH2X systems

daily water production is at least 30% with respect to silica gel. The benchmark assessment places the developed prototype within the broader field of thermally driven cooling and desalination technologies. Among the competing options, the benchmark is centred mainly on adsorption cooling and desalination systems because these technologies have the same solid sorbent operating principle as the ZHENIT prototype and can use low-temperature heat for the combined production of cooling and freshwater. Absorption refrigeration and hybrid refrigeration systems are considered as secondary references because they also belong to the broader field of thermally driven cooling technologies, but they are less directly comparable in terms of operating principle, functional scope, and system architecture. In particular, absorption refrigeration is commercially more mature but generally oriented towards cooling provision through liquid absorbent solutions, whereas hybrid refrigeration concepts can reduce the electrical demand of vapour compression systems at the cost of greater layout complexity due to the coupling of different thermodynamic cycles. The available literature on adsorption systems for ship applications is still limited, especially in terms of experimental evidence obtained under representative maritime conditions. For this reason, the ZHENIT prototype contributes to the advancement of the field by adapting the adsorption principle to a configuration intended for vessel installation, operation with seawater heat rejection, and exposure to ship motion. The main differentiating elements are the use of advanced sorbent materials, the reactor heat transfer arrangement based on liquid circulation, the possibility of producing chilled water and desalinated freshwater jointly or separately, and the adaptation of the system to maritime boundary conditions. The technology progressed from TRL 3 before the project to TRL 4 by means of integrated laboratory testing, while the on-board installation supports progression towards TRL 5 through the ongoing experimental campaign.

Overall, the technology benchmark and competitor analysis confirm that the four ZHENIT prototypes occupy distinct technological positions with respect to the current state of the art. The latent heat thermal energy storage prototype strengthens the role of compact storage systems for managing the temporal mismatch between waste heat availability and thermal demand. The ORC–ejector integrated heat pump extends organic Rankine cycle technology from electricity provision alone to multifunctional energy conversion. The isobaric expansion engine prototype provides the possibility of recovering mechanical or hydraulic output from low-temperature heat sources that are generally difficult to exploit. The sorption desalination and cooling prototype advances adsorption technology towards the combined supply of freshwater and cooling under maritime operating conditions. When considered together, the four prototypes define an integrated technological solution in which storage, conversion,

D 5.5 | Technology benchmark and competitor analysis of ZHENIT WH2X systems

mechanical recovery, and thermally driven supply of chilled water and freshwater can operate as complementary functions of the same waste heat recovery strategy. Their combined use could support a wider and more flexible strategy for waste heat recovery in vessel energy systems.

The main remaining challenges are associated with the progression from laboratory validation and prototype testing towards operation under representative maritime conditions. For all the technologies considered, future activities should focus on extended experimental campaigns, optimisation of operating strategies, improved control and monitoring, validation under dynamic thermal profiles, and integration with the thermal and electrical networks of vessels. Additional attention should be devoted to compactness, mass, footprint, reliability, durability, safety, manufacturability, and cost reduction, as these aspects have strong effects on the feasibility of practical on-board installation. On this basis, the results achieved within the ZHENIT project provide a relevant technological foundation for future replication activities and for the development of integrated waste heat recovery systems able to increase energy efficiency, reduce fuel consumption, and contribute to the decarbonisation of maritime transport.

Bibliography

- [1] European Commission, Fourth Annual Report from the European Commission on CO₂ Emissions from Maritime Transport (period 2018–2021), Brussels, 2023.
- [2] Wu, M., Li, K.X., Xiao, Y., and Yuen, K.F., Carbon Emission Trading Scheme in the shipping sector: Drivers, challenges, and impacts, *Marine Policy*, vol. 138, 2022. DOI: 10.1016/j.marpol.2022.104989
- [3] International Maritime Organization, Improving the energy efficiency of ships, accessed 25 January 2025, from <https://www.imo.org/en/OurWork/Environment/Pages/Improving%20the%20energy%20efficiency%20of%20ships.aspx>, 2025.
- [4] Mallouppas, G. and Yfantis, E.A., Decarbonization in Shipping industry: A review of research, technology development, and innovation proposals, *Journal of Marine Science and Engineering*, vol. 9, no. 4, pp. 415, 2021. DOI: 10.3390/jmse9040415
- [5] Singh, P.D.V. and Pedersen, E., A review of waste heat recovery technologies for maritime applications, *Energy Conversion and Management*, vol. 111, pp. 315-328, 2016. DOI: 10.1016/j.enconman.2015.12.073
- [6] Li, Y. and Shen, J., Thermodynamic, Economic, and Environmental Analysis and Optimization of a Multi-Heat-Source Organic Rankine Cycle for Large Marine Diesel Engine, *Processes*, vol. 13, no. 11, 3651, 2025. DOI: 10.3390/pr13113651
- [7] Fisher, R., Ciappi, L., Niknam, P.H., Braimakis, K., Karellas, S., Frazzica, A., and Sciacovelli, A., Innovative waste heat valorisation technologies for zero-carbon ships – A review,

D 5.5 | Technology benchmark and competitor analysis of ZHENIT
WH2X systems

- Applied Thermal Engineering*, vol. 253, 123740, 2024. DOI: 10.1016/j.applthermaleng.2024.123740
- [8] Zhang, W., Wang, J., Qin, G., Kuntal, S., Gong, F., and Yan, R., Review of the state-of-the-art of alternative marine fuels: A viable approach to zero-carbon shipping, *Cleaner Logistics and Supply Chain*, vol. 16, 100232, 2025. DOI: 10.1016/j.clscn.2025.100232
- [9] Kramer, J.V. and Steen, S., Sail-induced resistance on a wind-powered cargo ship, *Ocean Engineering*, vol. 261, 111688, 2022. DOI: 10.1016/j.oceaneng.2022.111688
- [10] Kolodziejcki, M. and Sosnowski, M., Review of Wind-Assisted Propulsion Systems in Maritime Transport, *Energies*, vol. 18, no. 4, 897, 2025. DOI: 10.3390/en18040897
- [11] Pan, P., Sun, Y., Yuan, C., Yan, X., and Tang, X., Research progress on ship power systems integrated with new energy sources: A review, *Renewable and Sustainable Energy Reviews*, vol. 144, 111048, 2021. DOI: 10.1016/j.rser.2021.111048
- [12] Huang, M., He, W., Incecik, A., Cichon, A., Królczyk, G., and Li, Z., Renewable energy storage and sustainable design of hybrid energy powered ships: A case study, *Journal of Energy Storage*, vol. 43, 103266, 2021. DOI: 10.1016/j.est.2021.103266
- [13] Grljusic, M., Medica, V., and Radica, G., Calculation of efficiencies of a ship power plant operating with waste heat recovery through combined heat and power production, *Energies*, vol. 8, no. 5, pp. 4273--4299, 2015. DOI: 10.3390/en8054273
- [14] Niknam, P.H., Ciappi, L., and Sciacovelli, A., Latent heat thermal energy storage system with pillow-plate heat exchangers topology – Assessment of thermo-fluid dynamic performance and application potential, *Applied Thermal Engineering*, vol. 265, 125606, 2025. DOI: 10.1016/j.applthermaleng.2025.125606
- [15] Zhu, S., Zhang, K., and Deng, K., A review of waste heat recovery from the marine engine with highly efficient bottoming power cycles, *Renewable and Sustainable Energy Reviews*, vol. 120, 109611, 2020. DOI: 10.1016/j.rser.2019.109611
- [16] Mondejar, M.E., Andreasen, J.G., Pierobon, L., Larsen, U., Thern, M., and Haglind, F., A review of the use of organic Rankine cycle power systems for maritime applications, *Renewable and Sustainable Energy Reviews*, vol. 91, pp. 126-151, 2018. DOI: 10.1016/j.rser.2018.03.074
- [17] Niknam, P.H., Fisher, R., Ciappi, L., and Sciacovelli, A., Optimally integrated waste heat recovery through combined emerging thermal technologies: Modelling, optimization and assessment for onboard multi-energy systems, *Applied Energy*, vol. 366, 123298, 2024. DOI: 10.1016/j.apenergy.2024.123298
- [18] Ciappi, L., Niknam, P.H., Fisher, R., and Sciacovelli, A., Application of Flat Plate Latent Heat Thermal Energy Storage for Waste Heat Recovery and Energy Flexibility in Maritime Sector, *ECOS 2023, Proceedings of the 36th International Conference on Efficiency, Cost, Optimization, Simulation and Environmental Impact of Energy Systems*, Las Palmas de Gran Canaria, Spain, pp. 2342-2353, 2023. DOI: 10.52202/069564-0211
- [19] Ciappi, L., Ding, Y., and Sciacovelli, A., Design of an innovative latent heat thermal energy storage prototype with pillow plates through analytical and computational fluid dynamics modelling, *Computational Thermal Sciences*, 2026. DOI: 10.1615/ComputThermalScien.2026063117

D 5.5 | Technology benchmark and competitor analysis of ZHENIT
WH2X systems

- [20] Piper, M., Olenberg, A., Tran, J.M., and Kenig, E.Y., Determination of the geometric design parameters of pillow-plate heat exchangers, *Applied Thermal Engineering*, vol. 91, pp. 1168-1175, 2015. DOI: 10.1016/j.applthermaleng.2015.08.097
- [21] Tran, J.M., Piper, M., Kenig, E.Y., and Scholl, S., Pillow-Plate Heat Exchangers: Fundamental Characteristics, in *Innovative Heat Exchangers*, Bart, H.-J. and Scholl, S., Eds., Cham, Switzerland: Springer, pp. 233-245, 2018.
- [22] Rubitherm Technologies GmbH, RT80HC, accessed 22 September 2024, from <https://www.rubitherm.eu/media/products/datasheets/Techdata - RT80HC EN 20102023.PDF>, 2023.
- [23] PCM Products, PlusICE Range, accessed 5 March 2024, from <https://www.pcmproducts.net/files/PlusICE%20Range%202021-1.pdf>, 2021.
- [24] Rubitherm Technologies GmbH, PX82, accessed 18 June 2024, from <https://www.rubitherm.eu/media/products/datasheets/Techdata - PX82 EN 03072020.PDF>, 2020.
- [25] Rubitherm Technologies GmbH, RT82, accessed 21 November 2024, from <https://www.rubitherm.eu/media/products/datasheets/Techdata - RT82 EN 09102020.PDF>, 2020.
- [26] Rubitherm Technologies GmbH, GR82, accessed 21 May 2024, from <https://www.rubitherm.eu/media/products/datasheets/Techdata - GR82 EN 03072020.PDF>, 2020.
- [27] Ciappi, L., Stebel, M., Smolka, J., Cappiotti, L., and Manfrida, G., Analytical and Computational Fluid Dynamics Models of Wells Turbines for Oscillating Water Column Systems, *Journal of Energy Resources Technology*, vol. 144, no. 5, 050903, 2022. DOI: 10.1115/1.4052216
- [28] Alva, G., Lin, Y., and Fang, G., An overview of thermal energy storage systems, *Energy*, vol. 144, pp. 341-378, 2018. DOI: 10.1016/j.energy.2017.12.037
- [29] Zhang, H., Baeyens, J., Caceres, G., Degreve, J., and Lv, Y., Thermal energy storage: Recent developments and practical aspects, *Progress in Energy and Combustion Science*, vol. 53, pp. 1-40, 2016. DOI: 10.1016/j.pecs.2015.10.003
- [30] Fisher, R., Ding, Y., and Sciacovelli, A., Hydration kinetics of K₂CO₃, MgCl₂ and vermiculite-based composites in view of low-temperature thermochemical energy storage, *Journal of Energy Storage*, vol. 38, 102561, 2021. DOI: 10.1016/j.est.2021.102561
- [31] Zhao, Y., Zhao, C.Y., Markides, C.N., Wang, H., and Li, W., Medium- and high-temperature latent and thermochemical heat storage using metals and metallic compounds as heat storage media: A technical review, *Applied Energy*, vol. 280, 115950, 2020. DOI: 10.1016/j.apenergy.2020.115950
- [32] Mabrouk, R., Naji, H., Benim, A.C., and Dhahri, H., A State of the Art Review on Sensible and Latent Heat Thermal Energy Storage Processes in Porous Media: Mesoscopic Simulation, *Applied Sciences (Switzerland)*, vol. 12, no. 14, 6995, 2022. DOI: 10.3390/app12146995

D 5.5 | Technology benchmark and competitor analysis of ZHENIT
WH2X systems

- [33] Zhao, C., Yan, J., Tian, X., Xue, X., and Zhao, Y., Progress in thermal energy storage technologies for achieving carbon neutrality, *Carbon Neutrality*, vol. 2, no. 1, 10, 2023. DOI: 10.1007/s43979-023-00050-y
- [34] Stekli, J., Irwin, L., and Pitchumani, R., Technical Challenges and Opportunities for Concentrating Solar Power With Thermal Energy Storage, *J Therm Sci Eng Appl*, vol. 5, no. 2, pp. 1-12, 2013. DOI: 10.1115/1.4024143
- [35] Pereira da Cunha, J. and Eames, P., Thermal energy storage for low and medium temperature applications using phase change materials – A review, *Applied Energy*, vol. 177, pp. 227-238, 2016. DOI: 10.1016/j.apenergy.2016.05.097
- [36] Kenisarin, M. and Mahkamov, K., Salt hydrates as latent heat storage materials: Thermophysical properties and costs, *Solar Energy Materials and Solar Cells*, vol. 145, pp. 255-286, 2016. DOI: 10.1016/j.solmat.2015.10.029
- [37] Bauer, T., Odenthal, C., and Bonk, A., Molten Salt Storage for Power Generation, *Chemie Ingenieur Technik*, vol. 93, no. 4, pp. 534-546, 2021. DOI: 10.1002/cite.202000137
- [38] Omara, A.A.M., Phase change materials for waste heat recovery in internal combustion engines: A review, *Journal of Energy Storage*, vol. 44, 103421, 2021. DOI: 10.1016/j.est.2021.103421
- [39] Xu, C., Zhang, H., and Fang, G., Review on thermal conductivity improvement of phase change materials with enhanced additives for thermal energy storage, *Journal of Energy Storage*, vol. 51, 104568, 2022. DOI: 10.1016/j.est.2022.104568
- [40] Marie, L.F., Landini, S., Bae, D., Francia, V., and O'Donovan, T.S., Advances in thermochemical energy storage and fluidised beds for domestic heat, *Journal of Energy Storage*, vol. 53, no. December 2021, 105242, 2022. DOI: 10.1016/j.est.2022.105242
- [41] EASE and EERA, European Energy Storage Technology Development Roadmap 2017, 2017.
- [42] Shu, G., Liang, Y., Wei, H., Tian, H., Zhao, J., and Liu, L., A review of waste heat recovery on two-stroke IC engine aboard ships, *Renewable and Sustainable Energy Reviews*, vol. 19, pp. 385-401, 2013. DOI: 10.1016/j.rser.2012.11.034
- [43] Kuiken, K., Diesel engines: for ship propulsion and power plants from 0 to 100,000 kW, *Target Global Energy Training*, 2008.
- [44] Manente, G., Ding, Y., and Sciacovelli, A., A structured procedure for the selection of thermal energy storage options for utilization and conversion of industrial waste heat, *Journal of Energy Storage*, vol. 51, 104411, 2022. DOI: 10.1016/j.est.2022.104411
- [45] Pandiyarajan, V., Chinnappandian, M., Raghavan, V., and Velraj, R., Second law analysis of a diesel engine waste heat recovery with a combined sensible and latent heat storage system, *Energy Policy*, vol. 39, no. 10, pp. 6011-6020, 2011. DOI: 10.1016/j.enpol.2011.06.065
- [46] Li, Z., Lu, Y., Huang, R., Chang, J., Yu, X., Jiang, R., Yu, X., and Roskilly, A.P., Applications and technological challenges for heat recovery, storage and utilisation with latent thermal energy storage, *Applied Energy*, vol. 283, 116277, 2021. DOI: 10.1016/j.apenergy.2020.116277

D 5.5 | Technology benchmark and competitor analysis of ZHENIT
WH2X systems

- [47] Scapino, L., Zondag, H.A., Van Bael, J., Diriken, J., and Rindt, C.C.M., Energy density and storage capacity cost comparison of conceptual solid and liquid sorption seasonal heat storage systems for low-temperature space heating, *Renewable and Sustainable Energy Reviews*, vol. 76, pp. 1314-1331, 2017. DOI: 10.1016/j.rser.2017.03.101
- [48] EnergyNest, ThermalBattery™, accessed 2 December 2024, from <https://energy-nest.com/thermal-battery/>, 2020.
- [49] Kocak, B., Fernandez, A.I., and Paksoy, H., Review on sensible thermal energy storage for industrial solar applications and sustainability aspects, *Solar Energy*, vol. 209, pp. 135-169, 2020. DOI: 10.1016/j.solener.2020.08.081
- [50] Novo, A.V., Bayon, J.R., Castro-Fresno, D., and Rodriguez-Hernandez, J., Review of seasonal heat storage in large basins: Water tanks and gravel-water pits, *Applied Energy*, vol. 87, no. 2, pp. 390-397, 2010. DOI: 10.1016/j.apenergy.2009.06.033
- [51] Eco-Tech Ceramics, Eco-Tech Ceram Eco Stock, accessed 16 July 2024, from <https://ecotechceram.com/en/>, 2022.
- [52] Lumenion GmbH, Lumenion Thermal Store, accessed 22 April 2025, from <https://lumenion.com/en/>.
- [53] Sunamp Ltd, Sunamp Thermino 300e Heat Battery, accessed 26 April 2025, from <https://www.theheatpumpwarehouse.co.uk/shop/heat-batteries/sunamp-heat-batteries/sunamp-thermino-300-e-heat-battery/>.
- [54] Baldi, F. and Gabriellii, C., A feasibility analysis of waste heat recovery systems for marine applications, *Energy*, vol. 80, pp. 654--665, 2015. DOI: 10.1016/j.energy.2014.12.020
- [55] Ancona, M.A., Baldi, F., Bianchi, M., Branchini, L., Melino, F., Peretto, A., and Rosati, J., Efficiency improvement on a cruise ship: Load allocation optimization, *Energy Conversion and Management*, vol. 164, pp. 42-58, 2018. DOI: 10.1016/j.enconman.2018.02.080
- [56] Huang, Y., Lan, H., Hong, Y.-Y., Wen, S., and Fang, S., Joint voyage scheduling and economic dispatch for all-electric ships with virtual energy storage systems, *Energy*, vol. 190, 116268, 2020. DOI: 10.1016/j.energy.2019.116268
- [57] Ouyang, T., Su, Z., Wang, F., Jing, B., Huang, H., and Wei, Q., Efficient and sustainable design for demand-supply and deployment of waste heat and cold energy recovery in marine natural gas engines, *Journal of Cleaner Production*, vol. 274, 123004, 2020. DOI: 10.1016/j.jclepro.2020.123004
- [58] Baldasso, E., Gilormini, T.J.A., Mondejar, M.E., Andreasen, J.G., Larsen, L.K., Fan, J., and Haglind, F., Organic Rankine cycle-based waste heat recovery system combined with thermal energy storage for emission-free power generation on ships during harbor stays, *Journal of Cleaner Production*, vol. 271, 122394, 2020. DOI: 10.1016/j.jclepro.2020.122394
- [59] Ouyang, T., Wang, Z., Zhao, Z., Lu, J., and Zhang, M., An advanced marine engine waste heat utilization scheme: Electricity-cooling cogeneration system integrated with heat storage device, *Energy Conversion and Management*, vol. 235, 113955, 2021. DOI: 10.1016/j.enconman.2021.113955

D 5.5 | Technology benchmark and competitor analysis of ZHENIT
WH2X systems

- [60] Brækken, A., Gabriell, C., and Nord, N., Energy use and energy efficiency in cruise ship hotel systems in a Nordic climate, *Energy Conversion and Management*, vol. 288, 117121, 2023. DOI: 10.1016/j.enconman.2023.117121
- [61] Wang, Z., Xia, R., Jiang, Y., Cao, M., Ji, Y., and Han, F., Evaluation and optimization of an engine waste heat assisted Carnot battery system for ocean-going vessels during harbor stays, *Journal of Energy Storage*, vol. 73, 108866, 2023. DOI: 10.1016/j.est.2023.108866
- [62] Frazzica, A., Manzan, M., Palomba, V., Brancato, V., Freni, A., Pezzi, A., and Vaglieco, B.M., Experimental Validation and Numerical Simulation of a Hybrid Sensible-Latent Thermal Energy Storage for Hot Water Provision on Ships, *Energies*, vol. 15, no. 7, 2596, 2022. DOI: 10.3390/en15072596
- [63] Manzan, M., Pezzi, A., Zandegiacomo de Zorzi, E., Freni, A., Frazzica, A., Vaglieco, B.M., Lucio, Z., and Claudio, D., Potential of thermal storage for hot potable water distribution in cruise ships, *Energy Procedia*, vol. 148, pp. 1105-1112, 2018. DOI: 10.1016/j.egypro.2018.08.044
- [64] Catapano, F., Frazzica, A., Freni, A., Manzan, M., Micheli, D., Palomba, V., Sementa, P., and Vaglieco, B.M., Development and experimental testing of an integrated prototype based on Stirling, ORC and a latent thermal energy storage system for waste heat recovery in naval application, *Applied Energy*, vol. 311, 118673, 2022. DOI: 10.1016/j.apenergy.2022.118673
- [65] Zhang, Q., Wang, S., Pan, D., and Li, J., Investigation on thermo-economic performance of shipboard waste heat recovery system integrated with cascade latent thermal energy storage, *Journal of Energy Storage*, vol. 64, 107171, 2023. DOI: 10.1016/j.est.2023.107171
- [66] Ouyang, T., Tan, X., Tuo, X., Qin, P., and Mo, C., Performance analysis and multi-objective optimization of a novel CCHP system integrated energy storage in large seagoing vessel, *Renewable Energy*, vol. 224, 120185, 2024. DOI: 10.1016/j.renene.2024.120185
- [67] Li, Z., Xu, Y., Fang, S., Wang, Y., and Zheng, X., Multiobjective Coordinated Energy Dispatch and Voyage Scheduling for a Multienergy Ship Microgrid, *IEEE Transactions on Industry Applications*, vol. 56, no. 2, pp. 989-999, 2020. DOI: 10.1109/TIA.2019.2956720
- [68] Li, Z., Xu, Y., Fang, S., Zheng, X., and Feng, X., Robust Coordination of a Hybrid AC/DC Multi-Energy Ship Microgrid With Flexible Voyage and Thermal Loads, *IEEE Transactions on Smart Grid*, vol. 11, no. 4, pp. 2782-2793, 2020. DOI: 10.1109/TSG.2020.2964831
- [69] Xu, L., Luo, X., Wen, Y., Wu, T., Wang, X., and Guan, X., Energy Management of Hybrid Power Ship System Using Adaptive Moth Flame Optimization Based on Multi-Populations, *IEEE Transactions on Power Systems*, vol. 39, no. 1, pp. 1711-1727, 2024. DOI: 10.1109/TPWRS.2023.3271363
- [70] Piper, M., Zibart, A., Tran, J.M., and Kenig, E.Y., A numerical study on turbulent single-phase flow and heat transfer in pillow plates, *IHTC 2014, Proceedings of the 15th*

D 5.5 | Technology benchmark and competitor analysis of ZHENIT
WH2X systems

- International Heat Transfer Conference, Kyoto, Japan, 8929, 2014. DOI: 10.1615/ihtc15.hex.008929*
- [71] Piper, M., Zibart, A., Tran, J.M., and Kenig, E.Y., Numerical investigation of turbulent forced convection heat transfer in pillow plates, *International Journal of Heat and Mass Transfer*, vol. 94, pp. 516-527, 2016. DOI: 10.1016/j.ijheatmasstransfer.2015.11.014
- [72] Loni, R., Najafi, G., Bellos, F., Rajaei, F., Said, Z., and Mazlan, M., A review of industrial waste heat recovery system for power generation with Organic Rankine Cycle: Recent challenges and future outlook, *Journal of Cleaner Production*, vol. 287, 125070, 2021. DOI: 10.1016/j.jclepro.2020.125070
- [73] Wieland, C., Schiffelechner, C., Dawo, F., and Astolfi, M., The organic Rankine cycle power systems market: Recent developments and future perspectives, *Applied Thermal Engineering*, vol. 224, 119980, 2023. DOI: 10.1016/j.applthermaleng.2023.119980
- [74] Wieland, C., Schiffelechner, C., Braimakis, K., Kaufmann, F., Dawo, F., Karellas, S., Besagni, G., and Markides, C.N., Innovations for organic Rankine cycle power systems: Current trends and future perspectives, *Applied Thermal Engineering*, vol. 225, 120201, 2023. DOI: 10.1016/j.applthermaleng.2023.120201
- [75] Song, J., Song, Y., and Gu, C.-w., Thermodynamic analysis and performance optimization of an Organic Rankine Cycle (ORC) waste heat recovery system for marine diesel engines, *Energy*, vol. 82, pp. 976-985, 2015. DOI: 10.1016/j.energy.2015.01.108
- [76] Lion, S., Taccani, R., Vlaskos, I., Scrocco, P., Vouvakos, X., and Kaiktsis, L., Thermodynamic analysis of waste heat recovery using Organic Rankine Cycle (ORC) for a two-stroke low speed marine Diesel engine in IMO Tier II and Tier III operation, *Energy*, vol. 183, pp. 48-60, 2019. DOI: 10.1016/j.energy.2019.06.123
- [77] Casisi, M., Pinamonti, P., and Reini, M., Increasing the energy efficiency of an internal combustion engine for ship propulsion with bottom ORCS, *Applied Sciences*, vol. 10, no. 19, 6919, 2020. DOI: 10.3390/app10196919
- [78] Macchi, E. and Astolfi, M., Organic Rankine Cycle (ORC) Power Systems: Technologies and Applications, 2016.
- [79] Colonna, P., Casati, E., Trapp, C., Mathijssen, T., Larjola, J., Turunen-Saaresti, T., and Uusitalo, A., Organic Rankine Cycle Power Systems: From the Concept to Current Technology, Applications, and an Outlook to the Future, *Journal of Engineering for Gas Turbines and Power*, vol. 137, no. 10, 100801, 2015. DOI: 10.1115/1.4029884
- [80] Orcan Energy, Efficiency Pack, accessed 12 October 2024, from <https://www.orcan-energy.com/en/solutions-marine.html>, 2017.
- [81] Mitsubishi Heavy Industries, Hydrocurrent™ Organic Rankine Cycle Module 125EJW - Compact and High-performance Waste Heat Recovery System Utilizing Low Temperature Heat Source, vol. 52, no. 4, pp. 53–55, 2015.
- [82] Calnetix Technologies, Hydrocurrent™ Organic Rankine Cycle (ORC) Module 125EJW - What Makes Hydrocurrent™ Superior The Optimal Heat-to-Power Solution for Marine Vessels, accessed 30 October 2025, from <https://www.calnetix.com/sites/default/files/Calnetix%20Hydrocurrent%20Brochure%20WEB.pdf>.

D 5.5 | Technology benchmark and competitor analysis of ZHENIT
WH2X systems

- [83] ENGIMMONIA, Sustainable technologies for future long distance shipping towards complete decarbonisation, accessed 2 December 2024, from <https://www.engimmonia.eu/>, 2023.
- [84] Stainchaouer, A., Schiffler, C., Wieland, C., Sakalis, G., and Spliethoff, H., Evaluating long-term operational data of a Very Large Crude Carrier: Assessing the diesel engines waste heat potential for integrating ORC systems, *Applied Thermal Engineering*, vol. 255, 123974, 2024. DOI: 10.1016/j.applthermaleng.2024.123974
- [85] Alfa Laval, Alfa Laval E-PowerPack, accessed 16 April 2025, from <https://www.alfalaval.co.uk/>, 2022.
- [86] Nesbitt, B., Handbook of Pumps and Pumping, *Elsevier Science*, 2006.
- [87] Encontech B.V., Energy Conversion Technologies, accessed 4 December 2024, from <https://www.encontech.nl/>, 2023.
- [88] Glushenkov, M., Kronberg, A., Knoke, T., and Kenig, E.Y., Heat Driven Pump for Reverse Osmosis Desalination, 2021.
- [89] Kronberg, A., Glushenkov, M., and Roosjen, S., Isobaric Expansion Engine Compressors: Thermodynamic Analysis of the Simplest Direct Vapor-Driven Compressors, *Energies*, vol. 15, no. 14, 5028, 2022. DOI: 10.3390/en15145028
- [90] Minetto, S., Fabris, F., Marinetti, S., and Rossetti, A., A review on present and forthcoming opportunities with natural working fluids in transport refrigeration, *International Journal of Refrigeration*, vol. 152, pp. 343–355, 2023. DOI: 10.1016/j.ijrefrig.2023.04.015
- [91] Ouadha, A. and El-Gotni, Y., Integration of an ammonia-water absorption refrigeration system with a marine Diesel engine: A thermodynamic study, *Procedia Computer Science*, vol. 19, pp. 754-761, 2013. DOI: 10.1016/j.procs.2013.06.099
- [92] Táboas, F., Bourouis, M., and Vallès, M., Analysis of ammonia/water and ammonia/salt mixture absorption cycles for refrigeration purposes in fishing ships, *Applied Thermal Engineering*, vol. 66, no. 1-2, pp. 603-611, 2014. DOI: 10.1016/j.applthermaleng.2014.02.065
- [93] Wu, W., Wang, B., Shi, W., and Li, X., An overview of ammonia-based absorption chillers and heat pumps, *Renewable and Sustainable Energy Reviews*, vol. 31, pp. 681--707, 2014. DOI: 10.1016/j.rser.2013.12.021
- [94] Zhang, Y., Palomba, V., and Frazzica, A., Understanding the effect of materials, design criteria and operational parameters on the adsorption desalination performance – A review, *Energy Conversion and Management*, vol. 269, 116072, 2022. DOI: 10.1016/j.enconman.2022.116072
- [95] Sztékler, K., Kalawa, W., Nowak, W., Mika, L., Gradziel, S., Krzywanski, J., and Radomska, E., Experimental study of three-bed adsorption chiller with desalination function, *Energies*, vol. 13, no. 21, 5827, 2020. DOI: 10.3390/en13215827
- [96] Ng, K.C., Thu, K., Saha, B.B., and Chakraborty, A., Study on a waste heat-driven adsorption cooling cum desalination cycle, *International Journal of Refrigeration*, vol. 35, no. 3, pp. 685-693, 2012. DOI: 10.1016/j.ijrefrig.2011.01.008
- [97] Palomba, V., Dino, G.E., Ghirlando, R., Micalef, C., and Frazzica, A., Decarbonising the shipping sector: A critical analysis on the application of waste heat for refrigeration in

D 5.5 | Technology benchmark and competitor analysis of ZHENIT
WH2X systems

- fishing vessels, *Applied Sciences*, vol. 9, no. 23, 5143, 2019. DOI: 10.3390/app9235143
- [98] Lu, Z. and Wang, R., Experimental performance study of sorption refrigerators driven by waste gases from fishing vessels diesel engine, *Applied Energy*, vol. 174, pp. 224-231, 2016. DOI: 10.1016/j.apenergy.2016.04.102
- [99] Elsaid, K., Taha Sayed, E., Yousef, B.A.A., Kamal Hussien Rabaia, M., Ali Abdelkareem, M., and Olabi, A.G., Recent progress on the utilization of waste heat for desalination: A review, *Energy Conversion and Management*, vol. 221, 113105, 2020. DOI: 10.1016/j.enconman.2020.113105
- [100] Garimella, S., Brown, A.M., and Nagavarapu, A.K., Waste heat driven absorption/vapor-compression cascade refrigeration system for megawatt scale, high-flux, low-temperature cooling, *International Journal of Refrigeration*, vol. 34, no. 8, pp. 1776-1785, 2011. DOI: 10.1016/j.ijrefrig.2011.05.017
- [101] Cao, T., Lee, H., Hwang, Y., Radermacher, R., and Chun, H.H., Modeling of waste heat powered energy system for container ships, *Energy*, vol. 106, pp. 408-421, 2016. DOI: 10.1016/j.energy.2016.03.072
- [102] Hafner, A., Gabriellii, C.H., and Widell, K., Refrigeration units in marine vessels - Alternatives to HCFCs and high GWP HFCs, Copenhagen, 2019.

Contact

The University of Birmingham

Lorenzo Ciappi - l.ciappi@bham.ac.uk

